PUBLICATIONS IN SCIENTIFIC JOURNALS

1. Synthesis, characterization and application of cerium phosphate as an ion exchanger, ***Desalination & Water Treatment*****,** 2012, 38, 126-314.

2. Acetalization of carbonyl compounds with pentaerythritol catalyzed by metal (IV) phosphates as solid acid catalysts, ***Journal of Industrial & Engineering Chemistry Research***, 2013**,** 52, 8969-8977.

3. Synthesis of monoesters and diesters using eco-friendly solid acid catalysts – cerium (IV) and thorium (IV) phosphates, ***Applied Catalysis A: General***, 2013**,** 467, 430-438.

4. Kinetics, thermodynamics and ion exchange characteristics of thorium phosphate: An inorganic ion exchanger, ***Indian Journal of Chemistry: A.*** 2014, 53A, 700-705.

5. A comparative study of proton transport properties of cerium (IV) and thorium (IV) phosphates, ***Electrochimica Acta,*** 2014, 148, 79-84.

6. Sorption and separation study of heavy metal ions using cerium phosphate: A cation exchanger, ***Desalination & Water Treatment*****,** 2015, 1-9.

PUBLICATIONS IN SCIENTIFIC PROCEEDINGS

1. Effect of microwave irradiation on the ion exchange characteristics of thorium phosphate**,** *DAE-BRNS 3rd International Symposium on Material Chemistry*, S R Bharadwaj, Kulshreshtha S K, Nigam S, Ravindran P V, Roy M, Verma S (Eds.), Chemistry Division, BARC, **ISMC-2010** (Dec. 2010) pg. 154.

PAPERS PRESENTED AT NATIONAL/INTERNATIONAL CONFERENCES

1. Synthesis, characterization and application of cerium phosphate as an ion exchanger, *DAE-BRNS Biennial Symposium on Emerging Trends in Separation Science and Technology (***SESTEC-2010***)*, IGCAR-Chennai, 1-4 March 2010.

2. Effect of microwave irradiation on the ion exchange characteristics of thorium phosphate, *DAE – BRNS 3rd International Symposium on Materials Chemistry* (**ISMC-2010**), BARC, Mumbai, 7th –11th Dec. 2010.

3. Synthesis, characterization and application of thorium phosphate as an ion Exchanger, *National Symposium on Advances in Separation and Purification Science & Technology* (**NSST-2011**), Department of Chemical Engineering, , G H Patel College of Engg. & Tech., Vallabh Vidhyanagar, 4th -5th Feb 2011.

4. Synthesis and characterization of cerium (iv) phosphate and its applicability as a cation exchanger, *Symposium on Modern Trends in Inorganic Chemistry* **(MTIC–XIV)***,* University of Hyderabad, Hyderabad, 10th –13th Dec. 2011.

5. Synthesis of mono esters and diesters using eco-friendly solid acid catalyst – cerium (IV) phosphate, *National Seminar on Catalysis for Sustainable Development, Department of Chemistry*, Faculty of Science, The M. S. University of Baroda, Vadodara, 27th –28th Jan. 2012.

ATTENDED SYMPOSIA, WORKSHOPS, TRAINING PROGRAMME FOR SELF DEVELOPMENT

1. Symposium on "**Emerging Trends in Catalysis**" organized by Catalysis Society of India, Baroda Chapter, 25-26 September 2009.

2. Workshop on "**Physical Techniques for the Investigation of Fast Ion Conducting Materials" held at Department of Physics**, Faculty of Science, The M. S. University of Baroda, Vadodara 390001, 20 - 22 March 2010.

3. **12th Orientation Programme on Catalysis Research**, National Centre of Catalysis Research (NCCR), IIT Madras, Chennai, 18th Nov. - 7th Dec. 2011

Desalination and Water Treatment
Publication details, including instructions for authors and subscription information:
http://www.tandfonline.com/loi/tdwt20

Synthesis, characterization and application of cerium phosphate as an ion exchanger

Tarun Parangi [a], Bina Wani [b] & Uma Chudasama [a]

[a] Applied Chemistry Department, Faculty of Technology & Engineering, The M.S. University of Baroda, Vadodara, 390 001, Gujarat, India Fax:

[b] Chemistry Division, Bhabha Atomic Research Centre, Trombay, Mumbai, 400 085, India

Available online: 10 Feb 2012

To cite this article: Tarun Parangi, Bina Wani & Uma Chudasama (2012): Synthesis, characterization and application of cerium phosphate as an ion exchanger, Desalination and Water Treatment, 38:1-3, 126-134

To link to this article: http://dx.doi.org/10.1080/19443994.2012.664312

Desalination and Water Treatment
www.deswater.com
1944-3994/1944-3986 © 2012 Desalination Publications. All rights reserved
doi: 10/5004/dwt.2012.2549

38 (2012) 126–134
January

Taylor & Francis
Taylor & Francis Group

Synthesis, characterization and application of cerium phosphate as an ion exchanger

Tarun Parangi[a], Bina Wani[b], Uma Chudasama[a,*]

[a]*Applied Chemistry Department, Faculty of Technology & Engineering, The M.S. University of Baroda, Vadodara 390 001, Gujarat, India*
Fax: +91 265 2423898; email: uvcres@gmail.com
[b]*Chemistry Division, Bhabha Atomic Research Centre, Trombay, Mumbai 400 085, India*

Received 9 December 2010; Accepted 11 July 2011

ABSTRACT

In the present endeavour, cerium phosphate (CP), an ion exchanger of the class of tetravalent metal acid (TMA) salt has been synthesized by soft chemistry route, sol gel method. Physical and ion exchange characteristics as well as chemical stability of the material in various acids, bases and organic solvent media has been studied. CP has been characterized using instrumental methods (FTIR, TGA/DSC, XRD and SEM). Distribution coefficient (K_d) of metal ions Mn^{2+}, Co^{2+}, Ni^{2+}, Cu^{2+}, Zn^{2+}, Cd^{2+}, Hg^{2+} and Pb^{2+} has been determined in aqueous as well as various electrolyte media/concentrations. The equilibrium exchange (varying temperature) of these metal ions with H^+ ions contained in CP has been studied and thermodynamic parameters equilibrium constant (K), standard Gibbs free energy ($\Delta G°$), enthalpy ($\Delta H°$) and entropy ($\Delta S°$) have been evaluated.

Keywords: Tetravalent metal acid salt; Inorganic ion exchanger; Cerium phosphate; Distribution coefficient (K_d); Thermodynamics of ion exchange; Cation exchanger

1. Introduction

Tetravalent metal acid (TMA) salts are inorganic cation exchangers in which protons present in the structural hydroxyl groups are responsible for cation exchange behaviour [1]. When a tetravalent metal is treated with phosphoric acid, M–O–P bonds are formed. In this process, a number of hydroxyl groups do not participate in the condensations which are referred to as pendant hydroxyl groups or defective P – OH, H of the P – OH contributing to cation exchange capacity (CEC) [2]. TMA salts are prepared by sol-gel routes and can be obtained both in amorphous and crystalline forms. TMA salts with varying water content, composition and crystallinity can be obtained varying several parameters such as mole ratio of reactants M:X (M = tetravalent metal, X = polyvalent anion), temperature of mixing, mode of mixing (metal salt solution to anion salt solution or vice versa), pH, rate of mixing, aging period etc. Variation in any of these parameters affects the structural hydroxyl groups, which in turn is reflected in their CEC and performance as a cation exchanger. Several studies have shown that cerium (IV) phosphates (CPs) are interesting inorganic materials for cation exchange [3]. Compared to zirconium, titanium and tin phosphates, which are well established ion exchangers, literature survey reveals that the cation exchange behaviour of cerium phosphate (CP) is not much explored [4]. Fibrous Cerium phosphate has received much attention as cation exchangers, used in the form of staples, cloths, ion exchange papers etc. [5–8]. However, for efficient metal separations column operations are preferred. In the several studies using

*Corresponding author.

Proceedings of DAE-BRNS Biennial Symposium on Emerging Trends in Separation Science and Technology, Kalpakkam, India, March 1–4, 2010

TMA salts as cation exchangers it is found that the amorphous materials are preferred to crystalline materials as they can be obtained in a range of mesh sizes suitable for column operations. Crystalline materials have shown the disadvantage of small grain size, restricting their application in column operation [1,9,10].

In the present endeavour, amorphous CP has been synthesized by soft chemistry route sol-gel method and characterized for spectral analysis (FTIR), thermal analysis (TGA and DSC), X-ray diffraction studies and SEM. Physical and ion exchange characteristics as well as chemical stability of the material in various acids, bases and organic solvent media has been assessed. Distribution coefficient (K_d) for metal ions Mn^{2+}, Co^{2+}, Ni^{2+}, Cu^{2+}, Zn^{2+}, Cd^{2+}, Hg^{2+} and Pb^{2+} has been determined in different electrolyte media/concentrations. Further, the equilibrium exchange (varying temperature) of these metal ions with H^+ ions contained in CP has been studied and thermodynamic parameters equilibrium constant (K), standard Gibbs free energy ($\Delta G°$), enthalpy ($\Delta H°$) and entropy ($\Delta S°$) have been evaluated.

2. Experimental

All chemicals and reagents used are of analytical grade. Double-distilled water was used for all the studies.

2.1. Synthesis of CP

CP has been synthesized by sol gel method. A solution containing $Ce(SO_4)_2$ $4H_2O$ [0.1 M, 50 ml in 10% (w/v) H_2SO_4] was prepared, to which NaH_2PO_4 $2H_2O$ [0.3 M, 50 ml] was added dropwise (flow rate 1 ml·min^{-1}) with continuous stirring for an hour at room temperature, when gelatinous precipitates were obtained. The resulting gelatinous precipitate was allowed to stand for 3 h at room temperature, then filtered, washed with conductivity water to remove adhering ions and dried at room temperature. The material was then broken down to the desired particle size [30–60 mesh (ASTM)] by grinding and sieving. 5 g of this material was treated with 50 ml of 1 M HNO_3 for 30 min with occasional shaking. The material was then separated from acid by decantation and treated with conductivity water to remove adhering acid. This process (acid treatment) was repeated at least 5 times. After final washing, the material was dried at room temperature. This material was used for all studies.

2.1.1. Physical and ion exchange characteristics

Physical characteristics such as appearance, percentage moisture content, apparent density, true density and ion exchange characteristics such as void volume fraction, concentration of fixed ionogenic groups and volume capacity for CP were studied according to known methods [11–13].

The synthesized material CP was observed for physical appearance such as colour, opacity/transparency, hardness etc. The percentage moisture content is calculated using the formula, *% moisture content* = 100 − *% solid* [where *% solid* = (*weight of dried material/weight of material before drying)* × 100)]. Apparent density is determined using the equation, *apparent density = weight of ion exchanger/volume of ion exchange bed*. The true density was determined by taking a definite amount of CP in previously weighed specific gravity bottle (W). The bottle was again weighed along with the ion exchanger (W_i). The bottle was now filled with water along with ion exchange material and weighed (W_{is}). The weight of the specific gravity bottle containing water is also noted (W_w). The true density is calculated by using equation, $D_{ie} = (W_i - W)/(W_w - W_{iw}) + (W_i - W)$. Void volume fraction is calculated using equation, *void volume fraction* = $1 - D_{col}/D_{ie}$. Concentration of fixed ionogenic group is calculated using the equation, $C_r = D_{ie} \times (100 - \%\ moisture) \times IEC/100$. Volume capacity of exchanger is evaluated using formula, $Q = (1 - void\ volume\ fraction) \times C_r$.

2.1.2. Chemical stability

The chemical stability of the material in various media - acids (HCl, H_2SO_4, HNO_3), bases (NaOH and KOH) and organic solvents (ethanol, benzene, acetone and acetic acid) was studied by taking 0.5 g of CP in 50 ml of the particular medium and allowing to stand for 24 h. The change in colour, nature, weight as well as solubility was observed. Further, to confirm the stability/solubility of exchanger in particular media, supernatant liquid was checked qualitatively for respective elements of exchanger.

2.1.3. pH titration curve

"pH titration curve" or the "potentiometric curve", a plot of pH versus number of milliequivalents of OH^- ions, gives an idea regarding the acidic nature of exchanger, weak or strong [11]. For cation exchangers, the acid sites can be titrated against an alkali hydroxide (used for neutralization) and a salt solution of same alkali metal (used as a supporting electrolyte). In the present case, 0.5 g of CP was placed in NaCl (0.1 M, 100 ml) solution. This solution mixture was titrated against NaOH (0.1 M) solution. After addition of every 0.5 ml of titrant, sufficient time was provided for establishment of equilibrium, till the pH is constant. A pH titration curve is obtained by plotting pH versus volume of NaOH (Fig. 1).

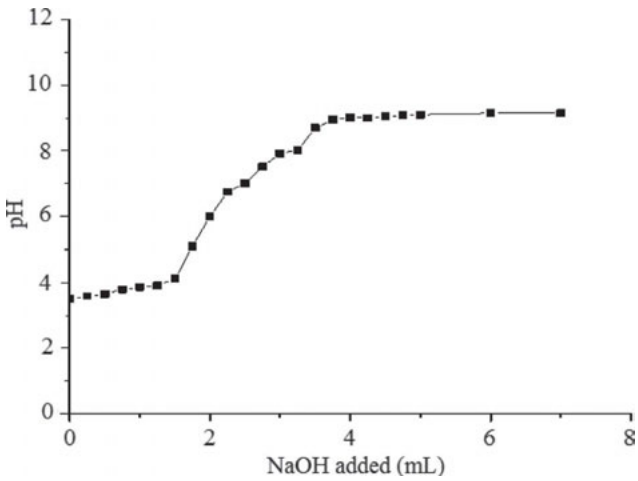

Fig. 1. pH Titration curve.

2.1.4. Cation exchange capacity (CEC) and effect of calcination on CEC

The Na^+ ion exchange capacity (CEC) of CP was determined by the column method by optimizing volume and concentration of sodium acetate solution [14]. In the first case, a fixed volume (250 ml) of sodium acetate solution of varying concentration (0.1 M, 0.2 M, 0.3 M, 0.4 M, 0.5 M, 0.6 M, 0.7 M) was passed through a glass column [30 cm × 1 cm (internal diameter)] containing 0.5 g of the exchanger, maintaining a flow rate of 0.5 ml·min^{-1} and effluent (containing H^+ ions eluted out) titrated against 0.1 M NaOH solution. The optimum concentration of eluant is thus determined. In the second case the eluant of optimum concentration was used and 10 ml fractions passed through the column keeping a flow rate 0.5 ml·min^{-1}. This experiment was conducted to find out the minimum volume necessary for a complete elution of the H^+ ions, which reflects the efficiency of the column. Using these optimized parameters Na^+ CEC was determined, using the formula aV/W, where a is molarity and V the amount of alkali used during titration, and W is the weight of the exchanger.

The effect of calcination on CEC was studied by heating several 1 g portions of the material for 2 h at different temperatures in the range 100°C to 500°C with 100°C intervals in a muffle furnace and Na^+ exchange capacity determined by the column method at room temperature.

2.2. Instrumentation

FTIR spectra was recorded using KBr pellet on Shimadzu (Model 8400S). Thermal analysis (TGA) was carried out on a Shimadzu (Model TGA 50) thermal analyzer at a heating rate of 10°C min^{-1} and DSC was analyzed on Shimadzu (Model DSC-50). X-ray diffractogram (2θ = 10 –80°) was obtained on X-ray diffractometer (Brucker AXS D8) with Cu-K_α radiation with nickel filter. SEM of the sample was scanned on Jeol JSM-5610-SLV scanning electron microscope.

2.3. Distribution studies

Distribution coefficient (K_d) is a measure of the fractional uptake of metal ions in solution, competing for H^+ ions, in case of a cation exchange material. Almost, all ion exchange reactions being reversible, at equilibrium, the favoured direction of an exchange reaction is determined by the relative affinity of the ion exchanger for the ions entering into the exchanger matrix.

The distribution coefficient (K_d) for Mn^{2+}, Co^{2+}, Ni^{2+}, Cu^{2+}, Zn^{2+}, Cd^{2+}, Hg^{2+} and Pb^{2+} was evaluated by batch method, in which 0.1 g of CP in the H^+ form was equilibrated with 20 ml of 0.001 M metal solution for 24 h at room temperature. The metal ion concentration before and after exchange was determined by EDTA titration.

Distribution studies have been carried out in aqueous as well as various electrolyte media like NH_4NO_3, HNO_3, $HClO_4$ and CH_3COOH of 0.02 and 0.20 M concentration. K_d was evaluated using the expression, $K_d = [(I\text{-}F)/F] \times V/W$ (ml·g^{-1}) where, I = total amount of the metal ion in the solution initially; F = total amount of metal ions left in the solution after equilibrium; V = volume of the metal ion solution; W = weight of the exchanger.

K_d was also evaluated varying temperatures (30°C to 60°C with 10°C interval). 20 ml, 0.002 M metal ion solution was equilibrated with 0.2 g of exchanger in stoppered conical flasks at a particular temperature for 6 h (maximum equilibrium time). The supernatant liquid was removed in each case after 6 h and the metal ion concentration evaluated by EDTA titration. From these experiments equilibrium values have also been determined.

2.4. Thermodynamics of ion exchange

2.4.1. Equilibrium time determination

0.1 g of exchanger was shaken with 0.002 M metal ion solution in stoppered conical flasks varying time in the range of 30 min to 6 h, with 30 min time interval at a particular temperature. A plot of the fractional attainment of equilibrium $U(\tau)$ versus time (t) gives an idea about maximum equilibrium time (Fig. 2).

2.4.2. Equilibrium experiments

The equilibrium experiments were performed by shaking 0.2 g of the exchanger particles at the desired temperature (30°C, 40°C, 50°C and 60°C) in a shaker

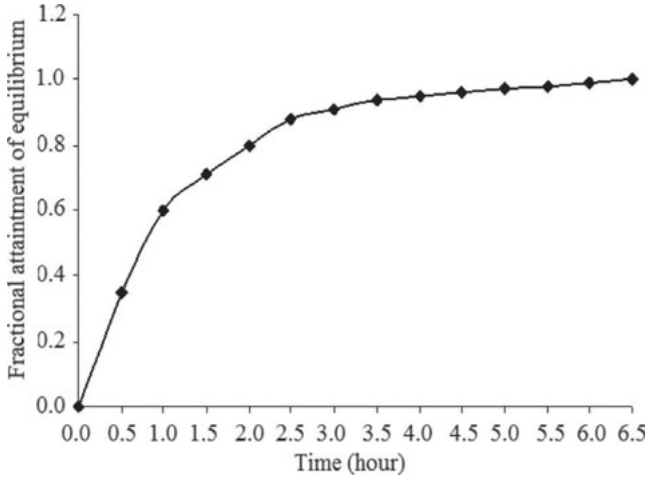

Fig. 2. Plot of $U(\tau)$ versus time (t).

bath for 6 h with 20 ml of a mixture of solution containing 0.06 M HCl and the appropriate metal ion of varying volume ratios (1, 3, 5,…19 ml 0.02 M metal ion solution and 19, 17, 15,...1 ml of 0.06 M HCl, respectively were prepared) having constant ionic strength (0.06 M). After equilibrium, the supernatant liquid was removed and metal ion estimated by EDTA titration.

3. Results and discussion

3.1. Characterization of CP

Physical and ion exchange characteristics of CP have been presented in Table 1. CP was obtained as yellow hard granules.

The Na^+ ion exchange capacity (CEC) in meq·g^{-1} evaluated by column method at room temperature is 2.48 meq·g^{-1} (using 220 ml 0.5 M of CH_3COONa solution). The Na^+ CEC of the calcined samples (Table 1) shows that CEC values decrease with increasing temperature, attributed to loss of moisture and condensation of structural hydroxyl groups.

A study on the chemical stability shows that CP is stable in acids and organic solvent media but not so stable in base medium (Table 1).

The FTIR spectra (Fig. 3) of CP exhibits a broad band in the region ~3400 cm^{-1} which is attributed to asymmetric and symmetric $^-$OH stretching vibration due to residual water and presence of structural hydroxyl groups, H^+ of the $^-$OH being cation exchange sites. These sites are also referred to as defective P-OH groups [2]. A sharp medium band at ~1630 cm^{-1} is attributed to aquo H–O–H bending [15]. The band at 1050 cm^{-1} is attributed to P=O stretching while the bands at 620 cm^{-1} and 500 cm^{-1} is attributed to Ce-O stretching [16].

Table 1
Physical and ion exchange characteristics of CP

Characteristics	Observation
Appearance	Yellow hard granules
Particle size	250–590 μ
% Moisture content	10.26%
True density	2.86 g·ml^{-1}
Apparent density	0.60 g·ml^{-1}
Void volume fraction	0.79
Concentration of fixed ionogenic groups	6.28 mmol·g^{-1}
Volume capacity of resin	1.31 meq·ml^{-1}
Nature of exchanger	Weak cation exchanger
CEC (Room Temperature)	2.45 meq g^{-1}
100°C	2.24 meq g^{-1}
200°C	1.89 meq g^{-1}
300°C	0.99 meq g^{-1}
400°C	0.20 meq g^{-1}
500°C	0.07 meq g^{-1}
Chemical stability	Maximum tolerable limits
i) Acids	1 N H_2SO_4, 2 N HNO_3, 5 N HCl
ii) Bases	0.5 N NaOH, 0.5 N KOH
iii) Organic solvents	Ethanol, Benzene, Acetone, Acetic acid

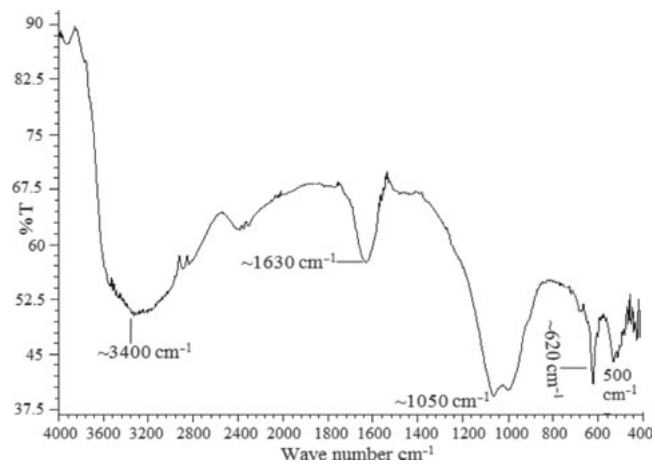

Fig. 3. FTIR of CP.

TGA (Fig. 4) exhibits two regions of weight loss. The first weight loss ~13% up to 120°C is attributed to loss of moisture/hydrated water, while the second weight loss ~8% in the range of 120–500°C is attributed to the condensation of structural hydroxyl groups.

DSC (Fig. 5) exhibits an endothermic peak at ~128°C, attributed to loss of moisture/hydrated water. Beyond this temperature no peaks are observed indicating absence of any phase change in the material upon thermal treatment in the range studied.

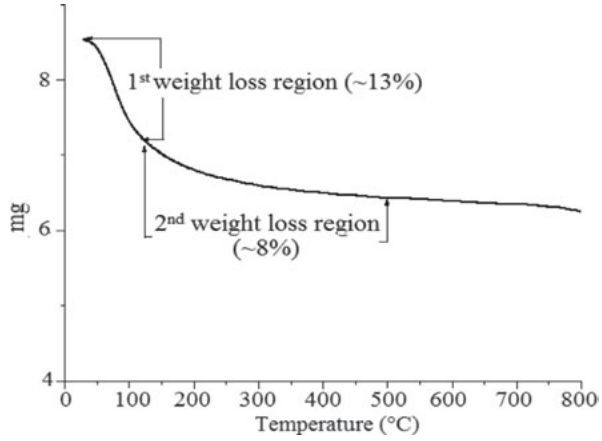

Fig. 4. TGA of CP.

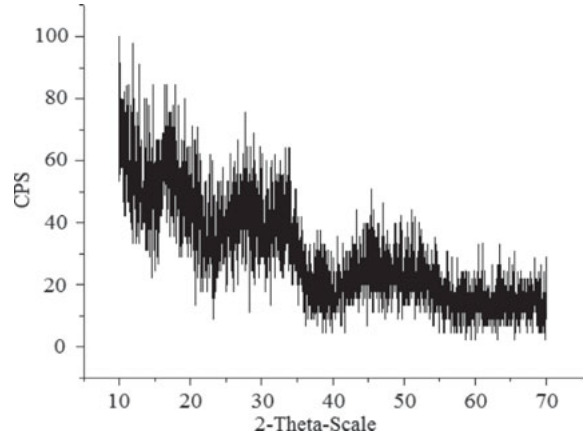

Fig. 6. XRD of CP.

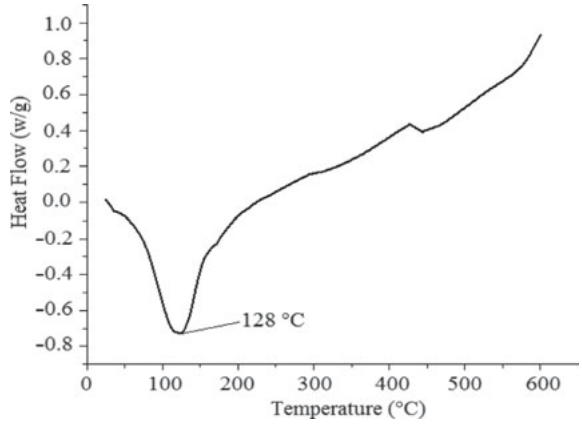

Fig. 5. DSC of CP.

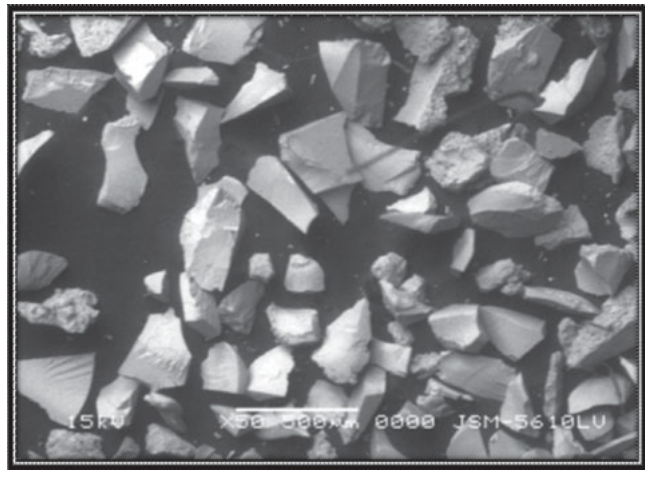

Fig. 7. SEM of CP.

Absence of sharp peaks in X-ray diffractogram (Fig. 6) of CP, indicates amorphous nature of the material. SEM (Fig. 7) of CP at room temperature, exhibits irregular particle size which indicates amorphous nature of the material which is also supported by XRD of the material.

3.2. Distribution studies

Selectivity/affinity of a particular metal ion towards an ion exchanger depends on (1) **the ion exchanger**, the factors responsible being particle size, the presence of functional groups that indicate the nature of the exchanger weak or strong, the ion exchange capacity, the degree of cross linking, and the structural complexity of the ion exchanger, (2) **the exchange media**, the factors responsible being concentration, pH, and the nature of the electrolyte, weak or strong, as well as the temperature, and (3) **the exchanging metal ion**, the factors responsible being ionic radius and ionic charge on the metal ion, with higher valent ions having more affinity for the exchanger [13,17]. Over and above these three factors the exchange process itself, i.e., the rate of exchange and equilibrium also play an important role in determining the selectivity. On immersing the exchanger in solution, equilibrium is established between the exchanger and the electrolyte solution, the rate of exchange depending on the size of the exchanging metal ion and the grain/particle size of the exchanger. Smaller cations have a greater tendency to be hydrated as a consequence of which the hydrated ionic radius is large. Larger ions being less hydrated, less energy is utilized for dehydration of the metal ions while occupying a site on the exchanger, plays a prominent role in determining the selectivity of metal ions [13,17].

The overall effect is a result of the contribution of the above mentioned factors. Depending on the predominant factor, the affinity of metal ions towards the ion exchanger varies in each case.

Separation factor, $\alpha = K_{d1} / K_{d2}$, where K_{d1} and K_{d2} are the distribution coefficients of the two constituent metal ions being separated on an ion exchange material in a particular electrolyte medium. The greater the deviation of α from unity, better is the separation. The efficiency of an ion exchange separation depends on the condition under which α has a useful value, or influencing in a direction favourable to separation. For a given metal ion pair, the electrolyte media in which the separation factor is the highest, is selected as the eluant. Thus, a study on distribution behaviour of metal ions in various electrolyte media gives an idea about the eluants that can be used for separation [13,17].

The distribution coefficient (K_d) values evaluated for the the metal ions under study towards CP have been presented in Table 2. In general it is observed that the K_d values are lower in high concentration of electrolyte and vice versa. Further, the K_d values in strong electrolyte media are lower as compared to weak electrolyte and aqueous media. This may be attributed to the high competition amongst ions for exchange in strong electrolyte media.

The most promising property of CP is the very high K_d value observed for Pb^{2+} in aqueous medium suggesting its separation from other metals/pollutants. No sorption is observed in case of Cu^{2+} (0.2 M HNO_3 and 0.2 M $HClO_4$), $Ni^{2+}$and Hg^{2+} (0.2 M $HClO_4$). Co^{2+}, Ni^{2+} and Zn^{2+} exhibit very low K_d values (0.2 M HNO_3) while Mn^{2+} and Co^{2+} exhibit very low K_d values (0.2 M $HClO_4$). Hg^{2+} exhibits very low K_d value in aqueous medium.

The observed selectivity order (Table 2) in aqueous medium is Zn^{2+} (0.74Å) > Ni^{2+} (0.72Å) > Mn^{2+} (0.80Å) > Co^{2+} (0.72Å) > Cu^{2+} (0.74Å) amongst the transition metal ions and Pb^{2+} (1.44Å) > Cd^{2+} (0.97Å) > Hg^{2+} (1.10Å) amongst the heavy metal ions, values in parenthesis being ionic radii of respective metal ions. The ionic radii being almost equivalent in case of transition metal ions, the selectivity order is probably dependant on rate of exchange/equilibrium and dissociation of salt, while selectivity order in case of heavy metal ions can be explained on the basis of size of ions and hence hydrated ionic radii. As explained earlier, larger ions being less hydrated, less energy is utilized for dehydration of the metal ions to occupy a site on the exchanger.

The effect of temperature on K_d and equilibrium values have been presented in Table 2. It is observed that both K_d and equilibrium values increase with increase in temperature. This could be attributed to increase in mobility of the ions with increasing temperature and higher affinity of metal ions towards the exchanger, compared to H^+ ions.

3.3. Thermodynamics of ion exchange

Thermodynamic parameters such as equilibrium constant (K), standard Gibbs free energy ($\Delta G°$), enthalpy ($\Delta H°$) and entropy ($\Delta S°$) have been evaluated using standard equations [11–13]. Results are summarized in Table 3. A plot of the fractional attainment of equilibrium $U(\tau)$ versus time (t) (Fig. 2) shows that the exchange equilibrium for CP appears to have attained within 4 h and hence all the equilibrium studies were performed after shaking for 6 h.

Equilibrium constant (K) values increase with increase in temperature for all metal ions under study (Table 3), indicating that the metal ions have higher affinity for the exchanger and that the mechanism is ion exchange [14].

Negative $\Delta G°$ values indicate that the exchange process is feasible and spontaneous in nature. In the present study, the free energy change for all the exchange reactions is negative, over the entire temperature range, indicating that the exchanger has a greater preference for metal ions than H^+ ions. The $\Delta G°$ values become more negative with increasing temperature, confirming that the exchange is favoured with increasing temperature. As dehydration is essential for ion exchange to occur [18], less negative $\Delta G°$ values observed may be attributed to metal ions that are heavily hydrated. In case of Pb^{2+} more negative $\Delta G°$ values are observed indicating that exchange takes place more readily in case of Pb^{2+}, being the least hydrated.

The enthalpy change ($\Delta H°$) for an ion exchange reaction can be either of the five reasons or a net effect of these factors: (1) the heat consumed in bond breaking, as H^+ is released from the resin (2) the heat released in the formation of bonds with the incoming cation (3) the heat corresponding to the energy required for crossing the barrier (distance between exchange phase and solution phase) (4) the enthalpy change accompanying hydration and dehydration of exchanging ion in the solution (5) introduction of a high degree of disorder into the resin matrix due to the ion exchange process. A negative enthalpy change ($\Delta H°$) indicates that the exchange reaction is exothermic and a positive enthalpy change indicates that the exchange reaction is endothermic.

In the present study, enthalpy change is positive in all cases, except Mn^{2+} and Ni^{2+}. As dehydration is a must for ion exchange to occur, some energy must be supplied, to the cation, as it leaves the hydration sphere to undergo ion exchange [18]. The observed order of $\Delta H°$ is: Pb^{2+} > Zn^{2+} > Cu^{2+} > Co^{2+} > Cd^{2+} > Hg^{2+} > Ni^{2+} > Mn^{2+}. Higher/positive values of enthalpy change indicate more endothermicity of the process and requirement of more energy for dehydration to occur. The $\Delta H°$ values indicate that probably complete dehydration occurs in case of Pb^{2+}. These observations are in keeping with high negative $\Delta G°$ values in case of Pb^{2+}.

Table 2
Distribution coefficient (K_d) (ml·g^{-1}) and equilibrium values (meq·g^{-1}) of metal ions

Metal ion	Ionic radius (A°)	K_d values in aqueous and various electrolyte media/concentration									K_d and Equilibrium values at different temperatures							
		Aqueous media	NH_4NO_3		HNO_3		$HClO_4$		CH_3COOH		30°C		40°C		50°C		60°C	
			0.02 M	0.2 M	0.02 M	0.2 M	0.02 M	0.2 M	0.02 M	0.2 M	K_d	EV	K_d	EV	K_d	EV	K_d	EV
Mn^{2+}	0.80	200.12	359.53	312.65	219.35	199.63	20.25	4.90	942.85	1032.00	336.36	0.370	468.75	0.375	480.00	0.443	685.00	0.475
Co^{2+}	0.72	180.00	105.85	27.14	13.05	2.78	16.29	7.95	211.45	184.00	61.00	0.150	68.00	0.161	83.00	0.170	97.00	0.200
Ni^{2+}	0.72	217.00	114.00	22.00	17.00	7.00	2.00	NS	205.00	135.00	37.10	0.144	42.12	0.164	66.00	0.178	111.00	0.024
Cu^{2+}	0.74	172.00	185.00	73.00	40.00	NS	3.00	NS	303.00	241.00	118.00	0.230	171.00	0.240	182.00	0.274	228.00	0.320
Zn^{2+}	0.74	266.00	174.00	65.01	56.00	14.00	30.00	15.00	273.00	190.00	57.00	0.213	69.00	0.242	87.00	0.268	91.00	0.276
Cd^{2+}	0.97	442.00	291.00	63.03	89.00	25.00	70.00	84.00	511.00	768.00	90.00	0.190	124.00	0.222	205.00	0.269	207.00	0.282
Hg^{2+}	1.44	19.09	50.42	28.87	56.47	35.04	18.00	NS	64.24	54.97	35.59	0.105	42.00	0.120	59.09	0.156	68.00	0.170
Pb^{2+}	1.10	3590.47	3780.00	2212.12	3418.18	279.51	1493.61	2642.85	5106.66	2141.17	568.00	0.343	601.00	0.347	3940.00	0.394	4000.00	0.402

NS = No sorption, EV = Equilibrium value.

Table 3
Thermodynamic parameters for M^{2+} - H^{+} exchange at various temperatures

Exchanging system	Temperature (K)	K_a	$\Delta G°$ (k J mol^{-1})	$\Delta H°$ (k J mol^{-1})	$\Delta S°$ (J mol^{-1} K^{-1})
Mn(II) – H(I)	303	3.45	–1.71	–36.47	–111.32
	313	8.83	–2.74		–91.35
	323	23.99	–4.26		–99.72
	333	428.33	–7.88		–104.38
Co(II) – H(I)	303	2.34	–1.07	12.71	45.52
	313	2.6	–1.24		44.6
	323	3.3	–1.6		44.34
	333	3.68	–1.80		43.62
Ni(II) – H(I)	303	1.45	–0.51	–5.06	–14.39
	313	1.57	–0.60		–14.21
	323	1.6	–0.61		–13.78
	333	1.74	–0.69		–13.64
Cu(II) – H(I)	303	2.70	–1.25	62.16	209.3
	313	4.32	–1.90		204.69
	323	8.02	–2.79		201.11
	333	23.89	–4.39		199.87
Zn(II) – H(I)	303	0.47	0.93	67.86	220.88
	313	7.01	–2.69		229.88
	323	10.87	–3.20		220.02
	333	23.06	–4.08		211.12
Cd(II) – H(I)	303	2.06	–0.91	9.87	35.67
	313	2.21	–1.03		34.87
	323	2.27	–1.10		34.00
	333	2.90	–1.47		34.10
Pb(II) – H(I)	303	0.41	1.10	143.97	471.50
	313	1.73	–0.71		462.25
	323	13.10	–3.45		456.40
	333	69.58	–5.87		449.99
Hg(II) – H(I)	303	3.77	–1.67	1.21	9.54
	313	3.88	–1.76		9.52
	323	3.96	–1.90		9.38
	333	4.15	–1.91		9.68

The entropy change normally depends on the extent of hydration of the exchangeable and exchanging ions along with any change in water structure around ions that may occur when they pass through the channels of exchange. $\Delta S°$ also follows same trend as $\Delta H°$. Higher values observed in case of Pb^{2+}, are attributed to greater dehydration, which indicates the greater disorder produced during the Pb^{2+} - H^{+} exchange.

4. Conclusions

CP exhibits promising ion exchange characteristics - good CEC, thermal stability and chemical stability, which are characteristics of a good ion exchange material. The most promising property of CP, is its high selectivity for Pb^{2+} and very low selectivity for Hg^{2+}, suggesting their removal from other metal ions/pollutants.

Acknowledgements

The authors thank DAE-BRNS for providing financial support and research fellowship to one of them (Tarun Parangi).

References

[1] K.G. Varshney and M.A. Khan, Inorganic Ion Exchangers in Chemical Analysis (M. Qureshi and K.G. Varshney, Eds). CRC Press, Boca Raton Florida (1991).
[2] A. Bhaumik and S. Inagaki, Mesoporous Titanium Phosphate Molecular Sieves with Ion-Exchange Capacity, J. Am. Chem. Soc., 123 (2001) 691–696.

[3] M. Nazaraly, G. Wallez, C. Chaneac, E. Tronc, F. Ribot, M. Quarton and J. P. Jolivet, The first structure of a Cerium (IV) Phosphate: Ab Initio Rietveld Analysis of $Ce^{(IV)}(PO_4)(HPO_4)_{0.5}(H_2O)_{0.5}$, Angew. Chem. Int. Ed., 44 (2005) 5691–5694.
[4] G. Alberti in Inorganic Ion Exchange Materials (Ed.: A Clearfield), CRC, Boca Roton, FL, (1982), chap. 2; b.
[5] A. Somya, M.Z.A. Rafiquee and K.G. Varshney, Synthesis, characterization and analytical applications of sodium dodecyl sulphate cerium (IV) phosphate: A new Pb (II) selective, surfactant-based intercalated fibrous ion exchanger, Colloids Surf., A, 336 (2009) 142–146.
[6] K.G. Varshney, M.Z.A. Rafiquee and A. Somya, Triton X–100 based cerium (IV) phosphate as a new Hg (II) selective, surfactant based fibrous ion exchanger: Synthesis, characterization and adsorption behaviour, Colloids Surf., A, 317 (2008) 400–405.
[7] K.G. Varshney, A. Agrawal and S.C. Mojumdar, Pyridine based cerium (IV) phosphate hybrid fibrous ion exchanger: synthesis, characterization and thermal behaviour, J. Therm. Calorim., 90(3) (2007) 731–734.
[8] K.G. Varshney, P. Gupta and N. Tayal, Kinetics of ion exchange of alkaline earth metal ions on acrylamide cerium (IV) phosphate: a fibrous ion exchanger, Colloids. Surf., B, 28 (2003) 11–16.
[9] K. Maheria and U. Chudasama, Synthesis and characterization of a new phase of titanium phosphate and its application in separation of metal ions, Indian J. Chem. Technol., 14 (2007) 423–426.
[10] A. Jayswal and U. Chudasama, Synthesis and Characterization of a New Phase of zirconium phosphate for the Separation of Metal Ions, J. Iran. Chem. Soc., 4(4) (2007) 510–515.
[11] F. Helfferich, Ion Exchange, McGraw-Hill (New York) 1962.
[12] R. Kunin, Ion Exchange Resin, Wiley (London) 1958.
[13] R. Thakkar and U. Chudasama, Synthesis and characterization of zirconium titanium phosphate and its application in separation of metal ions J. Hazard. Mater., 172 (2009) 129–137.
[14] P. Patel and U. Chudasama, Thermodynamics and Kinetics of ion exchange of a hybrid cation exchanger, zirconium diethylene triamine pentamethylene phosphonate, Indian J. Chem., sect. A, 49 (2010) 1318–1324.
[15] C.T. Seip, G.E. Granroth, M.W. Miesel and D.R. Talham, Langmuir-Blodgett Films of Known Layered Solids: Preparation and Structural Properties of Octadecylphosphonate Bilayers with Divalent Metals and Characterization of a Magnetic Langmuir-Blodgett Film, J. Am. Chem. Soc., 119 (1997) 7084–7094.
[16] A. Nilchi, M.M. Ghanadi and A. Khanchi, Characteristics of novel types substituted cerium phosphates, J. Radioanal. Nucl. Chem., 245(2) (2000) 589–594.
[17] R. Thakkar and U. Chudasama, Synthesis and Characterization of Zirconium Titanium Hydroxy Ethylidene Diphosphonate and Its Application in Separation of Metal Ions, Sep. Sci. Technol., 44 (2009) 3088–3112.
[18] A.E. Kurtuoglu and G. Atun, Determination of kinetics and equilibrium of Pb/Na exchange on clinoptilolite, Sep. Purif. Technol., 50 (2006) 62–70.

Applied Catalysis A: General 467 (2013) 430–438

Contents lists available at ScienceDirect

Applied Catalysis A: General

journal homepage: www.elsevier.com/locate/apcata

Synthesis of monoesters and diesters using eco-friendly solid acid catalysts—Cerium(IV) and thorium(IV) phosphates

Tarun Parangi[a], Bina Wani[b], Uma Chudasama[a,*]

[a] Applied Chemistry Department, Faculty of Technology & Engineering, The M.S. University of Baroda, Vadodara, 390001, Gujarat, India
[b] Chemistry Division, Bhabha Atomic Research Centre (BARC), Trombay, Mumbai, 400085, Maharashtra, India

ARTICLE INFO

Article history:
Received 1 April 2013
Received in revised form 18 July 2013
Accepted 20 July 2013
Available online xxx

Keywords:
Solid acid catalyst
Esterification
Inorganic ion exchanger
Cerium phosphate
Thorium phosphate
Tetravalent metal acid salt

ABSTRACT

In the present endeavour, amorphous cerium phosphate (CP) and thorium phosphate (TP) have been synthesized by sol–gel method and also under microwave irradiation to yield CP_M and TP_M. CP, TP, CP_M and TP_M have been characterized for elemental analysis (ICP-AES), spectral analysis (FTIR), thermal analysis (TGA), X-ray diffraction studies, SEM, EDX, surface area (BET) and surface acidity (NH_3-TPD). The potential use of these materials as solid acid catalysts has been explored by studying esterification as a model reaction. Monoesters such as ethyl acetate (EA), propyl acetate (PA), butyl acetate (BA), benzyl acetate (BzAc) and diesters such as diethyl malonate (DEM), diethyl succinate (DES), dibutyl phthalate (DBP), dioctyl phthalate (DOP) have been synthesized. Esterification conditions have been optimized by varying several parameters such as reaction time, catalyst amount and mole ratio of reagents. The catalytic activity has been compared and correlated with reference to surface acidity of the catalysts. It is found that catalytic activity of $CP_M > CP > TP_M > TP$. The regenerated catalysts could be reused upto two catalytic runs without significant loss in % yields of esters formed. The highlighting feature of the present work is the catalysts CP_M and TP_M that are synthesized in a much shorter reaction time with higher surface acidity giving good % yield of esters.

1. Introduction

Esterification is an industrially important reaction for synthesis of plasticizers, perfumes, fragrance in cosmetics, flavours in food, diluents in paints and coatings and intermediates in drugs, dye stuffs and fine chemicals [1,2]. The conventional catalyst used in esterification reactions is sulphuric acid, methanesulfonic acid or *p*-toluenesulfonic acid that are cited as potential environmentally hazardous chemicals, that pose problems such as difficulty in handling, causing an acidic waste water, difficulty of catalyst recovery, etc. [3–5]. In view of the deficiencies encountered, there is a global effort to replace the conventional homogeneous liquid acids by heterogeneous solid acids. The use of solid acids eliminates the corrosive action of liquid acids. Being heterogeneous in nature, separation from reaction mixture is easy and the catalyst can be regenerated and reused.

Several materials such as sulphated zirconia [6,7], zeolites [5,8,9], sulfonic acid based resins [10–13], heteropoly acids [6], MCM-41 based materials [14–17], organophosphonic acid-functionalized silica [18], metal oxides [19], pillared clay [19] etc. have been reported as solid acid catalysts for esterification reactions. Though, sulphated zirconia is a good esterification catalyst, it gets easily deactivated by losing the sulphate ions, thereby restricting recycling of the catalyst. The main disadvantage of heteropoly acids is low efficiency due to low surface area, rapid deactivation and poor stability and when supported on carbon the activity decreases [20]. Sulfonic acid based resin (Nafion-H) has also been found to be unsatisfactory due to its low operating temperature.

Tetravalent metal acid (TMA) salts are inorganic cation exchangers possessing the general formula $M(IV)(HXO_4)_2 \cdot nH_2O$ [M(IV) = Zr, Ti, Sn, etc. and X = P, W, Mo, As, Sb, etc.] where, H^+ of the structural hydroxyl groups are responsible for cation exchange, due to which TMA salts indicate good potential for application as solid acid catalysts, the acidic sites being Brønsted acid sites in nature.

From our laboratory, use of TMA salts as solid acid catalysts has been explored for esterification [21–28]. Much of the works done by us are on phosphates of Zr, Ti and Sn. However, not much work has been explored on phosphates of Ce and Th.

In the present endeavour, amorphous cerium phosphate (CP) and thorium phosphate (TP) have been synthesized by sol–gel method. Further, CP and TP have also been synthesized under microwave irradiation to yield CP_M and TP_M. The materials have been characterized for elemental analysis (ICP-AES), spectral analysis (FTIR), thermal analysis (TGA), X-ray diffraction studies, SEM, EDX, BET surface area and surface acidity (NH_3-TPD). Chemical

* Corresponding author. Tel.: +91 265 2434188x415; fax: +91 265 2423898.
E-mail addresses: juvenile34@gmail.com (T. Parangi), uvcres@gmail.com, uvc50@yahoo.com (U. Chudasama).

0926-860X/$ – see front matter © 2013 Elsevier B.V. All rights reserved.
http://dx.doi.org/10.1016/j.apcata.2013.07.043

stability of the materials in various acids, bases and organic solvent media has been studied and their potential use as solid acid catalysts has been explored and compared by studying esterification as a model reaction wherein mono esters such as ethyl acetate (EA), propyl acetate (PA), butyl acetate (BA), benzyl acetate (BzAc) and diesters such as diethyl malonate (DEM), diethyl succinate (DES), dibutyl phthalate (DBP), dioctyl phthalate (DOP) have been synthesized optimizing several parameters such as reaction time, catalyst amount and mole ratio of reagents.

2. Experimental

2.1. Chemicals

Thorium nitrate ($Th(NO_3)_4{\cdot}5H_2O$), ceric sulphate ($Ce(SO_4)_2{\cdot}4H_2O$) and sodium dihydrogen phosphate ($NaH_2PO_4{\cdot}2H_2O$) were procured from Loba Chemicals, Mumbai, while ethanol, 1-propanaol, 1-butanol, benzyl alcohol, octanol (2-ethyl 1-hexanol), acetic acid, phthalic anhydride, malonic acid, succinic acid, cyclohexane, xylene and toluene were obtained from Across Organics. Double-distilled water was used for all the studies.

2.2. Catalyst synthesis

CP and TP were synthesized by sol–gel method varying several parameters such as mole ratio of reactants, mode of mixing (metal salt solution to anion salt solution or vice versa), temperature, pH and rate of mixing. The main objective was to obtain a material with high cation exchange capacity (CEC) values which reflect on the protonating ability and thus the acidity in the materials. The term CEC is intended to describe the total available exchange capacity of an ion exchanger, as described by the number of functional groups on it. This value is constant for a given ion exchange material and is expressed in milli equivalents per gram, based on dry weight of material in given form (such as H^+). The Na^+ ion exchange capacity (CEC) of materials was determined by the column method [29] by optimizing volume and concentration of sodium acetate solution.

Several sets of materials were prepared varying conditions in each case using CEC as the indicative tool. (ESM – Tables 1 and 2 describe optimization of reaction parameters for synthesis of CP and TP respectively)

2.2.1. Synthesis of CP at optimized condition

A solution containing $Ce(SO_4)_2{\cdot}4H_2O$ [0.1 M, 50 mL in 10% (w/v) H_2SO_4] was prepared, to which $NaH_2PO_4{\cdot}2H_2O$ [0.3 M, 50 mL] was added dropwise (flow rate 1 mL min^{-1}) with continuous stirring for an hour at room temperature, when gelatinous precipitates were obtained (Step-I). The resulting gelatinous precipitate was allowed to stand for 3 h at room temperature, then filtered, washed with conductivity water to remove adhering ions and dried at room temperature (Step-II).

2.2.2. Synthesis of TP at optimized condition

An aqueous solution of $Th(NO_3)_4{\cdot}5H_2O$[0.1 M, 50 mL] was added drop wise (flow rate 1 mL min^{-1}) to an aqueous solution of $NaH_2PO_4{\cdot}2H_2O$ [0.2 M, 100 mL] with continuous stirring for an hour at room temperature, when gelatinous precipitates were obtained (Step-I). The resulting gelatinous precipitate was allowed to stand for 5 h at room temperature, then filtered, washed with double distilled water to remove adhering ions and dried at room temperature (Step-II).

2.2.3. Synthesis of CP and TP under microwave irradiation

Gelatinous precipitate obtained in step-I was subjected to microwave irradiation for optimum time and temperature (ESM – Table 3), then filtered, washed with double distilled water to remove adhering ions and dried at room temperature (Step-II).

2.2.4. Acid treatment

The above dried materials obtained in step-II were broken down to the desired particle size [30–60 mesh (ASTM)] by grinding and sieving. 5 g of this material was treated with 50 mL of 1 M HNO_3 for 30 min with occasional shaking. The material was then separated from acid by decantation and treated with double distilled water to remove adhering acid. This process (acid treatment) was repeated at least 5 times for both the materials. After final washing, the material was dried at room temperature.

2.3. Characterization

2.3.1. Chemical stability

The chemical stability of the catalysts in various acids (HCl, H_2SO_4, HNO_3), bases (NaOH and KOH) and organic solvent media (ethanol, propanol, butanol, benzyl alcohol, cyclohexane, toluene, xylene and acetic acid) was examined by taking 500 mg of each of the synthesized catalyst in 50 mL of the particular medium and allowed to stand for 24 h. The change in colour, weight and nature was observed.

2.3.2. Instrumentation

All synthesized materials were subjected to instrumental methods of analysis/characterization. CP and TP were analyzed for cerium, thorium and phosphorus by ICP-AES. FTIR spectra were recorded using KBr pellet on Shimadzu (Model 8400S). Thermal analysis (TGA) was carried out on a Shimadzu (Model TGA 50) thermal analyzer at a heating rate of 10 °C min^{-1}. X-ray diffractogram (2θ angles = 10°–90°, scanning time = 2°/min and sample run time = 8 min) was obtained on X-ray diffractometer (Brucker AXS D8) with Cu Kα radiation with nickel filter. SEM and EDX of the sample were scanned on Jeol JSM-5610-SLV scanning electron microscope. Surface area was determined by BET multipoint method using a Micromeretics Gemini 2220 series surface area analyzer. Surface acidity was determined on Chemisorb 2720, by a temperature programmed desorption (TPD) of ammonia. All materials were preheated at 150 °C, 200 °C and 700 °C temperatures and thereafter ammonia was chemisorbed at 120 °C and then desorption was carried out upto 700 °C at a heating rate of 10 °C min^{-1} in all cases. The products were analyzed by Ceres 800 Plus gas chromatograph (GC) using flame ionization detector.

2.4. Synthesis of esters

2.4.1. Synthesis of monoesters (EA, PA, BA and BzAc)

In a typical reaction, a 100 mL round bottomed flask equipped with a Dean and Stark apparatus, attached to a reflux condenser was used and charged with acetic acid (0.05–0.10 M), alcohol (0.05–0.10 M), catalyst (0.10–0.20 g) and a suitable solvent (15 mL). The reactions were carried out varying several parameters such as reaction time, catalyst amount, mole ratio of reactants and these parameters optimized. The temperature parameter has not been varied as the reaction temperature is sensitive to boiling points of reactants [ethanol (78 °C), 1-propanol (97 °C), 1-butanol (118 °C) and benzyl alcohol (205 °C)] as well as solvents used as azeotrope. Cyclohexane (80 °C) was used as a solvent for the synthesis of ethyl acetate and toluene (110 °C) for propyl acetate, butyl acetate and benzyl acetate. After completion of reaction, catalyst was separated by decantation and reaction mixture was distilled to obtain the product.

Table 1
Data of elemental analysis (ICP-AES) and EDX analysis.

Materials	ICP-AES analysis (%)		EDX analysis (atomic %)	
	M(IV)	P	M(IV)	P
CP (fresh)	33.15	15.11	34.95	65.05
CP (spent)	–	–	38.24	61.76
TP (fresh)	35.10	9.40	35.75	64.25
TP (spent)	–	–	37.52	62.48

For ICP-AES, detection limits = 0.10 ppm.

2.4.2. Synthesis of diesters (DEM, DES, DBP and DOP)

The diesters were synthesized in two steps. The mono ester was prepared in first step by taking equimolar proportion (0.025 mol) of acid and alcohol (malonic acid and ethanol for DEM, succinic acid and ethanol for DES, phthalic anhydride and 1-butanol for DBP, phthalic anhydride and 2-ethyl 1-hexanol for DOP) were taken in a round bottomed flask and the reaction mixture stirred at ~80 °C for DEM and DES, ~110 °C for DBP and ~140 °C for DOP for about 10–15 min in absence of any catalyst and solvent. The dicarboxylic acid and anhydride get completely converted to the monoester, so that the acid concentration at this stage is taken as the initial concentration. The obtained product (monoester) was then subjected to esterification reaction by addition of a second mole (0.025 mol) of respective alcohol, catalyst (0.10–0.20 g) and 15 mL solvent (toluene (110 °C) for DEM, DES and DBP, and xylene (140 °C) for DOP). The reactions were carried out optimizing several parameters such as reaction time, catalyst amount and mole ratio of reactants. The temperature parameter has not been varied as discussed in synthesis of monoesters. In all cases the round bottomed flask was fitted with Dean and Stark apparatus, with a condenser to remove water formed during the reaction. After completion of reaction, catalyst was separated by decantation and reaction mixture was distilled to obtain the product.

2.4.3. Calculation of % yield of esters

The yields of the mono and diesters formed were determined by titrating the reaction mixture with 0.1 M alcoholic KOH solution. The yields of the esters were calculated using the formula, % yield = $[(A - B)/A] \times M \times 100$, where A and B are acid values of the sample withdrawn before and after reaction and M is mole ratio of acid: alcohol. The yield of ester formed was also determined using GC. (Oven temperature: 150 °C, injector temperature: 200 °C, detector temperature: 220 °C and split ratio is 1:2).

2.5. Regeneration of catalyst

After separation of catalyst in reaction mixture by decantation, it is first refluxed in ethanol for 30 min to solubilize and remove adsorbed molecules, followed by drying at room temperature (~30 °C). This material was used as recycled catalyst. This regeneration procedure was followed in subsequent recycle reaction.

3. Results and discussion

3.1. Catalyst characterization

CP and TP were obtained as yellow and off white hard granules respectively. Elemental analysis performed by ICP-AES, for both CP and TP, show ratio of M:P to be 1:2, which is well supported by EDX analysis (ESM – Figs. 1 and 2) (Table 1).

Thermal behaviour of several TMA salts has been investigated and generally examined for loss of moisture ~80 °C, loss of external water molecules ~100–180 °C and for condensation of the structural hydroxyl groups ~180–500 °C and above [30]. TGA of CP and TP presented in Fig. 1 reveals that CP exhibits the first weight loss ~13% and the second weight loss ~8% while TP exhibits the first weight loss ~11% and the second weight loss ~9%. The first weight loss (up to ~120 °C) is attributed to loss of moisture/hydrated water while the second weight loss in the range 120–500 °C is attributed to condensation of structural hydroxyl groups.

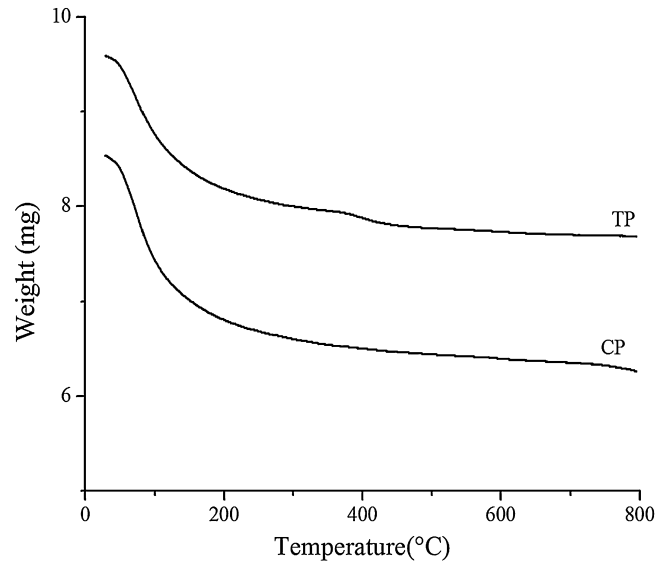

Fig. 1. TGA of CP and TP.

Based on the elemental analysis (ICP-AES) and thermal analysis (TGA) data, CP and TP, are formulated as $Ce(HPO_4)_2{\cdot}4.9H_2O$ and $Th(HPO_4)_2{\cdot}5.8H_2O$. The number of water molecules in each case is calculated using Alberti and Torracca (1968) formula [31]. (Table 1)

The FTIR spectra (Fig. 2) of CP and TP exhibits a broad band in the region ~3400 cm^{-1} which is attributed to asymmetric and symmetric —OH stretching vibration due to residual water and presence of structural hydroxyl groups, H^+ of the —OH being Brønsted acid sites in nature. These bands indicate the presence of structural hydroxyl groups/catalytic sites in the materials. These sites are also referred to as defective P—OH groups [29,32]. A sharp medium band at ~1630 cm^{-1} is attributed to aquo H—O—H bending [33]. The band at ~1050 cm^{-1} is attributed to P=O stretching while the bands at ~620 cm^{-1} and ~500 cm^{-1} is attributed to Metal–O stretching [34].

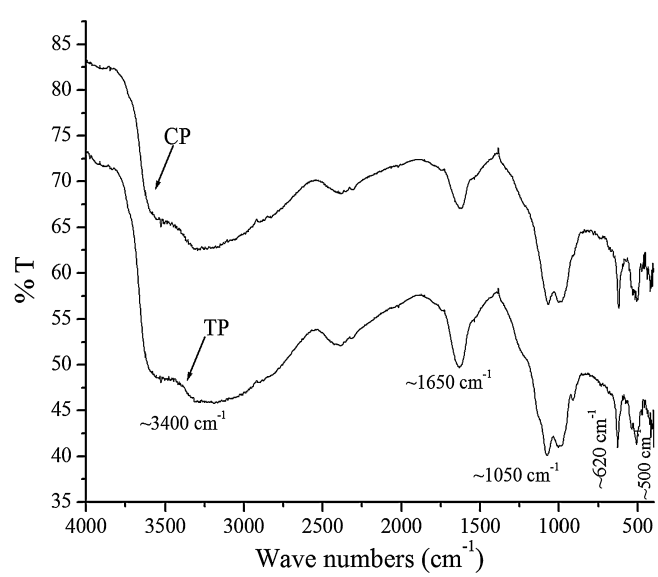

Fig. 2. FTIR spectra of CP and TP.

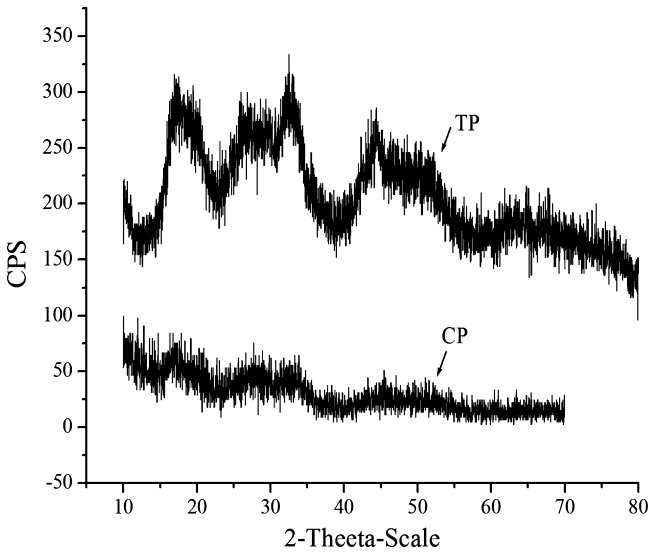

Fig. 3. XRD of CP and TP.

The Na^+ CEC values/protonating ability were observed to be 2.48, 1.45, 2.90 and 2.41 for CP, TP, CP_M and TP_M respectively.

CEC values decrease on calcination, at higher temperatures due to loss of hydrated water and condensation of structural hydroxyl groups (ESM – Table 4). This fact is also evident from the FTIR spectra of the calcined samples (ESM – Fig. 3). It is seen that the intensities of the peaks at $-3400\,cm^{-1}$ and $-1638\,cm^{-1}$ corresponding to the —OH group diminish as temperature increases [35].

CP and TP are found to be stable in acid media, maximum tolerable limits being (1 N H_2SO_4, 2 N HNO_3, 5 N HCl) and also stable in organic solvent media. They are however not so stable in base medium, maximum tolerable limits being (0.5 N NaOH and KOH).

The absence of sharp peaks in the X-ray diffractograms of CP and TP (Fig. 3), and CP_M and TP_M (Fig. 4) indicates amorphous nature of all the materials. SEM images of CP, TP, CP_M and TP_M (ESM – Figs. 4–7) show irregular morphology.

Surface area measurement has been performed by adsorption–desorption isotherm of N_2 which was recorded, at −196 °C after degassing the sample at 300 °C for 4 h. Surface area values of CP, TP, CP_M and TP_M are 20.71, 1.94, 1.40 and 1.22 in m^2/g respectively.

Table 2
Surface acidity and CEC values at 150, 200 and 700 °C preheating temperatures.

Samples	Calcination/preheating temperature (°C)	Total acidity (NH_3-TPD method) (mmol g^{-1})	CEC (meq g^{-1})
CP	150	0.95	2.04
	200	0.89	1.89
	700	–	–
CP_M	150	1.26	2.20
	200	0.45	2.00
	700	–	–
TP	150	0.78	0.70
	200	0.50	0.46
	700	–	–
TP_M	150	0.80	0.92
	200	0.76	0.70
	700	–	–

Surface acidity for all the materials was determined by NH_3-TPD at 150 °C, 200 °C and 700 °C preheating temperatures (Table 2 and Figs. 5–8). As already discussed earlier in the text, acidity in CP and TP is due to the presence of structural hydroxyl protons, H^+ of the —OH being the Brønsted acid sites. Further, surface acidity values of CP and TP depend on the size and charge of the cation. Smaller size and higher charge of the cation indicate greater tendency to release a proton, i.e. H^+ of the —OH groups present in CP and TP. In the present study Ce^{4+} and Th^{4+}, both ions being tetravalent as well as bearing common anion PO_4^{3-}, size of the cation Ce^{4+} (1.05 Å) and Th^{4+} (1.08 Å) seem to play a dominant role. Thus the acidity in the materials follows the order CP > TP and $CP_M > TP_M$. Decrease in surface acidity for CP and TP with increasing preheating temperatures could be attributed to condensation of structural hydroxyl groups as discussed above in thermal behaviour of these materials. This is well supported by CEC values, which reflect on the protonating ability and thus the acidity of the materials [36]. CEC values also decrease with increasing calcination/preheating temperature have already been discussed in FTIR spectra of calcined samples.

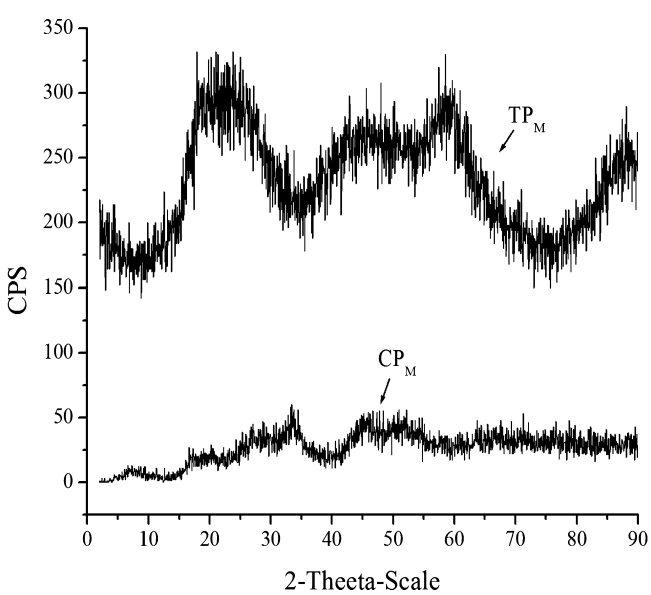

Fig. 4. XRD of CP_M and TP_M.

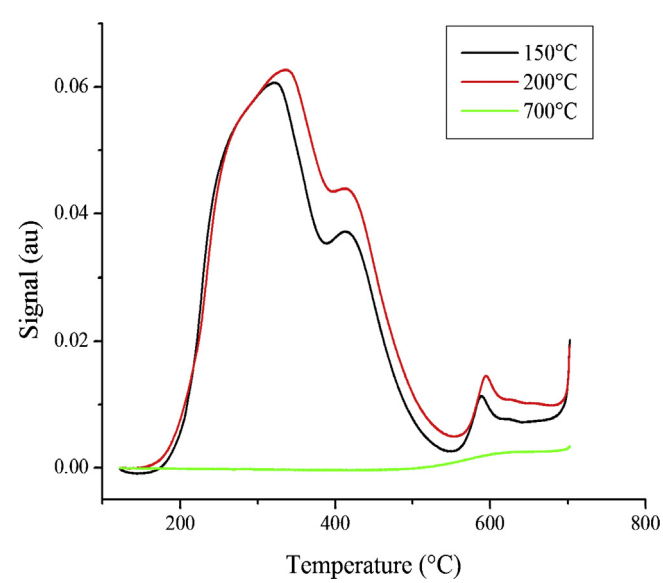

Fig. 5. NH_3-TPD patterns for CP at 150, 200 and 700 °C preheating temperatures.

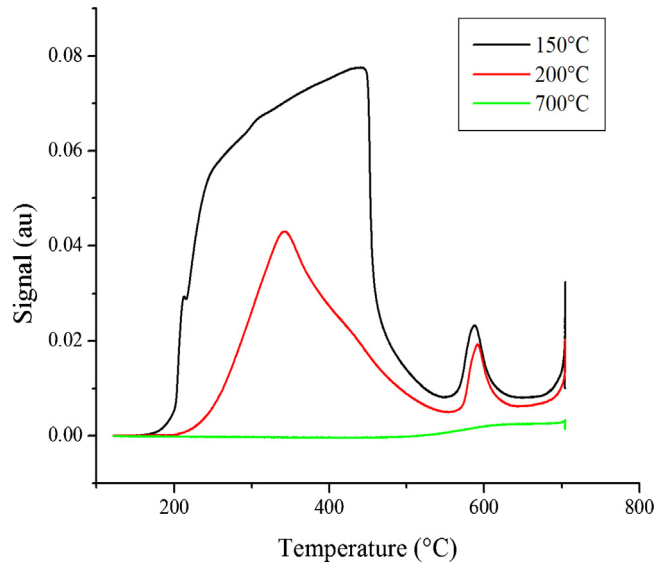

Fig. 6. NH_3-TPD patterns of CP_M at 150, 200 and 700 °C preheating temperatures.

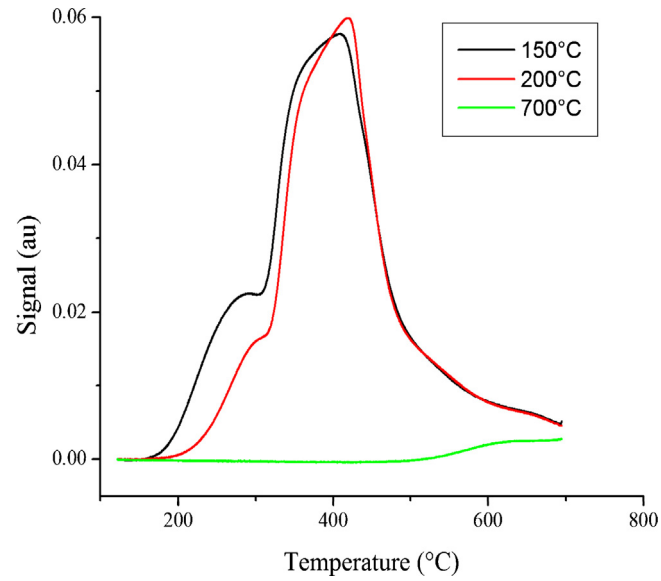

Fig. 8. NH_3-TPD patterns of TP_M at 150, 200 and 700 °C preheating temperatures.

3.2. Synthesis of monoesters

Monoester synthesis EA, PA, BA and BzAc is as presented in Scheme 1. Equilibrium constants of the esterification reactions are low. As in any equilibrium reaction, the reaction may be driven to the product side by controlling the concentration of one of the reactants (Le Chatlier's Principle). In order to obtain higher yield of esters, Le Chatlier's Principle has been followed. Solvents cyclohexane and toluene have been employed to remove the water formed during the reaction as a binary azeotrope. Monoesters EA, PA, BA and BzAc were synthesized as described in Section 2.

Firstly, reaction conditions were optimized using CP as solid acid catalyst for EA synthesis by varying parameters such as reaction time, catalyst amount and initial mole ratio of the reactants (Table 3 and a graphical presentation ESM – Figs. 8–10).

It is observed that as reaction time increases, percentage yield increases. However, there is not much gain in product after 8 h. With increasing amount of the catalyst, the % yield increases which is probably due to proportional increase in the number of active sites. The influence of reactant mole ratio was studied by increasing mole ration from 1:1.5 to 1.5:1 (acid:alcohol). According to Le Chatlier's Principle ester yields can be increased by increasing the concentration of either alcohol or acid. As observed from Table 3, the % yield of ester increases with increase in mole ratio of acid while decreases with increasing mole ratio of alcohol. This may be attributed to preferential adsorption of alcohol on the catalyst which results in blocking of active sites. For economic reasons also, the reactant that is usually less expensive of the two is taken in excess. In the present study, acids were used in excess.

Further, at optimized conditions synthesis of EA, PA, BA and BzAc was performed using CP, CP_M, TP and TP_M as solid acid catalysts, (mole ratio of reactants = 1:1.5 (alcohol:acid); catalyst amount = 0.15 g; reaction time = 8 h) (Table 4).

Esterification of monoesters EA, PA and BA has been reported [37] in absence of catalyst and exhibits poor yields. Therefore catalyst is a must for these reactions. In case of BzAc however, it is observed that with an excess of acetic acid and in the absence of any catalyst the yield is as high as 90.6% which is attributed to auto catalysis. In another report [38] high yields of BzAc were obtained with small amount of the catalyst but the reaction time was relatively high. Higher yields in case of benzyl acetate could be attributed to an enhanced nucleophilicity due to presence of aromatic ring in benzyl alcohol. The order of % yield of ester formed is BzAc > BA > PA > EA could be explained due to increase in carbon chain length in the respective alcohols used for ester formation. When the boiling point of the alcohol is less than the temperature of the reaction, most of the alcohol will end up in the vapor phase and not be available in the liquid phase. This is the reason why the heavier alcohols react more than the lighter ones. Turn over number (TON) reflects the effectiveness of a catalyst and this also follows the order of ester formation.

The order of monoesters formed with reference to performance of catalyst is CP exhibits higher yields in all cases compared to TP

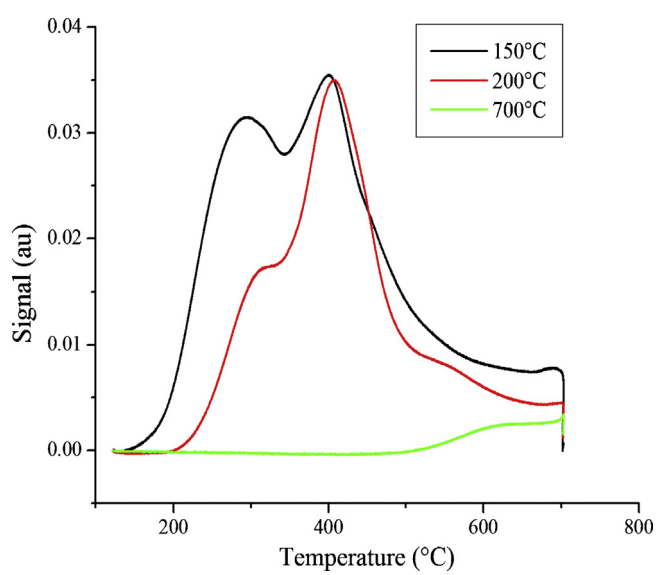

Fig. 7. NH_3-TPD pattern for TP at 150, 200 and 700 °C preheating temperatures.

$$\underset{\text{Acetic Acid}}{CH_3COOH} + \underset{\text{Alcohol}}{R\text{-}OH} \underset{\Delta}{\overset{H^+/\text{Catalyst}}{\rightleftharpoons}} \underset{\text{Monoester}}{CH_3COOR} + H_2O$$

R = $-C_2H_5$ for ethyl acetate, $-C_3H_7$ for propyl acetate, $-C_4H_9$ for butyl acetate and $-CH_2$-Ph for benzyl acetate

Scheme 1. Synthesis of monoesters (EA, PA, BA and BzAc).

Table 3
Optimization of reaction conditions for monoesters using CP.

Sr. no.	Reactants with their mole ratio	Product	Catalyst amount (g)	Time (h)	Temp. (°C)	% Yield CP
(A)	Time variation					
1	E + AA (1:1)	EA	0.05	1	80	12.2
2	E + AA (1:1)	EA	0.05	2	80	23.1
3	E + AA (1:1)	EA	0.05	3	80	25.2
4	E + AA (1:1)	EA	0.05	4	80	33.5
5	E + AA (1:1)	EA	0.05	5	80	39.6
6	E + AA (1:1)	EA	0.05	6	80	44.4
7	E + AA (1:1)	EA	0.05	7	80	48.2
8	E + AA (1:1)	EA	0.05	8	80	52.3
9	E + AA (1:1)	EA	0.05	9	80	53.1
10	E + AA (1:1)	EA	0.05	10	80	53.1
(B)	Catalyst amount variation					
12	E + AA (1:1)	EA	0.10	8	80	57.1
13	E + AA (1:1)	EA	0.15	8	80	59.1
14	E + AA (1:1)	EA	0.20	8	80	59.3
(C)	Mole ratio variation					
15	E + AA (1.5:1)	EA	0.15	8	80	41.8
16	**E + AA (1:1.5)**	**EA**	**0.15**	**8**	**80**	**74.4**

E = ethanol; AA = acetic acid.

while CP_M exhibits higher yields than TP_M could be attributed to higher surface acidity (Table 4, Figs. 9 and 10).

3.3. Synthesis of diesters

Reactions involved for diester synthesis are presented in Scheme 2 (DES and DEM) and Scheme 3 (DOP and DBP). The first step is so rapid that it can be carried out in the absence of catalyst. However, esterification of the second carboxylic group (second step) is very slow and needs to be facilitated by acid catalyst and the resulting water must be removed from the reaction mixture [39]. Firstly, reaction conditions were optimized using CP as solid acid catalyst for DEM synthesis by varying parameters such as reaction time, catalyst amount and initial mole ratio of the reactant. The optimized reaction conditions for diesters have been presented in Table 5 and a graphical presentation ESM – Figs. 11–13).

At optimized conditions synthesis of DEM, DES, DBP and DOP was performed using CP, TP, CP_M and TP_M (mole ratio of reactant = 1:2.5 (diacid/anhydride: alcohol), catalyst amount = 0.15 g and reaction time = 10 h) (Table 6).

In the present work, the % yields of DOP are higher than DBP which could be attributed to higher boiling point of 2-ethyl 1-hexanol compared to 1-butanol. Further, high yield in case DEM and DES compared to DOP and DBP is probably due to less steric hindrance felt by incoming ethanol from monoethyl malonate formed in the first step.

DEM synthesis has been reported by Prakash and co-workers using montmorillonite clay, but the yield is low (41%) and relatively high amount of catalyst (0.5 g) was used [38]. DOP formation has been catalyzed by zeolites [9], metallic oxides [40], solid super acids [13,41,42] and heteropoly acids [39,42]. Suter [43] has reported a non-catalytic process for the manufacture of DOP, at very high temperatures, at which autocatalysis occurs. In another report, DEM has been synthesized by Song and Jiang using the reaction of CO with $ClCH_2COOC_2H_5$. In this case high yield was observed but the reaction was carried out at high pressure [44]. DES synthesis and kinetics have been reported by Kolah et al. using amberlyst catalyst with good yields [45]. When homogeneous liquid acids are used as catalysts for synthesis of diesters, the result is a product that is coloured and of a poor quality. In the present work though

Table 4
% yields of monoesters using CP, TP, CP_M and TP_M at optimized condition.

Sr. no	Reactants	Product	CP		TP	
			% Yield	[a]TON	% Yield	[a]TON
1	E + AA	EA	74.4	33.7	70.7	32.0
2	P + AA	PA	75.6	37.8	72.1	36.0
3	B + AA	BA	78.5	42.9	74.8	40.9
4	BzA + AA	BzAc	81.3	53.6	78.0	51.4
(A)	Microwave irradiated catalysts		CP_M		TP_M	
			% Yield	[a]TON	% Yield	[a]TON
5	E + AA	EA	77.8	35.2	75.0	33.9
6	P + AA	PA	80.7	40.3	77.5	38.7
7	P + AA	BA	82.2	44.9	80.0	43.7
8	Bz + AA	BzAc	89.1	58.8	85.4	56.3

AA = acetic acid; E = ethanol; P = 1-propanol; B = 1-butanol; BzA = benzyl alcohol. Mole ratio of the reactants = 1:1.5 (alcohol:acid); reaction time = 8 h; catalyst amount = 0.15 g; reaction temperature 80 °C for EA; and 115 °C for PA, BA and BzAc.
[a] TON = turn over number, gram of ester formed per gram of catalyst.

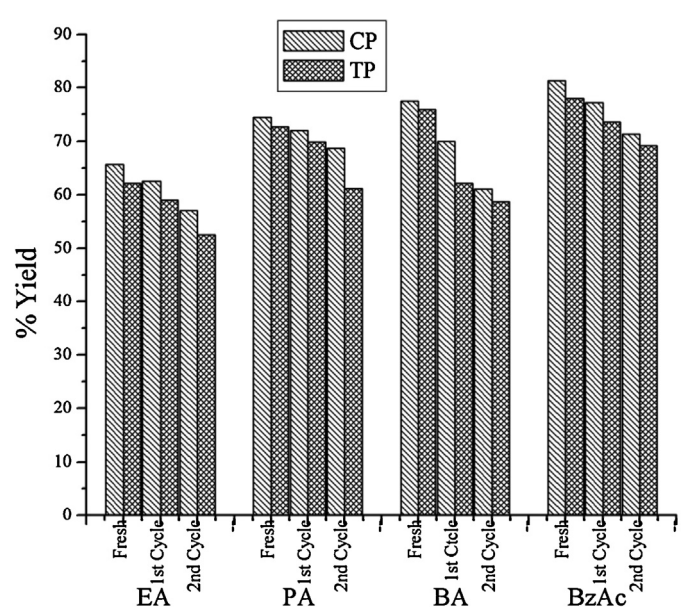

Fig. 9. Comparative catalytic performance of CP and TP for synthesis of monoesters.

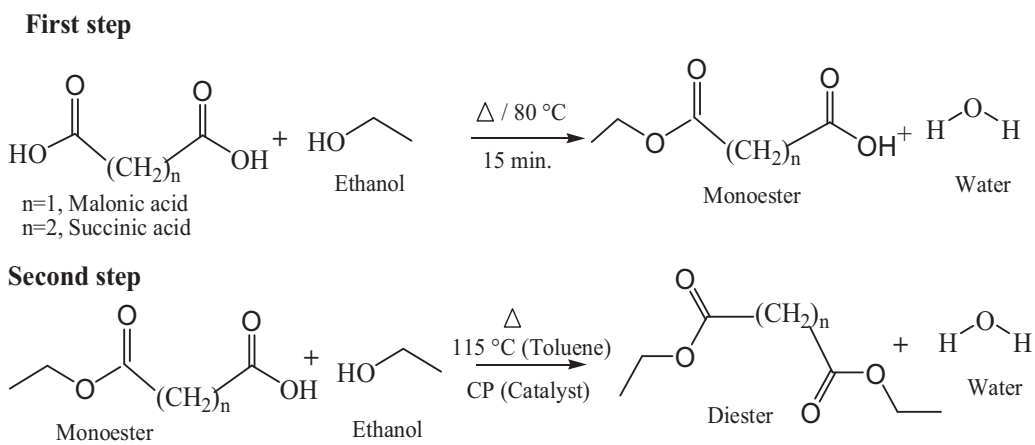

Scheme 2. Synthesis of DES and DEM.

the yields of diesters obtained are low, the advantage is that the diester is the single product and colourless.

The order of diesters formed with reference to performance of catalyst is CP that exhibits higher yields in all cases compared to TP while CP_M exhibits higher yields than TP_M (Table 6, Figs. 11 and 12).

During the course of the reaction, many a time the catalyst colour changes. This is probably due to the fact that reactant molecules come onto surface of catalyst and enters into reaction to give the product while a few of them get adsorbed on surface. In each subsequent run, the acid sites in catalysts were regenerated as described in Section 2. Almost 100% catalyst recovery is observed. After regeneration and reuse, decrease in yields are observed which is probably due to the deactivation of catalysts because of substrate molecules getting adsorbed on surface or also entering interstices of the catalyst material [36]. Reusability of CP and TP was tested by conducting two runs (Table 7, Figs. 9 and 11).

It is observed that there is only a marginal decrease in yields upto two catalytic runs. In recycled catalyst the yield decreased by 4–7% (Table 7). Further, EDX of spent CP (ESM – Fig. 14) (after 1st catalytic run) shows atomic % of Ce and P to be 38.24% and 61.76% respectively, and EDX of spent TP (ESM – Fig. 15) (after 1st catalytic run) shows atomic % of Th and P to be 37.52% and 62.48% respectively which shows decrease in atomic % of P compared to EDX of fresh CP (ESM – Fig. 1) (atomic % of Ce = 34.95 and atomic % of P = 65.05) and EDX of fresh TP (ESM – Fig. 2) (atomic % of Th = 35.75 and atomic % of P = 64.25). Decrease in yield of monoesters and diesters may be due to the leaching of P in catalysts.

Comparing catalyst efficiency/performance of CP and TP with M(IV) phosphates of the class of TMA salts (M(IV) = Zr, Ti and Sn) [3,27], the % yields are observed to be ranging from low to marginal to comparitive yields (ESM – Table 5).

3.4. Reaction mechanism in solid acid catalyzed esterification reaction

The mechanism of esterification can be different for the various solid acid catalysts and also depends on gas- or liquid-phase operation as well as the substrate. Chu et al. [46] claim that the esterification mechanism of acetic acid with butanol over carbon-supported HPA catalysts proceeds via a protonated alcohol intermediate, but most authors [47–49] proposed a protonated carboxylic acid as the reaction intermediate. The two possible

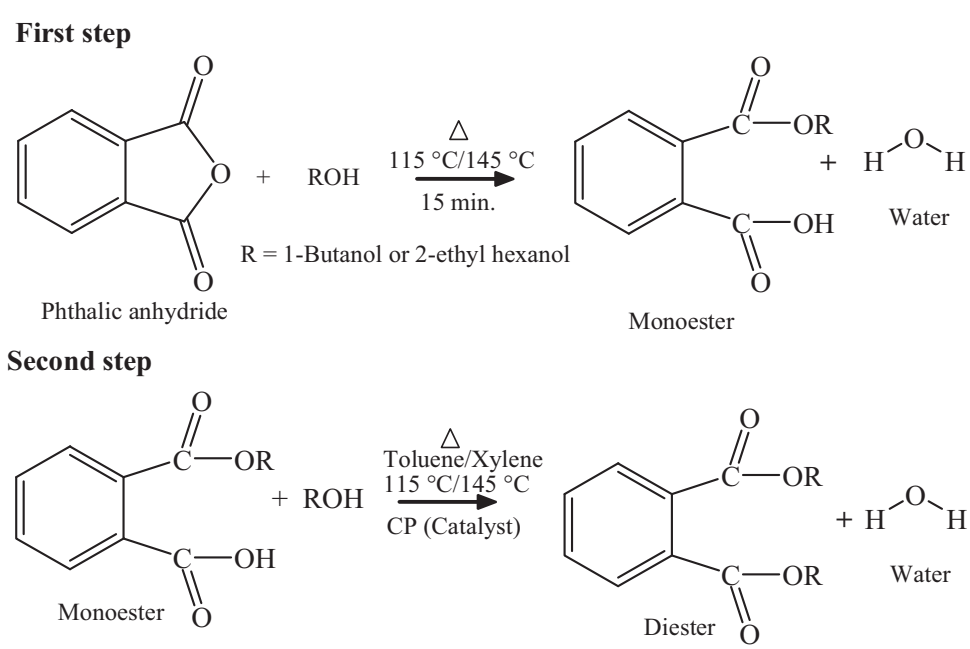

Scheme 3. Synthesis of DBP and DOP.

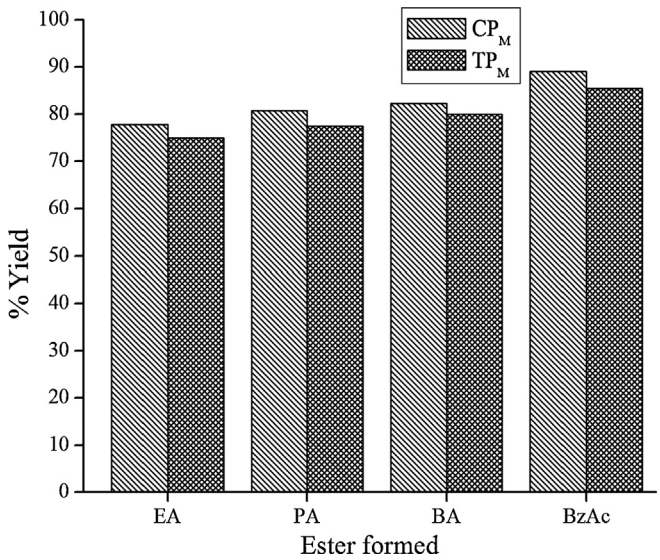

Fig. 10. Comparative catalytic performance of CP_M and TP_M for synthesis of monoesters.

Table 5
Optimization of reaction conditions for diesters using CP.

Sr. no.	Reactants with their mole ratio	Product	Catalyst amount (g)	Time (h)	Temp. (°C)	% Yield CP
(A)	Time variation					
1	E + MA (2:1)	DEM	0.05	1	115	56.2
2	E + MA (2:1)	DEM	0.05	2	115	57.1
3	E + MA (2:1)	DEM	0.05	3	115	61.8
4	E + MA (2:1)	DEM	0.05	4	115	65.7
5	E + MA (2:1)	DEM	0.05	5	115	69.4
6	E + MA (2:1)	DEM	0.05	6	115	72.3
7	E + MA (2:1)	DEM	0.05	7	115	74.1
8	E + MA (2:1)	DEM	0.05	8	115	75.6
9	E + MA (2:1)	DEM	0.05	9	115	75.8
10	E + MA (2:1)	DEM	0.05	10	115	75.9
11	E + MA (2:1)	DEM	0.05	11	115	76.0
12	E + MA (2:1)	DEM	0.05	12	115	76.0
(B)	Catalyst amount variation					
13	E + MA (2:1)	DEM	0.10	8	115	85.5
14	**E + MA (2:1)**	**DEM**	**0.15**	**8**	**115**	**91.5**
15	E + MA (2:1)	DEM	0.20	8	115	92.0
(D)	Mole ratio variation					
16	E + MA (2.2:1)	DEM	0.15	8	115	87.2
17	E + MA (2.4:1)	DEM	0.15	8	115	86.9

E = ethanol; MA = malonic acid. Bold values are for Optimized condition

intermediates, protonated ethanol and protonated acetic acid, are shown in Scheme 4.

The mechanism of diester formation over solid acid catalyst is similar to that of conventional mechanism involving the formation of protonated dicarboxylic acid, using proton donated by the catalyst, followed by nucleophilic attack of alcoholic group to yield the respective monoester. The second carboxylic group present in monoester gets further esterified by the same mechanism in a repeat reaction, which ultimately results in the diester formation [38].

Table 6
% yields of diesters using CP, TP, CP_M and TP_M at optimized condition.

Sr. no	Reactants	Product	CP		TP	
			% Yield	[a]TON	% Yield	[a]TON
1	E + MA	DEM	91.5	29.8	89.0	29.0
2	E + SA	DES	67.1	23.4	64.5	22.5
3	B + PhA	DBP	44.0	21.7	42.8	21.1
4	O + PhA	DOP	69.7	47.4	60.0	40.8
(A)	Microwave irradiated catalysts		CP_M		TP_M	
			% Yield	[a]TON	% Yield	[a]TON
5	E + MA	DEM	95.5	31.1	93.0	30.3
6	E + SA	DES	73.4	25.6	70.1	24.5
7	B + PhA	DBP	53.7	24.4	50.5	24.9
8	O + PhA	DOP	76.8	52.3	67.4	45.8

MA = malonic Acid; SA = succinic acid; PhA = phthalic anhydride.
Mole ratio of the reactants = 2:1 (alcohol:acid); reaction, time = 8 h. Catalyst amount = 0.15 g; reaction temperature 115 °C for DEM, DES and DBP, 140 °C for DOP.
[a] TON = turn over number, gram of ester formed per gram of catalyst.

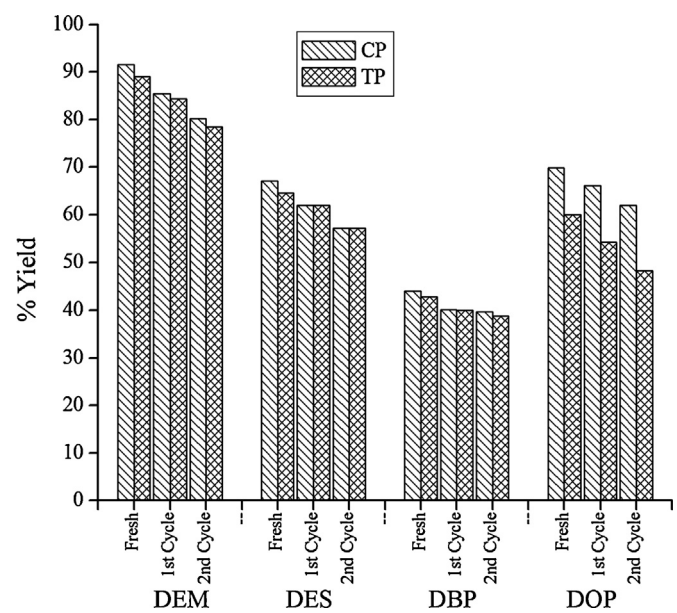

Fig. 11. Comparative catalytic performance of CP and TP for synthesis of diesters.

Table 7
Performance of recycled catalysts.

Recycled Catalyst	Catalytic Run	% Yield							
		EA	PA	BA	BzAc	DEM	DES	DBP	DOP
CP	First	72.1	88.2	72.0	73.2	85.4	61.9	40.1	66.1
	Second	67.8	87.3	66.1	67.8	80.2	57.1	39.6	62.0
TP	First	66.9	68.1	70.1	71.7	84.3	59.1	40.0	54.2
	Second	61.1	62.0	66.6	65.1	78.5	54.1	38.7	48.2

Reaction condition:
Monoesters: mole ratio of the reactants = 1:1.5 (alcohol:acid); reaction time = 8 h; catalyst amount = 0.15 g; reaction temperature 80 °C for EA; and 115 °C for PA, BA and BzAc; 115 °C for DEM, DES and DBP, 140 °C for DOP; diesters:mole ratio of the reactants = 2:1 (alcohol:acid); reaction time = 8 h. catalyst amount = 0.15 g; reaction temperature 115 °C for DEM, DES and DBP, 140 °C for DOP.

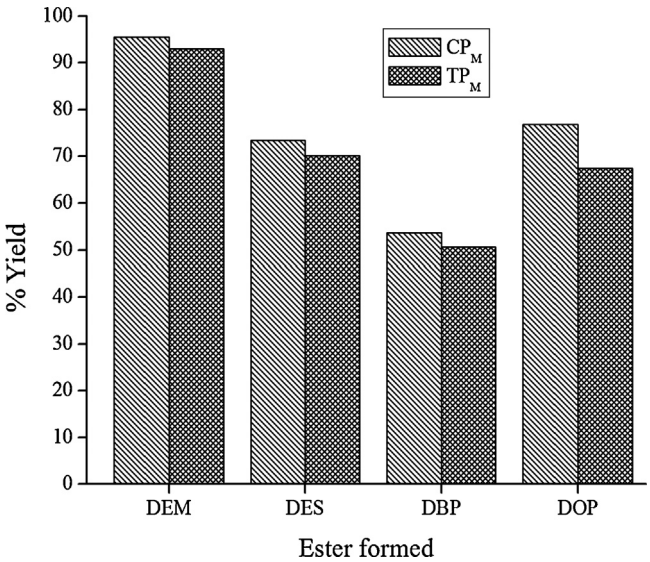

Fig. 12. Comparative catalytic performance of CP_M and TP_M for synthesis of diesters.

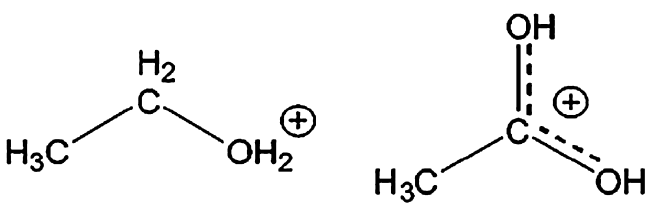

Scheme 4. Possible protonated intermediates in esterification reaction.

4. Conclusions

The study reveals good performance of all catalysts under study, with advantages of operational simplicity, mild reaction conditions as well as regeneration/reuse of catalysts. Further there is no catalyst or colour contamination in products formed, nor acid waste generation, a limitation in the conventional process. The highlighting feature of the present work is the synthesis of CP_M and TP_M under microwave irradiation in much shorter reaction time, with higher surface acidity including good % yields of esters formed.

Acknowledgement

The authors thank DAE-BRNS (BARC-Mumbai) for providing financial support and research fellowship to one of them (Tarun Parangi).

Appendix A. Supplementary data

Supplementary material related to this article can be found, in the online version, at http://dx.doi.org/10.1016/j.apcata.2013.07.043.

References

[1] J. Otera, Esterification, Wiley-VCH, Weinheim, Germany, 2003.
[2] F.A. Carey, Advanced Organic Chemistry, third ed., Plenum Press, New York, 1990.
[3] R. Thakkar, U. Chudasama, Green Chem. Lett. Rev. 2 (2) (2009) 61–69.
[4] G.D. Yadav, A.D. Murkute, Int. J. Chem. Reactor Eng. 1 (2003) 1–11.
[5] F.T. Sejidov, Y. Mansoori, N. Goodarzi, J. Mol. Catal. A: Chem. 240 (2005) 186–190.
[6] C.M. Garcia, S. Teixeira, L.L. Marciniuk, U. Schuchardt, Bioresour. Technol. 99 (2008) 6608–6613.
[7] J. Wang, H. Ma, B. Wang, J. Hazard. Mater. 157 (2008) 237–241.
[8] K.H. Chung, D.R. Chang, B.G. Park, Bioresour. Technol. 99 (2008) 7438–7443.
[9] Y. Ma, Q.L. Wang, H. Yan, X. Ji, Q. Qiu, Appl. Catal. A: Gen. 139 (1996) 51–57.
[10] A. Okudan, S. Baktir, A. Sagdic, Adv. Polym. Technol. (2012) 1–11.
[11] K.C.S. Figueiredo, V.M.M. Salim, C.P. Borges, Braz. J. Chem. Eng. 27 (4) (2011) 609–617.
[12] Y. Cheng, Y. Feng, Y. Ren, X. Liu, A. Gao, H. Benqiao, F. Yan, L. Jianxin, Bioresour. Technol. 113 (2012) 65–72.
[13] B. Zhang, J. Ren, X. Liu, Y. Guo, G. Lu, Y. Wang, Catal. Commun. 11 (2010) 629–632.
[14] T. Nishiguchi, Y. Ishii, S. Fujisaki, J. Chem. Soc. Perkin Trans. 1 (1999) 3023–3027.
[15] A.P. Toor, M. Sharma, G. Kumar, R.K. Wanchoo, Bull. Chem. React. Eng. Catal. 6 (1) (2011) 23–30.
[16] V. Brahamkhatri, A. Patel, Ind. Eng. Chem. Res. 50 (24) (2011) 13693–13702.
[17] L.A.S. Nascimento, L.M.Z. Tito, R.S. Angelica, C.F.F. Costa, J.R. Zamian, G.N.R. Filho, Appl. Catal. B: Environ. 101 (2011) 495–503.
[18] L.N. Helen, A.N. Zafiropoulos, A.F. Thomas, E.T. Samulski, W. Lin, J. Am. Oil Chem. Soc. 87 (2010) 445–452.
[19] P. Yin, L. Chen, Z. Wang, R. Qu, X. Liu, S. Ren, Bioresour. Technol. 110 (2012) 258–263.
[20] S. Shanmugam, B. Viswanathan, T.K. Varadarajan, J. Mol. Catal. A: Chem. 223 (2004) 143–147.
[21] P. Patel, A. Shivanekar, U. Chudasama, Indian J. Chem. 31A (1992) 803–805.
[22] A. Shivanekar, U. Chudasama, in: B. Vishwanathan, C.N. Pillai (Eds.), Recent Trends in Catalysis, Narosa Publishing House, New Delhi, 1990, pp. 489–497.
[23] A. Parikh, P. Patel, U. Chudasama, in: V. Murugesan, B. Arbindoo, M. Palanichamy (Eds.), Recent Trends in Catalysis, Narosa Publishing House, New Delhi, 1999, pp. 421–426.
[24] B. Beena, U. Chudasama, Indian J. Chem. Technol. 2 (1995) 339–340.
[25] S. Patel, U. Chudasama, Indian J. Chem. 41A (2002) 1864–1866.
[26] A. Parikh, U. Chudasama, Indian J. Chem. Technol. 10 (2003) 44–47.
[27] R. Joshi, H. Patel, U. Chudasama, Indian J. Chem. Technol. 15 (2008) 238–243.
[28] H. Patel, R. Joshi, U. Chudasama, Indian J. Chem. 47A (2008) 348–352.
[29] P. Patel, U. Chudasama, Indian J. Chem. 49A (2010) 1318–1324.
[30] R. Thakkar, U. Chudasama, Thermans (2008) 232–236.
[31] G. Alberti, E. Torracca, J. Inorg. Nucl. Chem. 30 (1968) 3075–3080.
[32] A. Bhaumik, S. Inagaki, J. Am. Chem. Soc. 123 (2001) 691–696.
[33] C.T. Seip, G.E. Granroth, M.W. Miesel, D.R. Talham, J. Am. Chem. Soc. 119 (1997) 7084–7094.
[34] A. Nilchi, M.M. Ghanadi, A. Khanchi, J. Radioanal. Nucl. Chem. 245 (2) (2000) 589–594.
[35] R. Thakkar, U. Chudasama, J. Hazard. Mater. 172 (2009) 129–137.
[36] S. Ghodke, U. Chudasama, Appl. Catal. A: Gen. 453 (2013) 219–226.
[37] K.R. Sharath, S. Vijayshree, N. Nagaraju, Indian J. Chem. Technol. 8 (2001) 362–367.
[38] C.R. Reddy, P. Iyengar, G. Nagendrappa, B.S. Jai Prakash, Catal. Lett. 101 (2005) 87–91.
[39] M. Arabi, J. Mol. Catal. A: Chem. 200 (2003) 105–110.
[40] M.M. Khodadadi, M.R. Gholami, Mater. Lett. 60 (2006) 715–719.
[41] L. GuanZhong, Appl. Catal. 133 (1995) 11–18.
[42] T.S. Thorat, V.M. Yadav, G.D. Yadav, Appl. Catal. 90 (1992) 73–76.
[43] H. Suter, Chem. Eng. Technol. 41 (17) (1969) 971–974.
[44] W.H. Song, X.Z. Jiang, Chin. Chem. Lett. 11 (2000) 1035–1036.
[45] A.K. Kolah, N.S. Asthana, D.T. Vu, C.T. Lira, J.D. Miller, Ind. Eng. Chem. Res. 47 (2008) 5313–5317.
[46] W. Chu, X. Yang, W. Ye, X. Wu, Appl. Catal. A: Gen. 145 (1996) 125–145.
[47] A. Corma, H. Garcia, S. Iborra, J. Primo, J. Catal. 120 (1989) 78–87.
[48] E. Santacesaria, D. Gelosa, P. Danise, S. Carra, J. Catal. 80 (1983) 427–436.
[49] I. Mochida, Y. Anju, A. Kato, T. Seiyama, J. Catal. 21 (1971) 263–269.

I&EC research
Industrial & Engineering Chemistry Research

Article

pubs.acs.org/IECR

Acetalization of Carbonyl Compounds with Pentaerythritol Catalyzed by Metal(IV) Phosphates as Solid Acid Catalysts

Tarun F. Parangi,[†] Bina N. Wani,[‡] and Uma V. Chudasama*,[†]

[†]Applied Chemistry Department, Faculty of Technology and Engineering, The M. S. University of Baroda, Vadodara 390 001, Gujarat, India

[‡]Chemistry Division, Bhabha Atomic Research Centre, Mumbai 400 085, Maharashtra, India

Supporting Information

ABSTRACT: In the present endeavor, amorphous cerium phosphate (CP) and thorium phosphate (TP) have been synthesized by the sol−gel method. Further, CP and TP also have been synthesized under microwave irradiation to yield CP_M and TP_M. The materials have been characterized for elemental analysis (inductively coupled plasma-atomic emission spectrometry, ICP-AES), spectral analysis (Fourier transform infrared spectroscopy, FTIR), thermal analysis (TGA), X-ray diffraction studies, scanning electron microscopy (SEM), energy dispersive X-ray (EDX) analysis, Brunauer−Emmett−Teller (BET) surface area analysis, and surface acidity (NH_3-temperature programmed desorption (TPD)). Chemical stability of the materials in various acids, bases, and organic solvent media has been studied, and their potential use as solid acid catalysts has been explored by studying acetal formation. A simple, efficient, and highly eco-friendly protocol is described for the acetalization of benzaldehyde, cyclohexanone, acetophenone and benzophenone with pentaerythritol by varying parameters such as reaction time, catalyst amount, and mole ratio of the reactants. The catalytic activity of CP, TP, CP_M, and TP_M has been compared and correlated with surface properties of the materials.

1. INTRODUCTION

Acetalization is an acid catalyzed reaction wherein acetals are derived from carbonyl compounds and alcohols, intensely used in organic synthesis to protect the carbonyl group of ketones and aldehydes, which is sometimes necessary in the manipulation of organic molecules with multiple functional groups.[1] Protection of the carbonyl groups of aldehydes and ketones can be accomplished by alcohols,[2] diols,[3] or trioxanes.[4] Most of the acetalization processes involve the reaction of carbonyl compound with ethylene glycol in the presence of an appropriate acid catalyst. The importance of acetals lies in the great synthetic utility and their stability to a variety of organic environments/reagents. Cyclic acetals and ketals are the most useful protective groups for the carbonyl functionality widely used in carbohydrate synthesis.[5]

Besides, there is interest of acetals as protecting groups, and many of them have found direct applications as solvents in fragrance industries,[6,7] cosmetics,[7] food and beverage additives,[8,9] pharmaceuticals,[10] the synthesis of enantiomerically pure compounds,[11,12] detergent and lacquer industries,[7] and polymer chemistry.[13] Acetals have been also used in motor oils, lubricating oils, and hydraulic fluids and as an invert-emulsion for drilling petroleum operations.[14,15]

A number of acetalization procedures include the use of corrosive protic acids (HCl, H_2SO_4), Lewis acids ($ZnCl_2$, $FeCl_3$),[1,16] *p*-toluenesulphonic acid,[17] camphorsulphonic acid,[18] iodine,[19] formic acid,[20] and a series of cationic diphosphine Lewis acidic complexes of Pt(II), Pd(II), Rh(III), etc.[21,22] However, acetalization procedures mentioned above require expensive reagents, tedious workup procedures, and neutralization of the strongly acidic media leading to the production of harmful wastes. Hence, these methods suffer limitations, derived from high E-factors and low atom utilization as the catalysts are irreversibly lost.[23] In this context, the use of heterogeneous acid catalysts for the reaction is attractive and it may allow one to carry it out without the generation of wastes.

There is a strong interest in the use of solid acid catalysts as replacements to conventional homogeneous catalysts such as mineral and organic acids, due to environmental concerns. Though the conventional catalysts are very effective, they produce highly corrosive media and chemically reactive waste streams, whose treatment can be both difficult and hazardous. In contrast, solid acid catalysts are easier to handle, and the general operation of a large chemical process is safer and ecofriendly. The obtained product is of high purity, and finally, there is the possibility of recycling and reuse of catalysts.[24] Environmentally benign solid acid catalysts such as SO_4^{-2}/ZrO_2, SO_4^{-2}/TiO_2,[25] Ce exchanged montmorillonite,[26] acidic zeolites,[27−29] mesoporous silica[30] and siliceous mesoporous material,[31,32] $Al(HSO_4)_3$,[33] SBA-15,[34] and $CeCl_3$[35] have been reported to be active for the acetalization reactions. Lachter et al.[15] have reported catalytic activity of ion exchange resins such as niobium phosphate and amberlyst-35 as solid acid catalyst for the acetalization of hexanal with 2-ethyl-hexanol and also observed higher performance of niobium phosphate compared with Amberlyst-35.

Pentaerythritol (PET) is an alcohol with formula $C(CH_2OH)_4$ [2,2-bis(hydroxymethyl)propane-1,3-diol]. It is a white, crystalline polyol with the neopentane backbone, a

Received: March 2, 2013
Revised: May 21, 2013
Accepted: June 6, 2013
Published: June 6, 2013

versatile building block for the preparation of many polyfunctional compounds. The pentaerythritol react with carbonyl compounds to give pentaerythritol acetals which are useful in many fields. They can be applied as plasticizers and vulcanizers of various polymeric materials, as raw materials for production of valuable resins and lacquers, as physiologically active substances,[36] as defoamers for washing solution containing anionic surfactant, in motor oils, lubricating oils, and hydraulic fluids.[15] 1,2-Diacetal is an efficient protecting group for vicinal 1,2-diol units in carbohydrates. Acetonide formation is the commonly used protection for 1,2-(*cis*)- and 1,3-diols, which have extensively been used in carbohydrate chemistry to selectively mask the hydroxyls of different sugars.[36]

Kannan et al.[36] have reported acetalization of pentaerythritol with several carbonyl compounds in the presence of an Al-pillared saponite. Firouzabadi et al.[37] have described application of solid silica chloride, an easily available and efficient catalyst for the preparation of diacetal of pentaerythritol from aldehydes that gives good yields with short reaction times. Pandurangan et al.[38] have reported synthesis of diacetal from pentaerythritol with carbonyl compounds using MCM-41 molecular sieves. However, catalyst regeneration and reuse studies have not been reported.[37,38]

Tetravalent metal acid (TMA) salts are inorganic cation exchangers possessing the general formula M(IV)-$(HXO_4)_2 \cdot nH_2O$ [M(IV) = Zr, Ti, Sn, etc. and X = P, W, Mo, As, Sb, etc.], where H^+ of the structural hydroxyl groups is responsible for cation exchange, since TMA salts indicate good potential for application as solid acid catalysts, the acidic sites being Brønsted acid sites in nature. TMA salts have been widely used as solid acid catalysts by us. A variety of reactions such as dehydration of alcohols,[24] ketalization of ketones,[3] esterification,[39−47] and coumarin synthesis by Pechmann condensation[48,49] have been reported from our laboratory.

Many of the works done by us are on phosphates of Zr, Ti, and Sn. However, not much work has been explored on phosphates of Ce and Th. It has been earlier reported that Ce exchanged H−Y zeolites and K-10 montmorillonite clays possess more acid sites and produce a larger amount of acetal compared to other rare earth exchanged zeolites and clays.[26]

In the present endeavor, amorphous cerium phosphate (CP) and thorium phosphate (TP) have been synthesized by the soft chemistry route sol−gel method. Further, CP and TP have also been synthesized under microwave irradiation to yield CP_M and TP_M. The materials have been characterized for elemental analysis (inductively coupled plasma-atomic emission spectrometry, ICP-AES), spectral analysis (Fourier transform infrared spectroscopy, FTIR), thermal analysis (TGA), X-ray diffraction studies, scanning electron microscopy (SEM), energy dispersive X-ray (EDX) analysis, Brunauer−Emmett−Teller (BET) surface area analysis, and surface acidity (NH_3-temperature programmed desorption (TPD)). Chemical stability of the materials in various acids, bases, and organic solvent media has been studied, and their potential use as solid acid catalysts has been explored by studying acetal formation. A simple, efficient, and highly eco-friendly protocol is described for the acetalization of benzaldehyde, cyclohexanone, acetophenone, and benzophenone with PET by varying parameters such as reaction time, catalyst amount, and mole ratio of the reactants. The catalytic activity of CP, TP, CP_M, and TP_M have been compared and correlated with surface properties of the materials.

2. EXPERIMENTAL SECTION

2.1. Chemicals. Thorium nitrate ($Th(NO_3)_4 \cdot 5H_2O$), ceric sulfate ($Ce(SO_4)_2 \cdot 4H_2O$), and sodium dihydrogen phosphate ($NaH_2PO_4 \cdot 2H_2O$) were procured from Loba Chemicals, Mumbai, while pentaerythritol, benzaldehyde, cyclohexanone, acetophenone, benzophenone, and toluene were obtained from Across Organics. Double-distilled water was used for all the studies.

2.2. Catalyst Synthesis. CP and TP were synthesized by the sol−gel method varying several parameters such as mole ratio of reactants, mode of mixing (metal salt solution to anion salt solution or vice versa), temperature, pH, and rate of mixing. The main objective was to obtain a material with high CEC/protonating ability. Several sets of materials were prepared varying conditions in each case using CEC as the indicative tool. (Supporting Information Tables 1 and 2 describe optimization of reaction parameters for synthesis of CP and TP, respectively.)

2.2.1. Synthesis of CP at Optimized Condition. A solution containing $Ce(SO_4)_2 \cdot 4H_2O$ [0.1 M, 50 mL in 10% (w/v) H_2SO_4] was prepared, to which $NaH_2PO_4 \cdot 2H_2O$ [0.3 M, 50 mL] was added dropwise (flow rate 1 $mL \cdot min^{-1}$) with continuous stirring for an hour at room temperature, when gelatinous precipitates were obtained (Step-I). The resulting gelatinous precipitate was allowed to stand for 3 h at room temperature, then filtered, washed with conductivity water to remove adhering ions, and dried at room temperature (Step-II).

2.2.2. Synthesis of TP at Optimized Condition. An aqueous solution of $Th(NO_3)_4 \cdot 5H_2O$ [0.1 M, 50 mL] was added dropwise (flow rate 1 $mL \cdot min^{-1}$) to an aqueous solution of $NaH_2PO_4 \cdot 2H_2O$ [0.2M, 100 mL] with continuous stirring for an hour at room temperature, when gelatinous precipitates were obtained (Step-I). The resulting gelatinous precipitate was allowed to stand for 5 h at room temperature, then filtered, washed with double distilled water to remove adhering ions, and dried at room temperature (Step-II).

2.2.3. Synthesis of CP and TP under Microwave Irradiation. Gelatinous precipitate obtained in Step-I was subjected to microwave irradiation for optimum time and temperature (Supporting Information Table 3), then filtered, washed with double distilled water to remove adhering ions, and dried at room temperature (Step-II).

2.2.4. Acid Treatment. The above dried materials obtained in Step-II were broken down to the desired particle size [30−60 mesh (ASTM)] by grinding and sieving. Five g of this material was treated with 50 mL of 1 M HNO_3 for 30 min with occasional shaking. The material was then separated from acid by decantation and treated with double distilled water to remove adhering acid. This process (acid treatment) was repeated at least 5 times for both the materials. After the final washing, the material was dried at room temperature.

2.3. Characterization. *2.3.1. Chemical Stability.* The chemical stability of the catalysts in various acids (HCl, H_2SO_4, HNO_3), bases (NaOH and KOH), and organic solvent media (ethanol, propanol, butanol, benzyl alcohol, cyclohexane, toluene, xylene, and acetic acid) was examined by taking 500 mg of each of the synthesized catalysts in 50 mL of the particular medium and allowed to stand for 24 h. The change in color, weight, and nature was observed.

2.3.2. Cation Exchange Capacity (CEC). The protonating ability of catalysts was determined as Na^+ CEC using a column

method by optimizing volume and concentration of sodium acetate solution.[50]

2.3.3. Instrumentation. All synthesized materials were subjected to instrumental methods of analysis/characterization. FTIR spectra were recorded using KBr pellet on Shimadzu (Model 8400S). ^{1}H NMR spectra was performed on a Bruker (300 MHz in DMSO, internal standard TMS). Thermal analysis (TGA) was carried out on a Shimadzu (Model TGA 50) thermal analyzer at a heating rate of 10 °C·min^{-1}. The X-ray diffractogram (2θ = 10−80°) was obtained on an X-ray diffractometer (Bruker AXS D8) with Cu Kα radiation with nickel filter. SEM and EDX of the sample were scanned on a Jeol JSM-5610-SLV scanning electron microscope. Surface area was determined by the BET multipoint method using a Micromeretics Gemini 2220 series surface area analyzer. Surface acidity was determined on a Chemisorb 2720, by a temperature programmed desorption (TPD) of ammonia. All materials were preheated at 150, 200, and 700 °C temperatures, and thereafter, ammonia was chemisorbed at 120 °C; then, desorption was carried out up to 700 °C at a heating rate of 10 °C·min^{-1} in all cases.

2.4. Experimental Setup for Acetal Formation. In a typical reaction, a 100 mL round bottomed flask equipped with a Dean and Stark apparatus, attached to a reflux condenser, was used and charged with carbonyl compound (5−20 mmol), PET (5−10 mmol), catalyst (0.1−0.6 g), and toluene as solvent (10 mL) in nitrogen atmosphere. The reactions were carried out varying several parameters such as reaction time, amount of catalyst, mole ratio of reactants, etc., and these parameters were optimized. The progress of the reaction was monitored by TLC (20% of ethyl acetate in petroleum ether). After cooling, the catalyst was filtered off and washed with CH_2Cl_2. The crude product was isolated by distillation and purified through recrystallization in ethanol.

2.5. Regeneration of Catalyst. After separation of catalyst in reaction mixture by decantation, it is first refluxed in ethanol for 30 min to solubilize and remove adsorbed molecules, followed by drying. This material was used as recycled catalyst. This regeneration procedure was followed in the subsequent recycle reaction.

3. RESULTS AND DISCUSSION

3.1. Catalyst Characterization. CP and TP were obtained as yellow and off white hard granules, respectively. Elemental analysis performed by ICP-AES, for CP, shows % Ce = 33.15 and % P = 15.11 and, for TP, shows % Th = 35.10 and % P = 9.40 with ratio of metal−P as 1:2. This is well supported by EDX (Supporting Information Figure 1) for CP which shows atomic % of Ce and P to be 34.95% and 65.05%, respectively, and (Supporting Information Figure 2) for TP which shows atomic % of Th and P to be 35.75% and 64.25%, respectively.

CP and TP are found to be stable in acidic media, maximum tolerable limits being 1 N H_2SO_4, 2 N HNO_3, and 5 N HCl, and also stable in organic solvent media. They are however not so stable in a basic medium, maximum tolerable limits being 0.5 N NaOH and KOH.

CEC (cation exchange capacity) values reflect on the protonating ability and thus the acidity in the materials. The Na^+ CEC values were observed to be 2.48, 1.48, 2.90, and 2.41 for CP, TP, CP_M, and TP_M, respectively.

The FTIR spectra (Supporting Information Figure 3) of CP and TP exhibits a broad band in the region of ∼3400 cm^{-1} which is attributed to asymmetric and symmetric −OH stretching vibration due to residual water and the presence of structural hydroxyl groups, H^+ of the −OH being a Brønsted acid site in nature. These bands indicate the presence of structural hydroxyl groups/catalytic sites in the materials. These sites are also referred to as defective P−OH groups.[50,51] A sharp medium band at ∼1630 cm^{-1} is attributed to aquo H−O−H bending.[52] The band at ∼1050 cm^{-1} is attributed to P═O stretching while the bands at ∼620 and ∼500 cm^{-1} are attributed to metal−O stretching.[53]

TGA of CP and TP is presented in Supporting Information Figure 4. CP exhibits the first weight loss of ∼13% and the second weight loss of ∼8% while TP exhibits the first weight loss of ∼11% and the second weight loss of ∼9%. The first weight loss (up to ∼120 °C) is attributed to loss of moisture/hydrated water while the second weight loss in the range of 120−500 °C is attributed to condensation of structural hydroxyl groups.

CEC values decrease on calcination, due to loss of hydrated water and condensation of structural hydroxyl groups at higher temperatures (Supporting Information Table 4). This fact is also evident from the FTTR spectra of the calcined samples (Supporting Information Figure 5). It is seen that the intensities of the peaks at −3400 and −1638 cm^{-1} corresponding to the −OH group diminish as temperature increases.

The absence of sharp peaks in the X-ray diffractograms of CP and TP (Supporting Information Figure 6) and CP_M and TP_M (Supporting Information Figure 7) indicates an amorphous nature of all the materials. SEM images of CP, TP, CP_M, and TP_M (Supporting Information Figures 8 to 11) show irregular morphology.

The surface area measurement has been performed by an adsorption desorption isotherm of N_2 which was recorded at −196 °C after degassing the sample at 300 °C for 4 h. Surface area values of CP, TP, CP_M, and TP_M are 20.71, 1.94, 1.40, and 0.0026 m^2/g, respectively.

Surface acidity for all the materials was determined by NH_3-TPD at 150, 200, and 700 °C preheating temperatures (Table 1 and Figures 1, 2, 3, and 4). As already discussed earlier in the text, acidity in CP and TP is due to the presence of structural hydroxyl protons, H^+ of the −OH being the Brønsted acid sites. Further, surface acidity values of CP and TP depend on the size and charge of the cation. Smaller size and higher charge of the cation indicates greater tendency to release a proton, i.e., H^+ of

Table 1. Surface Acidity and CEC Values at 150, 200, and 700 °C Preheating Temperatures

samples	calcination/preheating temperature (°C)	total acidity (NH_3-TPD method) (mL·g^{-1})	CEC (meq·g^{-1})
CP	150	22.28	2.04
	200	21.00	1.89
	700	0.60	
CP_M	150	29.72	2.20
	200	10.52	2.00
	700	0.82	
TP	150	18.15	0.70
	200	11.77	0.46
	700	0.47	
TP_M	150	18.94	0.92
	200	17.93	0.70
	700	0.50	

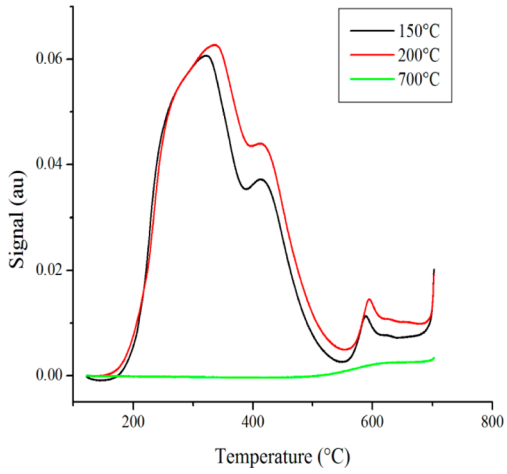

Figure 1. NH_3-TPD patterns for CP at 150, 200, and 700 °C preheating temperatures.

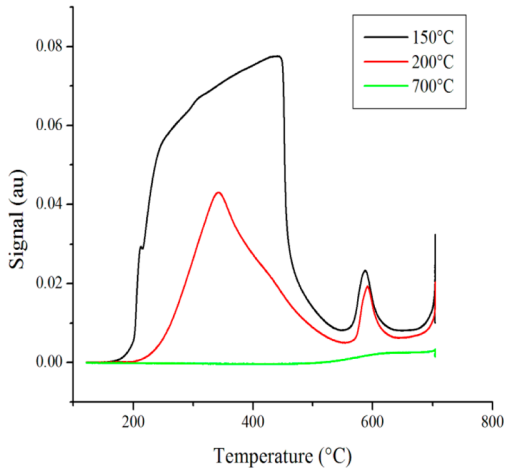

Figure 2. NH_3-TPD patterns for CP_M at 150, 200, and 700 °C preheating temperatures.

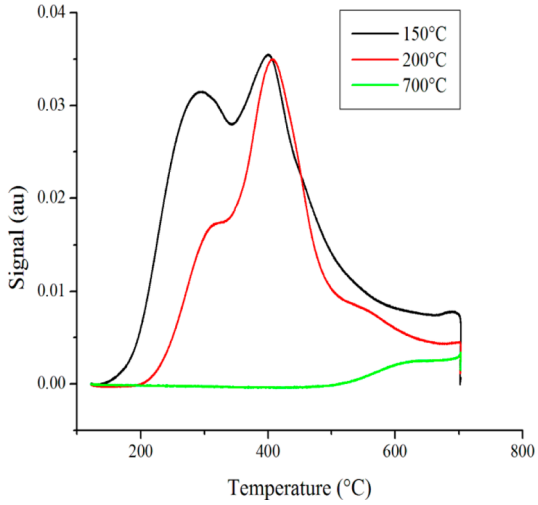

Figure 3. NH_3-TPD patterns for TP at 150, 200, and 700 °C preheating temperatures.

the −OH groups present in CP and TP. In the present study, both Ce^{4+} and Th^{4+} ions are tetravalent as well as bear common anion PO_4^{3-}, and the size of the cation Ce^{4+} (1.05 Å) and Th^{4+}

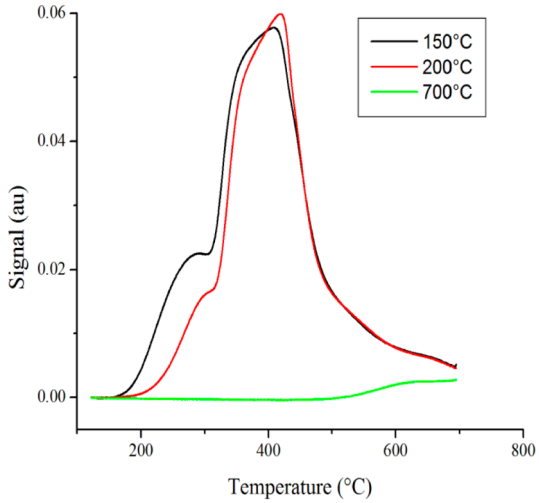

Figure 4. NH_3-TPD patterns for TP_M at 150, 200, and 700 °C preheating temperatures.

(1.08 Å) seems to play a dominant role. Thus, the acidity in the materials follows the order CP > TP (CP_M > TP_M). A decrease in surface acidity for CP and TP with increasing preheating temperatures could be attributed to condensation of structural hydroxyl groups as discussed above in thermal behavior of these materials. This is well supported by CEC values, which reflect on the protonating ability and thus the acidity of the materials.[49] CEC values also decrease with increasing calcination/preheating temperature, as has already been discussed in FTIR spectra of calcined samples.

3.2. Acetalization of Carbonyl Compounds with PET.

Acetal formation is a reversible reaction, which proceeds by a two-step mechanism.[23] Scheme 1 envisages the mechanism of

Scheme 1. General Mechanism for Acetalization of Carbonyl Compounds

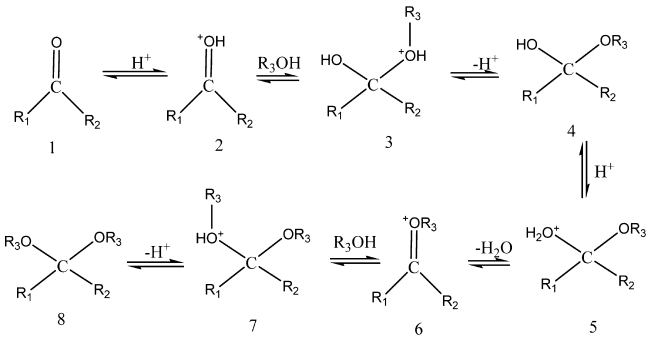

the acetal formation of carbonyl compounds using solid acid catalyst. In the mechanism presented (Scheme 1), carbonyl compound is first protonated by the Brønsted acid sites (H^+ ions of the catalyst) to produce the intermediate 2 which then combines with alcohol to form the hemiacetal 4 liberating a significant amount of heat.[54−56] Protonation of 4 leads to intermediate 5 which undergoes subsequent dehydration to give 6. Reaction of 6 with a molecule of alcohol gives intermediate 7. This step is also an exothermic reaction, and last, removal of a proton from 7 leads to the formation of the acetal 8.[23,54−56]

In the present study, acetalization of benzaldehyde ($\Delta_f H^\circ_{liquid}$ = −87.1 kJ/mol),[57] cyclohexanone ($\Delta_f H^\circ_{liquid}$ = −156.4 kJ/

mol),[57] acetophenone ($\Delta_f H°_{liquid}$ = −142.5 kJ/mol),[57] and benzophenone ($\Delta_f H°_{solid}$ = −34 kJ/mol)[57] with PET ($\Delta_f H°_{solid}$ = −920.5 kJ/mol)[57] has been performed as described in the Experimental Section. First, reaction conditions were optimized using CP as solid acid catalyst for preparation of diacetal from benzaldehyde and ketones (cyclohexanone and acetophenone/benzophenone) with PET by varying parameters such as reaction time, catalyst amount, and initial mole ratio of the reactants. The optimized reaction conditions are presented in Supporting Information Tables 5 to 7 and a graphical presentation (Figures 5, 6, and 7).

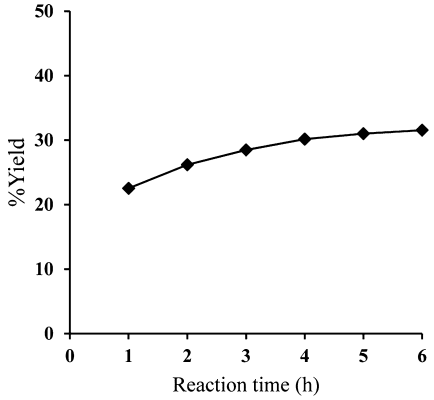

Figure 5. Reaction time variation for preparation of diacetal from benzaldehyde with PET using CP.

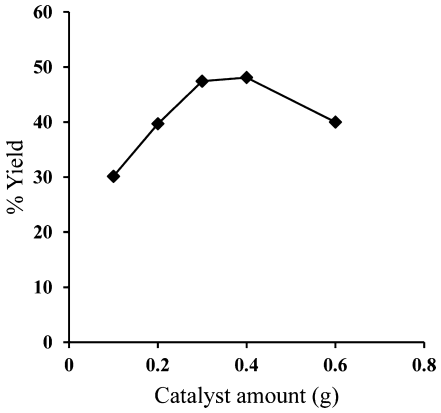

Figure 6. Catalyst amount variation for preparation of diacetal from benzaldehyde with PET using CP.

The effect of reaction time on the product yield of diacetal formed in all cases was studied at refluxing temperature (110 °C) using toluene as solvent with 1:1 mol ratio of PET−benzaldehyde/ketones and 0.1 g of catalyst (CP). The reaction reached equilibrium within 4 h (benzaldehyde), 6 h (cyclohexanone), and 8 h (acetophenone and benzophenone). With increasing catalyst amount, which was varied from 0.1 g to 0.6 g, % yield increases probably due to an increase in the number of acid sites. With reference to the mechanism described in Scheme 1, step 1 is protonation whereas step 3 is formation of hemiacetal followed by deprotonation. For deprotonation to occur, an optimum acidity is required, or else if acidity is higher, then the further reaction to form the acetal is inhibited or reaction slows down; thus, the excess acid amount may promote the occurrence of the reverse reaction. Therefore, in

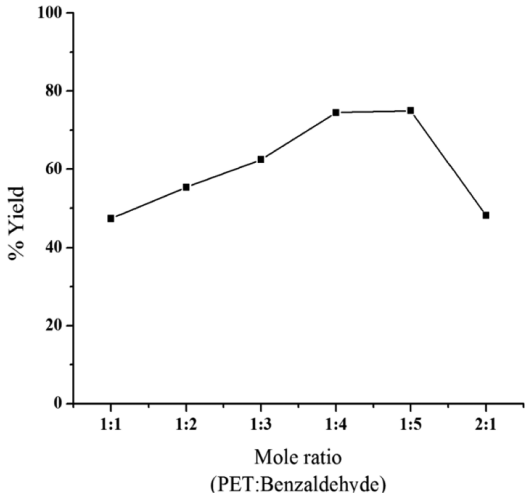

Figure 7. Variation of mole ratio of reactants for preparation of diacetal from benzaldehyde with PET using CP.

all cases, the optimum catalyst amount was taken as 0.3 g (Supporting Information Tables 5 to 7).

Acetal formation is a reversible reaction, the reverse reaction being acetal hydrolysis with the same mechanism going in the backward direction to give alcohol and carbonyl compound. Considering thermodynamics of the acetal reaction, equilibrium constants of the acetal reaction are low.[58] As in any equilibrium reaction, the reaction may be driven to the product side (forward direction) by controlling the concentration of one of the reactants or removing water molecules formed continuously to avoid the reverse reaction (Le Chatlier's Principle). In the present study, in order to obtain higher yields of acetal, Le Chatlier's Principle has been followed. A Dean and Stark apparatus has been used for removal of water as binary azoetrope using toluene as solvent. Further, mole ratio of the reactants PET to carbonyl compound has been varied taking one of the reactants in excess. Thus, precautions are taken to avoid the backward reaction to arrive at maximum yields. The presented % yields are isolated yields.

The influence of mole ratio of reactants on product yield was studied using 0.3 g of catalyst at the refluxing temperature at optimized reaction time. The mole ratios of PET−benzaldehyde/ketones were varied from 1:1 to 1:5 and 2:1. It is observed that, when the mole ratio increased from 1:1 to 1:4, the product yield increased which is attributed to an increase in chemisorption of benzaldehyde/ketones on the Brønsted acid sites which leads to the polarization of the carbonyl bond where PET makes a nucleophilic attack. Further, for mole ratio 2:1, the yield decreased which may be due to the dilution of benzaldehyde/ketones. In the present study, 1:4 mol ratios of PET−benzaldehyde/ketones were used. Diacetal of PET was observed as the single product over all mole ratios of PET and benzaldehyde/ketones.

At optimized condition, acetalization of benzaldehyde, cyclohexanone, acetophenone, and benzophenone with PET was performed using TP, CP_M, and TP_M (reaction time = 4 h (benzaldehyde), 6 h (cyclohexanone), and 8 h (acetophenone and benzophenone); catalyst amount = 0.3 g; mole ratio of PET−benzaldehyde/ketones = 1:4; reaction temperature = 110 °C; Table 2).

In all the reactions, acetal derivative of benzaldehyde (dibenzal acetal) was obtained with high % yield. This is

Table 2. % Yields of Diacetals from Benzaldehyde/Ketones with PET using CP, TP, CP_M, and TP_M

no.	reactants[a]	time (h)	% yield[b] CP	TP
1	PET−benzaldehyde	4	74.51	68.13
2	PET−cyclohexanone	6	72.00	59.45
3	PET−acetophenone	8	61.00	54.74
4	PET−benzophenone	8	48.25	44.16
	(A) Catalyst Reusability			
5	PET−benzaldehyde 1st cycle	4	70.00	64.00
6	PET−benzaldehyde 2nd cycle	4	64.18	59.20
7	PET−cyclohexanone 1st cycle	6	68.25	56.20
8	PET−cyclohexanone 2nd cycle	6	61.36	53.41
9	PET−acetophenone 1st cycle	8	58.75	50.42
10	PET−acetophenone 2nd cycle	8	53.65	48.00
11	PET−benzophenone 1st cycle	8	42.13	37.76
12	PET−benzophenone 2nd cycle	8	38.45	33.47
	(B) Microwave Irradiated Catalysts			
			CP_M	TP_M
1	PET−benzaldehyde	4	86.18	72.34
2	PET−cyclohexanone	6	80.36	68.50
3	PET−acetophenone	8	73.41	62.20
4	PET−benzophenone	8	54.00	48.31

[a]Mole ratio of reactants, PET−benzaldehyde/ketones = 1:4; catalysts amount = 0.3 g; reaction temperature = 110 °C (toluene). [b]Yields based on conversion of carbonyl compound taken.

probably due to the fact that aldehyde undergoes nucleophilic addition more readily than ketones. Compared to benzophenone and acetophenone, benzophenone is more bulky than acetophenone and shows the lowest reactivity and thus low yields. The rate determining step of acetalization is the formation of a cation from the protonated hemiacetal. Hence, the bulkiness of hemiacetals might prevent the attack of the alcohol on the carbonyl carbon atom thereby effecting a change in the rate-determining step. Further, the electron withdrawing power of the phenyl group (1 for acetophenone and 2 for benzophenone) in these compounds reduces the easy release of the pair of electrons on the carbonyl carbon during the reaction. However, cyclohexanone is more reactive toward nucleophiles than both acetophenone and benzophenone.[23] Therefore, the reactivity of the ketones decrease in the order cyclohexanone > acetophenone > benzophenone (Table 2). Order of % yields obtained is CP > TP, and CP_M > TP_M could be attributed to higher surface acidity (Table 2, Figures 8 and 9).

During the course of the reaction, many a time, the catalyst color changes. This is probably due to the fact that reactant molecules come onto the surface of the catalyst and enter into the reaction to give the product while a few of them get adsorbed on the surface. In each subsequent run, the acid sites in the catalysts were regenerated as described in the Experimental Section. After regeneration and reuse, decreases in yields are observed which is probably due to the deactivation of catalysts because of substrate molecules getting adsorbed on the surface or also entering interstices of the catalyst material.[49]

It is observed that there is only a marginal decrease in yields up to two catalytic runs. In recycled catalyst, the yield decreased by 4−7% (Figure 10). When catalyst was used as such (without regeneration), a 7−10% decrease in yields was observed (Supporting Information Table 8). Further, EDX of spent CP (Supporting Information Figure 12; after first catalytic run)

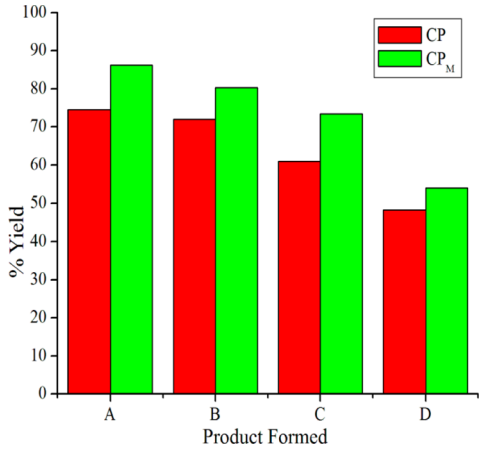

Figure 8. Comparative catalytic performance of CP and CP_M for preparation of diacetals: A = dibenzal acetal; B = acetal derivative of cyclohexanone; C = acetal derivative of acetophenone; D = acetal derivative of benzophenone.

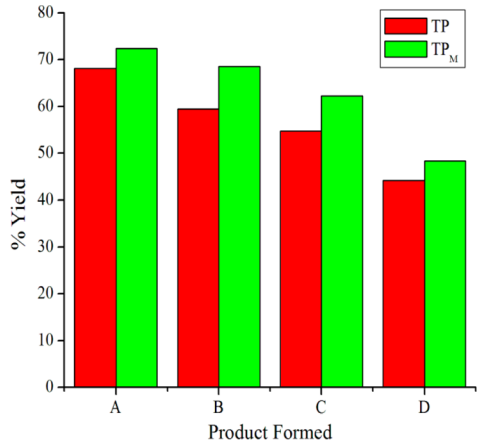

Figure 9. Comparative catalytic performance of TP and TP_M for preparation of diacetals: A = dibenzal acetal; B = acetal derivative of cyclohexanone; C = acetal derivative of acetophenone; D = acetal derivative of benzophenone.

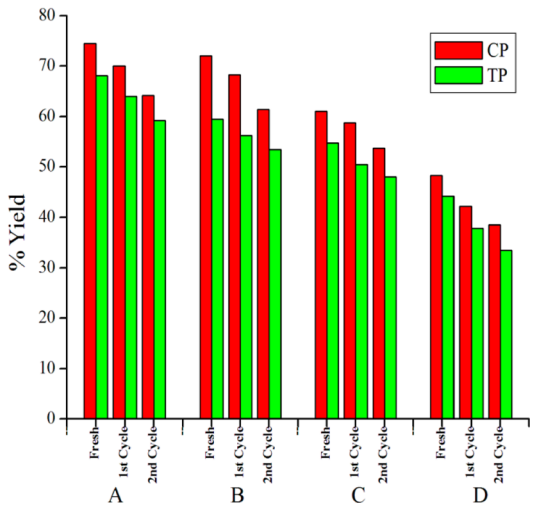

Figure 10. Reusability of CP and TP for preparation of diacetals: A = dibenzal acetal; B = acetal derivative of cyclohexanone; C = acetal derivative of acetophenone; D = acetal derivative of benzophenone.

shows atomic % of Ce and P to be 37.97% and 62.03%, respectively, and EDX of spent TP (Supporting Information Figure 13; after first catalytic run) shows atomic % of Th and P to be 37.65% and 62.35%, respectively, which shows a decrease in atomic % of P compared to fresh CP and TP. A decrease in yield of acetal derivatives may be due to the leaching of P in catalysts.

3.3. Characterization of the Products. The isolated products were characterized by FTIR, ^{1}H NMR spectroscopy, and melting point. Heats of formation ($\Delta_f H°$) values of products have been estimated on the basis of $\Delta_f H°$ values of reactants.[58]

Dibenzal Aceatal. IR Absorptions. ν_{max}/cm^{-1} 2910 (CH), 2862 (CH), 1600 (C═C aromatic), 1460 (C═C aromatic), 1390 (CH), 1050 (C−O−C), 805 (C_6H_5), 710 (C_6H_5).

NMR Data. δH (100 MHz; $CDCl_3$; Me_4Si), 3.51 (6H, m, H_{ax}, H_{eq}), 4.70 (2H, d, J 11.7, 2 H_{eq}), 5.42 (2H, s, 2 × PhCH), 7.10−7.60 (10H, m, 2 × Ph). Melting point: 155 °C (ethanol). $\Delta_f H°_{solid}$ = −521.1 kJ/mol.

Acetal Derivative of Cyclohexanone. IR Absorptions. ν_{max}/cm^{-1} 2960 (CH), 2870 (CH), 1140 (C−O−C).

NMR Data. δH H(100 MHz; $CDCl_3$; Me_4Si) 1.4−1.7 (20H, m, 2 × $(CH_2)_5$), 3−3.5 (8H, m, $(CH_2O)_4$). Melting point: 116 °C (ethanol). $\Delta_f H°_{solid}$ = −661.7 kJ/mol.

Acetal Derivative of Acetophenone. IR Absorptions. ν_{max}/cm^{-1} 2970 (CH), 2890 (CH), 1600 (C═C aromatic), 1468 (C═C aromatic), 1365 (CH), 1150 (C−O−C), 790 (C_6H_5), 700 (C_6H_5).

NMR Data. δH (100 MHz; $CDCl_3$; Me_4Si) 1.51 (6H, s, 2 × Me), 3.15 (2H, dd, J 11.1, 2.4, 2 × H_{eq}), 3.30 (2H, d, J 11.1, 2 × H_{ax}), 3.60 (2H, d, J 11.7, 2 × H_{ax}), 4.48 (2H, dd, J 11.7, 2 × H_{eq}), 7.25−7.70 (10H, m, 2 × Ph). Melting point: 146 °C (ethanol). $\Delta_f H°_{solid}$ = −633.9 kJ/mol.

Acetal Derivative of Benzophenone. IR Absorptions. ν_{max}/cm^{-1} 2975 (CH), 2880 (CH), 1615 (C═C Aromatic), 1480 (C═C Aromatic), 1390 (CH), 1050 (C−O−C), 755 (C_6H_5), 770 (C_6H_5).

NMR Data. δH (100 MHz; $CDCl_3$; Me_4Si) 3.6 (8H, s, $(CH_2O)_4$), 7.14−7.32 (20H, m, 2 × $(Ph)_2$). Melting point: 160 °C (ethanol). $\Delta_f H°_{solid}$ = −416.9 kJ/mol.

4. CONCLUSIONS

The work outlined herein reveals the promising use of CP and TP as solid acid catalysts in acetal formation with high selectivity of the products, advantages being operational simplicity, mild reaction conditions, no catalyst contamination in products formed, no acid waste generation, and regeneration and reuse of catalysts, and last, products formed are colorless, a limitation in the conventional process. Further, the catalysts CP_M and TP_M are synthesized (under microwave condition) in a much shorter reaction time with higher surface acidity, and good % yields of diacetal are encouraging.

■ ASSOCIATED CONTENT

Ⓢ Supporting Information

Eight tables, showing optimization of reaction conditions for catalyst synthesis and preparation of diaceatal including reusability of the catalysts, and thirteen figures, showing catalyst characterization. This material is available free of charge via the Internet at http://pubs.acs.org.

■ AUTHOR INFORMATION

Corresponding Author

*Address: Applied Chemistry Department, Faculty of Technology and Engineering, The M. S. University of Baroda, Post Box No. 51, Kalabhavan, Vadodara 390 001, Gujarat, India. Phone: +91 9426344434. E-mail: uvcres@gmail.com.

Notes

The authors declare no competing financial interest.

■ ACKNOWLEDGMENTS

The authors thank DAE-BRNS for providing financial support and a research fellowship to T. Parangi.

■ REFERENCES

(1) Greene, T. W. *Protective Groups in Organic Synthesis*; Wiley: New York, 1981; p 114.

(2) Srivastava, P.; Srivastava, R. A novel method for the protection of amino alcohols and carbonyl compounds over a heterogeneous, reusable catalyst. *Catal. Commun.* **2008**, *9*, 645−649.

(3) Patel, S.; Chudasama, U.; Ganeshpure, P. Ketalization of ketones with diols catalyzed by metal (IV) phosphates as solid acid catalysts. *J. Mol. Catal. A: Chem.* **2003**, *194*, 267−271.

(4) Chandan, S.; Malik, H. Protection of the carbonyl group as 1,2,4-trioxane and its regeneration under basic conditions. *Org. Lett.* **2005**, *7*, 5673−5676.

(5) Wang, P.; Kong, A. G.; Wang, W. J.; Zhu, H. Y.; Shan, Y. K. Facile preparation of ionic liquid functionalized magnetic nano-solid acid catalyst for acetalization reaction. *Catal. Lett.* **2010**, *135*, 159−164.

(6) Climent, M. J.; Velty, A.; Corma, A. Design of a solid catalyst for the synthesis of a molecule with blossom orange scent. *Green Chem.* **2002**, *4*, 565−569.

(7) Bauer, K.; Garbe, D.; Surburg, H. *Common Fragrances and Flavour Materials*, 2nd ed.; VCH: New York, 1990.

(8) Clode, D. M. Carbohydrate cyclic acetal formation and migration. *Chem. Rev.* **1979**, *79*, 491−513.

(9) Ley, S. V.; Priepke, H.W. M. Eintopfsynthese einer trisaccharideinheit des gemeinen polysaccharid-antigens von *Streptococci* der Gruppe B unter verwendung cyclohexan-1,2-diacetal(CDA)-geschützter rhamnoside. *Angew. Chem.* **1994**, *106*, 2412−2414.

(10) Bruns, K.; Conard, J.; Steigel, A. Stereochemistry of cyclic compounds-I: Synthesis and conhgurational assignment of diawereomeric 2,4-dioxaspir[5.5]undec-8-enes. *Tetrahedran* **1979**, *35*, 2523−2530.

(11) Cheung, M. K.; Douglas, N. L.; Hinzen, B.; Ley, S. V.; Pannecoucke, X. One-pot synthesis of tetra- and pentasaccharides from monomeric building blocks using the principles of orthogonality and reactivity tuning. *Synlett* **1997**, *3*, 257−260.

(12) Narasaka, K.; Inone, M.; Yamada, T.; Sugiomori, J.; Iwasawa, N. Asymmetric diels−alder reaction by the use of a chiral titanium catalyst with molecular sieves 4A. Remarkable solvent effect on the enantioselectivity. *Chem. Lett.* **1987**, 2409−2412.

(13) Elliot, A. J. *1,3-Dioxalane Polymers in Comprehensive Heterocyclic Polymers1,3-Dioxalane Polymers in Comprehensive Heterocyclic Polymers*; Pergamon Press: Oxaford, UK, 1984; p 6.

(14) Hille, M.; Wittkus, H.; Scholz, H. J.; Weimlet, F. Use of acetals. U.S. Patent 5,759,963, 1998.

(15) Barros, A. O.; Faisca, A. T.; Latcher, E. R.; Nascimento, R. S. V.; Gil, R. A. S. Acetalization of hexanal with 2-ethyl hexanol catalyzed by solid acids. *J. Braz. Chem. Soc.* **2011**, *22* (2), 359−363.

(16) Bornstein, J.; Bedell, S. F.; Drummond, P. E.; Kosoloki, C. F. The synthesis of α-amino-*o*-tolualdehyde diethylacetal. *J. Am. Chem. Soc.* **1956**, *78*, 83−86.

(17) McKinzie, C. A.; Stocker, J. H. Preparation of ketals. A reaction mechanism. *J. Org. Chem.* **1955**, *20*, 1695−1701.

(18) Boulineau, F. P.; Wei, A. Stereoselective synthesis of [^{13}C]methyl 2-[^{15}N]amino-2-deoxy-β-D-glucopyranoside derivatives. *Carbohydr. Res.* **2001**, *334*, 271−279.

(19) Kartha, K. P. R. Iodine, a novel catalyst in carbohydrate reactions I. *o*-Isopropylidination of carbohydrates. *Tetrahedron Lett.* **1986**, *27*, 3415−3416.
(20) Winnik, F. M.; Carver, J. P.; Krepinsky, J. J. Syntheses of model oligosaccharides of biological significance. Synthesis of a tetramannoside and of two lyxose-containing Trisaccharides. *J. Org. Chem.* **1982**, *47*, 2701−2707.
(21) Cataldo, M.; Neiddu, F.; Gavagnin, R.; Pinna, F.; Strukul, G. Hydroxy complexes of palladium (II) and platinum (II) as catalysts for the acetalization of aldehydes and ketones. *J. Mol. Catal. A: Chem.* **1999**, *142*, 305−316.
(22) Neiddu, E.; Cataldo, M.; Pinna, F.; Strukul, G. Acetalization of α,β-unsaturated carbonyl compounds catalyzed by complexes of Pt(II). *Tetrahedron Lett.* **1999**, *40*, 6987−6990.
(23) Thomas, B.; Sreedharan, P.; Sugunan, S. Synthesis of dimethyl acetal of ketones: Design of solid acid catalysts for one-pot acetalization reaction. *Microporous Mesoporous Mater.* **2005**, *80*, 65−72.
(24) Patel, S.; Chudasama, U.; Ganeshpure, P. Metal(IV) phosphates as solid acid catalysts for selective cyclodehydration of 1,*n*-diols. *Green Chem.* **2001**, *3*, 143−145.
(25) Lin, C. H.; Lin, S. D.; Yang, Y. H.; Lin, T. P. The synthesis and hydrolysis of dimethyl acetals catalyzed by sulfated metal oxides. An efficient method for protecting carbonyl groups. *Catal. Lett.* **2001**, *73* (2−4), 121−125.
(26) Tateiwa, J.; Hiriuchi, H.; Uemura, S. Ce^{3+}-Exchanged montmorillonite (Ce^{3+}-Mont) as a useful substrate-selective acetalization catalyst. *J. Org. Chem.* **1995**, *60*, 4039−4043.
(27) Corma, A.; Climent, M. J.; Garcia, H.; Primo, J. Formation and hydrolysis of acetals catalysed by acid faujasites. *Appl. Catal., A: Gen.* **1990**, *59*, 333−340.
(28) Ballini, R.; Bosica, G.; Frullanti, B.; Maggi, R.; Sartori, G.; Schroer, F. 1,3-Dioxolanes from carbonyl compounds over zeolite HSZ-360 as a reusable, heterogeneous catalyst. *Tetrahedron Lett.* **1998**, *39*, 1615−1618.
(29) Algarre, F.; Corma, A.; Garcia, H.; Primo, J. Acid zeolites as catalysts in organic reactions. Highly selective condensation of 2-alkylfurans with carbonylic compounds. *Appl. Catal., A: Gen.* **1995**, *128*, 119−126.
(30) Iwamoto, M.; Tanaka, Y.; Sawamura, N.; Namba, S. Remarkable effect of pore size on the catalytic activity of mesoporous silica for the acetalization of cyclohexanone with methanol. *J. Am. Chem. Soc.* **2003**, *125* (43), 13032−13033.
(31) Climent, M. J.; Corma, A.; Iborra, S.; Navarro, M. C.; Primo, J. Use of mesoporous MCM-41 aluminosilicates as catalysts in the production of fine chemicals: Preparation of dimethylacetals. *J. Catal.* **1996**, *161*, 783−789.
(32) Tanaka, Y.; Sawamura, N.; Iwamoto, M. Highly effective acetalization of aldehydes and ketones with methanol on siliceous mesoporous material. *Tetrahedron Lett.* **1998**, *39*, 9457−9460.
(33) Mirjalili, B. F.; Zolfigol, A. M.; Bamoniri, C. A.; Hazar, A. $Al(HSO_4)_3$ as an efficient catalyst for acetalization of carbonyl compounds under heterogeneous or solvent-free conditions. *J. Braz. Chem. Soc.* **2005**, *16*, 877−880.
(34) Mayoral, E. P.; Martin-Aranda, R. M.; Lopez-Peinado, A. J.; Ballestreos, P.; Zukla, A.; Cejka, J. Green synthesis of acetals/ketals: Efficient solvent-free process for the carbonyl/hydroxyl group protection catalyzed by SBA-15 materials. *Top. Catal.* **2009**, *52*, 148−152.
(35) Silveria, C. C.; Mendes, S. R.; Ziembowiscz, F. I.; Lenardao, E. J.; Perin, G. The use of anhydrous $CeCl_3$ as a recyclable and selective catalyst for the acetalization of aldehydes and ketones. *J. Braz. Chem. Soc.* **2010**, *21*, 371−374.
(36) Kannan, V.; Sreekumar, K.; Gil, A.; Vicente, M. A. Acetalation of pentaerithritol catalyzed by an Al-pillared saponite. *Catal. Lett.* **2011**, *141*, 1118−1122.
(37) Firouzabadi, H.; Iranpur, N.; Hazarkhani, H. New applications of solid silica chloride (SiO_2-Cl) in organic synthesis. Efficient preparation of diacetals of 2,2-bis(hydroxymethyl)-1,3-propanediol from different substrates and their transthioacetalization reactions. Efficient regeneration of carbonyl compounds from acetals and acylals. *Phosphorus, Sulfur Silicon* **2002**, *177*, 2847−2858.
(38) Rabindran, B. J.; Pandurangan, A. $H_3PW_{12}O_{40}$ supported on MCM-41 molecular sieves: An effective catalyst for acetal formation. *Appl. Catal., A: Gen.* **2005**, *295*, 185−192.
(39) Patel, P.; Shivanekar, A.; Chudasama, U. Use of zirconium tungstate in acid catalysis: Some esterification reactions. *Indian J. Chem.* **1992**, *31A*, 803−805.
(40) Shivanekar, A.; Chudasama, U. *Recent Trends in Catalysis*; Vishwanathan, B., Pillai, C. N., Eds.; Narosa Publishing House: New Delhi, 1990; p 489−497.
(41) Parikh, A.; Patel, A.; Chudasama, U. *Recent Trends in Catalysis*; Murugesan, V., Arbindoo, B., Palanichamy, M., Eds.; Narosa Publishing House, New Delhi, 1999; p 421−426.
(42) Beena, B.; Chudasama, U. A comparative study of the Brønsted acidity of zirconium phosphate and zirconium phenyl phosphonate. *Indian J. Chem. Tech.* **1995**, *2*, 339−340.
(43) Patel, S.; Chudasama, U. Synthesis, characterization and catalytic application of tin phosphate. *Indian J. Chem.* **2002**, *41A*, 1864−1866.
(44) Parikh, A.; Chudasama, U. Metal (IV) tungstates as solid acid catalysts for the synthesis of phthalate diester-dioctyl phthalate (DOP). *Indian J. Chem. Tech.* **2003**, *10*, 44−47.
(45) Joshi, R.; Patel, H.; Chudasama, U. Synthesis of monoester and diesters using eco-friendly solid acid catalysts M(IV) Tungstates and phosphates. *Indian J. Chem. Technol.* **2008**, *15*, 238−243.
(46) Patel, H.; Joshi, R.; Chudasama, U. Use of zirconium (IV) phosphate as a solid acid catalyst in some esterification reactions. *Indian J. Chem.* **2008**, *47A*, 348−352.
(47) Thakkar, R.; Chudasama, U. Synthesis of mono and diesters using eco-friendly solid acid catalyst - zirconium titanium phosphate. *Green Chem. Lett. Rev.* **2009**, *2* (2), 61−69.
(48) Joshi, R.; Chudasama, U. Synthesis of coumarins via the Pechmann condensation using inorganic ion exchangers as solid acid catalysts. *J. Sci. Ind. Res.* **2008**, *67*, 1092−1097.
(49) Ghodke, S.; Chudasama, U. Solvent free synthesis of coumarins using environment friendly solid acid catalysts. *Appl. Catal., A: Gen.* **2013**, *453*, 219−226.
(50) Patel, P.; Chudasama, U. Thermodynamics and kinetics of ion exchange of a hybrid cation exchanger, zirconium diethylene triamine pentamethylene phosphonate. *Indian J. Chem., Sect. A* **2010**, *49*, 1318−1324.
(51) Bhaumik, A.; Inagaki, S. Mesoporous titanium phosphate molecular sieves with ion-exchange capacity. *J. Am. Chem. Soc.* **2001**, *123*, 691−696.
(52) Seip, C. T.; Granroth, G. E.; Miesel, M. W.; Talham, D. R. Langmuir-Blodgett films of known layered solids: preparation and structural properties of octadecylphosphonate bilayers with divalent metals and characterization of a magnetic Langmuir-Blodgett film. *J. Am. Chem. Soc.* **1997**, *119*, 7084−7094.
(53) Nilchi, A.; Ghanadi, M. M.; Khanchi, A. Characteristics of novel types substituted cerium phosphates. *J. Radioanal. Nucl. Chem.* **2000**, *245* (2), 589−594.
(54) Agirre, I.; García, I.; Requies, J.; Barrio, V. L.; Guemez, M. B.; Cambra, J. F.; Arias, P. L. Glycerol acetals, kinetic study of the reaction between glycerol and formaldehyde. *Biomass Bioenergy* **2011**, *35*, 3636−3642.
(55) Agirre, I.; Barrio, V. L.; Güemez, B.; Cambra, J. F.; Arias, P. L. Catalytic reactive distillation process development for 1,1 diethoxy butane production from renewable sources. *Bioresour. Technol.* **2011**, *102*, 1289−1297.
(56) Chopade, S. P.; Sharma, M. M. Reaction of ethanol and formaldehyde: Use of versatile cation-exchange resins as catalyst in batch reactors and reactive distillation columns. *React. Funct. Polym.* **1997**, *32* (1), 53−65.
(57) Domalski, E. S. Selected values of heats of combustion and formation of organic compound containing C, H, N, O, P and S. *J. Phys. Chem. Ref. Data* **1972**, *1* (2), 221.
(58) Rui, P. V.; Pereira, C. S. M.; Silva, V. M. T. M.; Loureiro, J. M.; Rodrigues, A. E. Glycerol valorization as biofuel: Thermodynamic and

kinetic study of the acetalization of glycerol with acetaldehyde. *Ind. Eng. Chem. Res.* **2013**, *52*, 1538−1547.

Indian Journal of Chemistry
Vol 53A, June 2014, pp. 700-705

Kinetics, thermodynamics and ion exchange characteristics of thorium phosphate: An inorganic ion exchanger

Tarun Parangi[a], Bina Wani[b] & Uma Chudasama[a, *]

[a]Applied Chemistry Department, Faculty of Technology & Engineering, The MS University of Baroda, Vadodara 390 001, Gujarat, India

[b]Chemistry Division, Bhabha Atomic Research Centre, Mumbai 400 085, Maharashtra, India

Email: uvcres@gmail.com

Received 7 May 2013; re-revised and accepted 13 May 2014

Amorphous thorium phosphate, an inorganic cation exchanger of the class of tetravalent metal acid salts, has been synthesized by sol-gel method and subjected to physical, ion exchange and instrumental methods of characterization. Equilibrium constant values increase with increase in temperature for the transition metal ions (Co^{2+}, Ni^{2+}, Cu^{2+}, Zn^{2+}) and heavy metal ions (Cd^{2+}, Hg^{2+}, Pb^{2+}) under study, indicating that the metal ions have higher affinity for the exchanger and that the mechanism is ion exchange. $\Delta G°$ values for all the exchange reactions are negative and become more negative with increasing temperature indicating increase in feasibility and spontaneity of the exchange process. $\Delta H°$ is positive in all cases indicating complete dehydration of ions for exchange to take place. R^2 values are found to be close to unity for both Langmuir and Freundlich isotherms, providing a good fit to the experimental data for sorption of all the metal ions studied. Efficient metal ion separations have been performed which is supported by symmetrical bell shaped curves and the percentage of metal eluted. A study on regeneration and reuse of the ion exchanger shows that TP is effective up to four cycles without much decline in performance.

Keywords: Inorganic ion exchanger, Ion exchanger, Cation exchanger, Thorium phosphate, Ion exchange thermodynamics

Amongst inorganic ion exchangers, tetravalent metal acid (TMA) salts are widely studied and have attracted attention due to their excellent thermal and chemical stability, and selectivity towards certain metal ions[1-3]. There are several reports[4-11] on use of thorium phosphate as a cation exchanger, however, systematic studies on thermodynamics and kinetics of ion exchange as well as its use in metal ion separations is lacking.

In the present endeavour, an amorphous thorium phosphate (TP) in granular form with an appreciable cation exchange capacity (CEC) has been synthesized by sol-gel method. The material has been subjected to physico-chemical, ion exchange and instrumental methods of characterization. Thermodynamic and adsorption studies have been performed to explore the possible use of TP as cation exchanger. The distribution coefficient (K_d) values have been determined under different conditions. Based on the separation factor, α, a few binary and ternary metal ion separations have been performed.

Experimental

All chemicals and reagents used were of analytical grade. Deionized water was used for all the studies.

The ion exchanger, thorium phosphate (TP) was synthesized as follows: An aqueous solution of $Th(NO_3)_4 \cdot 5H_2O$ (0.1 *M*, 50 mL) was added drop wise (flow rate 1 mL/min) to an aqueous solution of $NaH_2PO_4 \cdot 2H_2O$ (0.2 *M*, 100 mL) with continuous stirring for an hour at room temperature. A gelatinous precipitate was obtained, which was allowed to stand for 5 h at room temperature, then filtered, washed with deionized water to remove adhering ions and dried at room temperature. The material was then broken down to the desired particle size (30–60 mesh (ASTM)) by grinding and sieving, and then subjected to acid treatment[12,13]. This material was used for all studies.

TP was characterized by elemental analysis (ICP-AES), spectral analysis (FTIR), thermal analysis (TGA and DSC), XRD and SEM.

TP particles of definite mesh size (30–60 mesh ASTM) were used for exchange studies with. For equilibrium time determination, 0.1 g of exchanger was shaken with 0.002 *M* metal ion solution in stoppered conical flasks, for varying time in the range of 30 min to 6 h, with 30 min time interval at a particular temperature (303 K).

The equilibrium experiments were performed by shaking 100 mg of the exchanger particles at the desired temperature (303–333 K with 10 K interval) in a shaker bath for 6 h with 20 mL of a mixture of solution containing 0.06 *M* HCl and the appropriate metal ion in varying volume ratios (1, 3, 5,…19 mL, 0.02 *M* metal ion solution and 19, 17, 15,...1 mL of 0.06 *M* HCl, respectively were prepared) having constant ionic strength (0.06 *M*).

Adsorption/ion exchange of metal ions under study was carried out in the *p*H range 1–7. To 0.1 g of the exchanger, 10 mL of 0.002 *M* metal ion solution was added and *p*H adjusted in acidic range using dilute HNO_3 and in alkaline range using dilute NaOH and the mixture was shaken for 30 min.

Metal ion solution (10 mL) of 0.002 *M* was equilibrated in stoppered conical flasks at the desired temperatures (303–333 K with 10 K interval) and at specific time intervals with increments of 10 min. (10–200 min). In each case, the *p*H of the solution was adjusted to the value at which maximum sorption of respective metal ion takes place.

In all experiments, the metal ion concentration was evaluated by EDTA titration[2]. For adsorption experiments, the %uptake was calculated using the formula, $[(C_o–C_e)/C_o]\times100$, where C_o is the initial concentration of metal ion in mg/L and C_e is the final concentration of metal ion in mg/L.

K_d was evaluated at optimum conditions by batch process (optimum metal ion concentration, *p*H of maximum adsorption for maximum equilibrium time) using 0.1 g of the exchanger in aqueous as well as various electrolyte media like NH_4NO_3, HNO_3, $HClO_4$ and CH_3COOH of 0.02 and 0.2 *M* concentration at room temperature. K_d was determined using the expression, $K_d = [(I-F)/F] \times V/W$ (mL/g) where I = total amount of the metal ion in the solution initially, F = total amount of metal ions left in the solution after equilibrium, V = volume of the metal ion solution, and, W = weight of the exchanger in g[12,16].

For the metal ions under study, BTC was determined by known method[12,16]. A breakthrough curve was obtained by plotting the ratio C_e/C_o against the effluent volume, where C_o and C_e are the concentrations of the initial solution and effluent, respectively. BTC was calculated using the formula, $(C_oV_{(10\%)})/W$ (mmol/g) where C_o is concentration of metal ion in mol/L, $V_{(10\%)}$ is the volume of metal ion solution passed through column when exit concentration reaches 10% of the initial concentration in mL and W is the weight of the exchanger in g[12,16].

For elution studies (single metal), the column was prepared as reported earlier[12,16]. The metal ion solution (0.001 *M*, 10 mL) was loaded onto the column and eluted with eluents like HNO_3, $HClO_4$, CH_3COOH, and NH_4NO_3 of 0.02 and 0.2 *M* concentration.

For binary and ternary separations, the mixture of metal ion solutions (0.001 *M*, 10 mL of each metal ion) to be separated was loaded onto the column. The separation was achieved by passing suitable eluent through the column.

The amount of metal ion recovered was calculated in terms of percentage elution expressed as, $\%E = (C_e/C_o)\times100$ where C_e is the concentration of the metal ion in the eluted solution and C_o is the concentration of metal ion loaded onto the column.

Regeneration and reuse of the ion exchanger (TP) was performed in the case of Pb^{2+} by batch method. Pb^{2+} solution (0.006 *M*) was treated with 0.1 g of TP and kept for 6 h (maximum equilibrium time) after which the metal ion concentration was determined by EDTA titration and K_d value was determined. Pb^{2+} exchanged onto TP was eluted out by treating with HNO_3 (1 *M*, 50 mL) till Pb^{2+} was completely removed. This regenerated TP was used to determine K_d value for Pb^{2+}. The process was repeated until a wide variation in K_d values was observed. The %retention in K_d values, $K_{d(R)}$, was determined using the expression, $K_{d(R)} = [K_{d(C)}/K_d]\times100$ where K_d = initial value obtained, $K_{d(C)} = K_d$ determined in each subsequent cycle.

Results and discussion

TP was obtained as white hard granules. Physical and ion exchange characteristics of TP have been presented in Table 1. Elemental analysis shows Th:P ratio as 1:2 (Table 1).

The Na^+ CEC evaluated by column method at room temperature is 1.45 meq/g. The Na^+ CEC of the calcined samples (Table 1) shows that CEC values decrease with increasing temperature, which is attributed to the loss of moisture and condensation of structural hydroxyl groups.

A study on the chemical stability shows that TP is stable in acids and organic solvent media but not so stable in base medium (Table 1).

The FTIR spectrum of TP exhibits a broad band in the region ~3400 cm^{-1}, which is attributed to asymmetric and symmetric -OH stretching vibration due to residual water and presence of structural hydroxyl groups, H^+ of the -OH being cation exchange sites. These sites are also referred to as defective P-OH groups[3]. A sharp medium band at ~1630 cm^{-1} is attributed to aquo H-O-H bending[17,18]. The band at 1050 cm^{-1} is attributed to P=O stretching, while the bands at 620 cm^{-1} and 500 cm^{-1} are attributed to Th-O stretching[9,10].

TGA exhibits two regions of weight loss. The first weight loss of ~13% up to 120 °C is attributed to loss of moisture/hydrated water and the second weight loss of ~8% in the range of 120–500 ºC is attributed to the condensation of structural hydroxyl groups.

DSC exhibits an endothermic peak at ~133 ºC, attributed to loss of moisture/hydrated water. Beyond this temperature, no peaks are observed indicating absence of any phase change in the material upon thermal treatment in the range studied.

Absence of sharp peaks in XRD indicates amorphous nature of the material. SEM image at room temperature, exhibits irregular morphology.

Thermodynamics of ion exchange has been studied for Cu^{2+}, Zn^{2+}, Co^{2+}, Ni^{2+} (transition metal ions) and Pb^{2+}, Cd^{2+}, Hg^{2+} (heavy metal ions) and results presented in Table 2. Equilibrium constant (K) values increase with increase in temperature for all metal ions under study (Table 2), indicating that the metal ions have higher affinity for the exchanger and that the mechanism is ion exchange[19-21].

The $\Delta G°$ for all the exchange reactions is negative, over the entire temperature range, indicating that the exchanger has a greater preference for metal ions than H^+ ions. The $\Delta G°$ values become more negative with increasing temperature, confirming that the exchange is favoured with increasing temperature. At any given temperature, $\Delta G°$ follows the order (increasing negativity): $Cu^{2+} > Zn^{2+} > Ni^{2+} > Co^{2+}$ amongst the transition metal ions and $Pb^{2+} > Cd^{2+} > Hg^{2+}$ amongst the heavy metal ions. $\Delta H°$ is positive in all cases and follows the order: $Cu^{2+} > Zn^{2+} > Ni^{2+} > Co^{2+}$ and $Pb^{2+} > Cd^{2+} > Hg^{2+}$. Higher/positive values of enthalpy change indicate higher endothermicity of the exchange process and requirement of more energy for dehydration to occur[13,18,22]. The $\Delta H°$ values indicate that probably complete dehydration occurs in the case of Cu^{2+} and Pb^{2+}. Further, trends in $\Delta H°$ values are also supportive of trends in $\Delta G°$ values. The entropy change ($\Delta S°$) also follows the same trend as $\Delta H°$. Higher values observed in the case of Cu^{2+} and Pb^{2+}, are attributed to greater dehydration, which indicates the greater disorder produced during the exchange.

Langmuir constants (b and V_m) and Freundlich constants (K and $1/n$) were obtained from the slopes and intercepts of the linear plots (Supplementary data, Table S1). R^2 values are found to be close to unity for both the isotherms and provide a good fit to the experimental data for sorption of all the metal ions taken (except Hg^{2+} for Freundlich isotherm). Variation in R^2 values is attributed to the fact that the surface adsorption is not a monolayer with a single site. Two or more sites with different affinities may be involved in metal ion sorption[2]. In the present

Table 1 — Physical and ion exchange characteristics of thorium phosphate

Appearance	White hard granules
Particle size	250-590 μ
Moisture content	8.07%
True density	2.98 g/mL
Apparent density	1.50 g/mL
Void volume fraction	0.88
Conc. of fixed ionogenic groups	6.52 mmol/g
Volume capacity of resin	3.23 meq/mL
Nature of exchanger	Weak cation exchanger
CEC (Room temp.)	1.48 meq/g
100 °C	1.39 meq/g
200 °C	0.46 meq/g
300 °C	0.28 meq/g
400 °C	0.16 meq/g
500 °C	0.10 meq/g
Chemical stability	Max. tolerable limits
Acids	1 *N* H_2SO_4, 2 *N* HNO_3, 3 *N* HCl
Bases	0.5 *N* NaOH, 0.5 *N* KOH
Organic solvents	Ethanol, Benzene, Acetone, Acetic acid, Toluene, Xylene
Elemental analysis (ICP-AES)	Th = 35.10% and P = 9.40%

Table 2 — Thermodynamic parameters for M^{2+} - H^+ exchange with thorium phosphate

System	Temp. (K)	K_a	ΔG^0 (kJ/mol)	ΔH^0 (kJ/mol)[a]	ΔS^0 (J/mol K)
$Co^{2+} – H^+$	303-333	1.52-1.67	-0.53-0.72	2.69	10.62-10.22
$Ni^{2+} – H^+$	303-333	1.73-2.65	-0.69-1.34	12.04	42.06-40.23
$Cu^{2+} – H^+$	303-333	2.31-16.26	-1.05-3.86	69.37	230.69-220..46
$Zn^{2+} – H^+$	303-333	2.08-3.10	-0.92-1.56	43.59	145.62-137.57
$Cd^{2+} – H^+$	303-333	1.78-6.96	-0.68-2.68	40.74	136.60-130.41
$Hg^{2+} – H^+$	303-333	1.48-3.44	-0.49-1.71	18.47	63.93-60.64
$Pb^{2+} – H^+$	303-333	4.75-249.63	-9.95-15.11	138.14	462.39-441.94

[a]Average values calculated from the van't Hoff isochore equation.

study, low values of b indicate favorable adsorption. V_m values reflecting the maximum adsorption capacity of metal ions towards exchanger follows the order: $Cu^{2+} > Zn^{2+} > Ni^{2+} > Co^{2+}$ amongst transition metal ions and $Pb^{2+} > Cd^{2+} > Hg^{2+}$ amongst heavy metal ions at 303 K. The values of $1/n$ and R_L are between 0 and 1, which indicates normal isotherm and favourable adsorption respectively and agree with reported results[23,24].

K_d values determined in aqueous medium by batch process at optimum condition and break through capacity (BTC) values determined by column method follow the same order: $Cu^{2+} > Zn^{2+} > Ni^{2+} > Co^{2+}$ amongst the transition metal ions and $Pb^{2+} > Cd^{2+} > Hg^{2+}$ amongst the heavy metal ions (Table 3), confirming order of metal ion affinity towards TP.

The elution behaviour of the single metal ions under study was studied with different eluents such as HNO_3, $HClO_4$, CH_3COOH and NH_4NO_3 (Table 4). Good elution is observed due to presence of single metal ion and non-interference of elements. All elution curves are symmetrical bell shaped, indicating elution efficiency. Higher concentration of eluent and acids in general, are better eluents. HNO_3 (0.2 M) is the best eluent for most metal ions. The percentage of metal eluted is in keeping with the fact that metal ions with high K_d values are less eluted and vice-versa[13,16,25].

A study on distribution behaviour of metal ions in various electrolyte media gives an idea about the eluents that can be used for separation[13,16,25]. For a given metal ion pair, the electrolyte media in which the separation factor is the highest, is selected as the eluent.

Efficient binary separations for the following metal ion pairs: Ni^{+2}-Cu^{+2}, Co^{+2}-Cu^{+2}, Ni^{+2}-Zn^{+2}, Hg^{+2}-Pb^{+2}, Cd^{+2}-Hg^{+2} and Cd^{+2}-Pb^{+2} were carried out, which is supported by symmetrical bell shaped curves and % metal eluted (Fig. 1). In ternary separations for Co^{2+}- Ni^{2+}- Cu^{2+} (transition metal ions) and Hg^{2+}- Cd^{2+}- Pb^{2+} (heavy metal ions), three distinct peaks were observed (Fig. 1), however, with tailing effects for every metal ion eluted. The percentage of metal eluted was also lower as compared to single and binary metal ion separations (Supplementary data, Table S2).

A study on regeneration and reuse shows that the exchanger, once used, can be converted back to its original form by desorption of the metal ions with

Table 3 — Breakthrough capacity (mmol/g) and distribution coefficient (K_d) values (mL/g) for thorium phosphate

Metal ion	Ionic radii (Å)	BTC (mmol/g)	DW	K_d (mL/g)[a]							
				NH_4NO_3		HNO_3		$HClO_4$		CH_3COOH	
				0.02 M	0.2 M	0.02 M	0.2 M	0.02 M	0.2 M	0.02 M	0.2 M
Co^{2+}	0.72	0.24	87.94	72.94	18.86	5.56	18.99	9.27	3.00	124.80	69.30
Ni^{2+}	0.72	0.32	167.78	144.30	151.21	27.60	NS	24.17	19.00	88.20	73.31
Cu^{2+}	0.74	0.45	270.43	207.00	74.19	49.66	NS	17.37	NS	287.32	118.80
Zn^{2+}	0.74	0.34	180.36	134.40	94.15	48.31	24.12	86.47	NS	181.42	140.26
Cd^{2+}	0.97	0.47	245.00	179.20	65.10	20.00	NS	23.75	NS	235.42	180.90
Hg^{2+}	1.44	0.22	80.18	143.00	136.50	150.40	118.10	186.20	178.21	140.40	128.30
Pb^{2+}	1.10	0.96	2390.16	1400.00	978.20	560.76	78.72	526.77	89.26	2980.42	1788.58

[a]K_d values obtained at optimum conditions; Maximum deviation in K_d values = ±3.
NS = No sorption.

Table 4 — Percentage elution of various metal ions in different electrolyte media using thorium phosphate

Metal ion	E (%)[a]							
	NH_4NO_3		HNO_3		$HClO_4$		CH_3COOH	
	0.02 M	0.2 M	0.02 M	0.2 M	0.02 M	0.2 M	0.02 M	0.2 M
Co^{2+}	90.19	92.15	94.60	96.10	93.13	94.11	90.19	92.15
Ni^{2+}	92.15	93.36	96.93	97.95	93.50	94.89	91.83	93.33
Cu^{2+}	91.17	93.13	94.10	97.05	95.05	96.00	90.40	91.17
Zn^{2+}	88.27	90.23	94.00	95.09	91.21	95.00	86.27	92.15
Cd^{2+}	88.51	91.68	93.06	95.71	92.00	94.00	90.00	91.09
Hg^{2+}	91.42	92.38	94.28	88.14	94.26	94.76	89.52	91.42
Pb^{2+}	80.31	84.22	84.69	95.05	85.57	87.75	79.59	82.26

[a]Eluent volume = 70 mL and 60 mL for 0.02 M and 0.2 M electrolytes respectively.
Maximum deviation in %elution of metal ions = ±2.

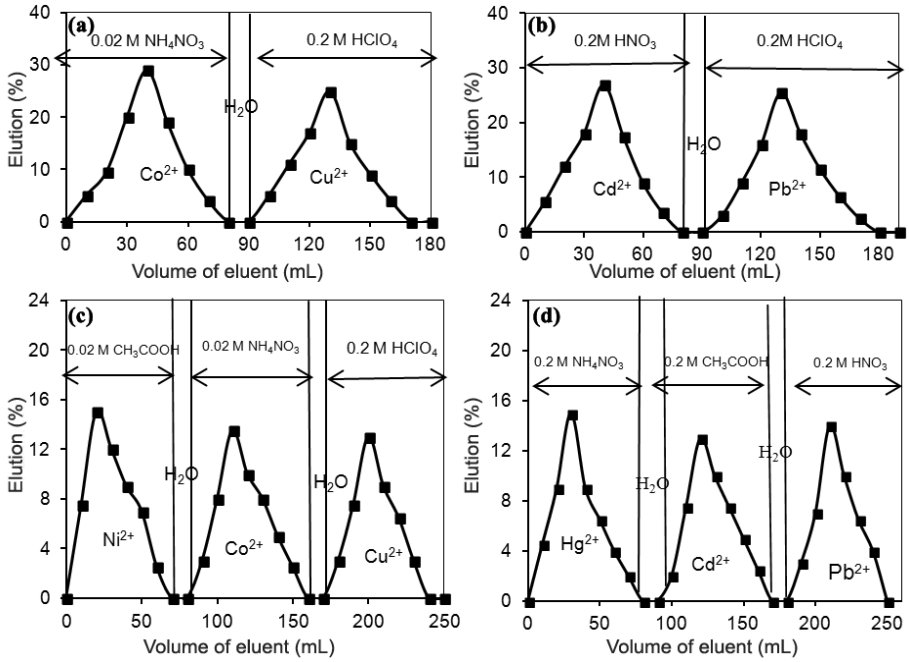

Fig. 1– Binary separation of (a) Co^{2+} - Cu^{2+}, (b) Cd^{2+} - Pb^{2+}, and, Ternary separation of (c) Ni^{2+} - Co^{+2} - Cu^{+2} and (d) Hg^{2+} - Cd^{2+} - Pb^{2+} using TP.

1 *M* HNO_3. It is observed that K_d values is almost the same (~100 %) up to 4 cycles, indicating that TP can be regenerated and reused without much decline in performance.

In the present study, the ion exchanger, thorium phosphate, exhibits promising ion exchange characteristics i.e., good CEC, thermal and chemical stability, good regeneration capacity and high affinity for Cu^{2+} and Pb^{2+}. Feasibility of ion exchange has been studied and correlated with K, $\Delta G°$, $\Delta H°$ and $\Delta S°$ values. Data evaluated from isotherm studies undertaken was found to match with Langmuir and Freundlich isotherm models. High selectivity for Cu^{2+} and Pb^{2+} indicates good separation characteristics (Ni^{2+}-Cu^{2+} and Co^{2+}-Cu^{2+}, Cd^{2+}-Pb^{2+} and Hg^{2+}-Pb^{2+}). Efficient metal ion separations carried out using TP indicates high potential for this material to be used as a cation exchanger.

Supplementary data

Supplementary data associated with this article i.e., Tables S1 and S2, are available in the electronic form at http://www.niscair.res.in/jinfo/ijca/IJCA_53A(06)700-705_SupplData.pdf.

Acknowledgement

The authors thank DAE-BRNS for providing financial support and research fellowship to one of them (TP).

References

1 Varshney K G & Khan M A, *Inorganic Ion Exchangers in Chemical Analysis,* edited by M Qureshi & K G Varshney, (CRC Press, Boca Raton Florida) 1991, p. 177-270.
2 Maheria K & Chudasama U, *J Indian Inst Sci*, 86 (2006) 515.
3 Bhaumik A & Inagaki S, *J Am Chem Soc*, 123 (2001) 691.
4 Khan A A, Inamuddin & Alam M M, *React Funct Polymers*, 63(2) (2005) 119.
5 Varshney K G & Tayal N, *Langmuir,* 17 (2001) 2589.
6 Varshney K G, Tayal N, Khan A A & Niwas R, *Colloids Surfaces A: Phys Chem Eng Aspects,* 181 (2001) 123.
7 Varshney K G, Agrawal A & Mojumdar S C, *J Therm Anal Calor,* 90(3) (2007) 721.
8 Khan A A & Inamuddin, *J App Polym Sci*, 105 (2007) 2806.
9 Islam M & Patel R, *J Hazard Mater,* 156 (2008) 509.
10 Islam M & Patel R, *J Hazard Mater,* 172 (2009) 707.
11 Islam M, Mishra P C & Patel R, *Chem Eng J*, 166 (2011) 978.
12 Patel P & Chudasama U, *J Scient Ind Res,* 69 (2010) 756.
13 Thakkar R & Chudasama U, *J Hazard Mater* 172 (2009) 129.
14 Helfferich F, *Ion Exchange*, (McGraw-Hill, New York) 1962.
15 Kunin R, *Ion Exchange Resin*, (Wiley, London) 1958.
16 Patel P & Chudasama U, *Ion Exchange Lett,* 4 (2011) 7.
17 Seip C T, Granroth G E, Miesel M W & Talham D R, *J Am Chem Soc*, 119 (1997) 7084.
18 Patel P & Chudasama U, *Indian J Chem,* 49A (2010) 1318.
19 Jayswal A & Chudasama U, *J Scient Ind Res*, 66 (2007) 945.
20 Tagami L, Onelia Aparecida Andreo dos Santos, Eduardo Falabella Sousa-Aguiar, Pedro Augusto Arroyo & Maria

Angelica Simoes Dornellas de Barros, *Acta Scient Technol*, 23 (2001) 1351.

21 Pehlivan E, Ersoz M, Pehlivan M, Yildiz S & Duncan H, *J Coll Interface Sci*, 170 (1995) 320.

22 Kurtuoglu A E & Atun G, *Sep Purif Technol*, 50 (2006) 62.

23 Voudrias E, Fytianos K & Bozani E, *Global Nest: The Int J*, 4 (2002) 75.

24 Akpomie G K, Ogbu I C, Osunkunle A A, Abuh M A & Abonyi M N, *J Emerg Trends Engg App Sci,* 3(2) (2012) 354.

25 Patel P & Chudasama U, *Sep Sci Technol*, 46 (2011) 1346.

Electrochimica Acta 148 (2014) 79–84

Contents lists available at ScienceDirect

Electrochimica Acta

journal homepage: www.elsevier.com/locate/electacta

A Comparative Study of Proton Transport Properties of Cerium (IV) and Thorium (IV) Phosphates

Tarun Parangi [a], Bina Wani [b], Uma Chudasama [a,*]

[a] Applied Chemistry Department, Faculty of Technology & Engineering, The M.S. University of Baroda, Vadodara 390001, Gujarat,India
[b] Chemistry Division, Bhabha Atomic Research Centre, Mumbai 400085, Maharashtra, India

ARTICLE INFO

Article history:
Received 21 June 2014
Received in revised form 2 October 2014
Accepted 10 October 2014
Available online 14 October 2014

Keywords:
Cerium phosphate
thorium phosphate
tetravalent metal acid salt
proton conduction
impedance
activation energy

ABSTRACT

In the present endeavour, amorphous cerium phosphate (CP) and thorium phosphate (TP) have been synthesized by sol-gel method. Further, CP and TP have also been synthesized under microwave irradiation to yield CP_M and TP_M. The materials have been characterized for elemental analysis (ICP-AES), spectral analysis (FTIR), thermal analysis (TGA and DSC), X-ray diffraction studies, SEM, EDX and surface acidity (NH_3-TPD). Chemical stability of the materials in various acids, bases and organic solvent media has been studied. The proton transport properties of these materials have been explored and compared by measuring conductance at different temperatures using an impedance analyzer. It is observed that conductivity decreases with increasing temperature in all cases and mechanism of transportation is proposed to be Grotthuss type. Trends in specific conductance of CP, TP, CP_M and TP_M has been compared and correlated based on cation exchange capacity values and surface acidity. Mechanism of conductance in these materials has been discussed based on conductivity (σ) data and activation energy (E_a).

1. Introduction

As a new clean energy, fuel cell technology has attracted worldwide attention for its enormous promise in efficient and environment friendly power source for mobile and stationary power application. Therefore, there has been intensification of research aimed at discovering new proton conducting materials and determining their conduction mechanism, which is driven by the potential use of such compounds in fuel cells, sensors, water electrolysis units and other electrochemical devices. An entire class of materials has gained increasing interest as proton conductors: polymers, oxide ceramics, intercalation compounds etc. A brief overview of the past and present state on solid-state proton conductors has been reported [1–3].

Proton conductors are often considered to be electrolytes in which hydrogen is transported towards and evolved at the cathode during electrolysis. Proton transport includes transport of proton (H^+) and any assembly that carries protons (OH^-, H_2O, H_3O^+, NH_4^+, HS^-etc.). The transport of protons (H^+) between relatively stationary host anions is termed the 'Grotthuss' or 'free-proton' mechanism [4]. The Grotthuss mechanism requires close proximity of water molecules which are held firmly but free to rotate. Transport by any other species is termed "Vehicle mechanism". Vehicle mechanism is most frequently encountered in aqueous solution and other liquids/melts. In solids, vehicle mechanism is usually restricted to materials with open structures (channels, layers) to allow passage of large ions and molecules. Compounds with smaller amounts of water would be expected to conduct by the vehicle mechanism in which a nucleophilic group such as H_2O or NH_3 acts as a proton carrier. The classification of proton conductors, according to the method of preparation, chemical composition, structural dimensionality, mechanism of conduction etc., has been summarized in a comprehensive book on proton conductors [5].

The crystal structure and proton conductivity of cerium pyrophosphate have been investigated to explore its potential electrolyte applications for intermediate temperature fuel cell [6]. Casciola et al. have reported ac conductivity of cerium phosphate in hydrogen form at relative humidities (from 11 to 90%) at temperatures from 20 to 60 °C. The measured conductivities values lie in the ranges from 3×10^{-4} S/cm (at 20 °C and 90% relative humidities) [6]. M-V Le et al. have reported proton conductors of cerium pyrophosphate for intermediate temperature fuel cell [7]. Its conductivity, measured with impedance spectroscopy, is higher than 10^{-2} S/cm in the intermediate temperature range, with a maximum value 3.0×10^{-2} S/cm at

* Corresponding author. Tel.: + 91 265 2434188x415/942 634 4434; fax: +91 265 2 423 898.
E-mail addresses: juvenile34@gmail.com (T. Parangi), uvcres@gmail.com (U. Chudasama).

http://dx.doi.org/10.1016/j.electacta.2014.10.032
0013-4686/

180 °C. When 10 mol% Mg is doped on the Ce site of CeP_2O_7, the maximum conductivity is raised to 4.0×10^{-2} S/cm at 200 °C. Onoda et al. have been reported synthesis and electrical conductivity of bulk tetravalent Gd doped cerium pyrophosphate in various conditions (dry, H_2O and D_2O) [8]. Nicole et al. have reported structure and electronic properties of cerium orthophosphate [9]. EG Moaral et al. have reported impedance analysis of Sr-substituted $CePO_4$ with mixed protonic and p-type electronic conduction. The reported conductivity is $\sim 3.5 \times 10^{-3}$ S/cm at 600 °C [10]. Zhongfang Li et al. have reported synthesis and characteristics of proton-conducting membranes based on cerium sulfophenyl phosphate (CeSSP) and poly (2,5-benzimidazole) [11]. The proton conductivity of membrane doped in 38 wt. % CeSSP reaches 0.14 S/cm at 180 °C under 100% humidity. Khan et al. have reported electrical conductivity study of an organic-inorganic composite cation-exchanger: polypyrrole thorium phosphate [12]. The conductivities values lie in the semiconducting region, in the order of 10^{-6} to 10^{-4} S/cm range at 50 to 150 °C temperature range at an interval of 20 °C. Clearfield has discussed structural concepts in inorganic proton conductors [2]. Barboux et al. have examined ac conductivity of fibrous cerium phosphates $Ce(HPO_4)_2 \cdot nH_2O$ by the complex impedance method as a function of temperature and water pressure [13], the bulk conductivity is of the order of 10^{-5} S/cm while the surface conductivity is 10^{-4} S/cm. The conductivity increased very slowly as the water content rose to a value of $n = 3$, beyond this water level the conductivity increased rapidly.

Inorganic ion exchangers of the class of tetravalent metal acid (TMA) salts exhibit the general formula $M(IV)(HXO_4)_2 \cdot nH_2O$ where M (IV) = Zr, Ti, Sn etc. and X = P, Mo, W, As, Sb, etc. TMA salts possess structural hydroxyl protons that are responsible for their ion-exchange behaviour. The number of protons present in the structural hydroxyl groups indicates the potential of TMA salts to exhibit solid state proton conduction. When these –OH groups are hydrated, the protons can move easily on the surface, thus accounting for their conductivities, which depend strongly on relative humidity, surface area and degree of crystallinity. Alberti and coworkers have shown that the surface conducts protons a thousand times faster than bulk protons. M(IV) phosphates of the class of TMA salts hold great promise as proton conducting materials possessing high conductivity and thermal stability at medium temperatures. From our laboratory, we have reported proton transport properties of amorphous M(IV) phosphates and tungstates where M(IV) = Zr, Sn and Ti and compared their proton conduction behaviour [14–18]. However not much work has been explored on phosphates of Ce(IV) and Th(IV).

In the present endeavour, amorphous cerium phosphate (CP) and thorium phosphate (TP) have been synthesized by soft chemistry route sol-gel method. Further, CP and TP have also been synthesized under microwave irradiation to yield CP_M and TP_M. The materials have been characterized for elemental analysis (ICP-AES), spectral analysis (FTIR), thermal analysis (TGA and DSC), X-ray diffraction studies, SEM, EDX and surface acidity (NH_3-TPD). Chemical stability of the materials in various acids, bases and organic solvent media has been studied. The transport properties of these materials have been explored by measuring specific proton conductance at different temperatures in the range 30–120 °C at 10 °C intervals, using a Solartron Dataset Impedance Analyzer (SI 1260) over the frequency range 1 Hz–10 MHz at a signal level below 1 V. Based on the specific conductance data and Arrhenius plots, a suitable mechanism has been proposed and the conductance performance of CP, TP, CP_M and TP_M compared.

Table 1
Data of elemental analysis (ICP-AES) and EDX analysis.

Materials	ICP-AES analysis (%)		EDX analysis (atomic %)	
	M(IV)	P	M(IV)	P
CP (Fresh)	33.15	15.11	34.95	65.05
CP (Spent)	–	–	38.24	61.76
TP (Fresh)	35.10	9.40	35.75	64.25
TP (Spent)	–	–	37.52	62.48

* For ICP-AES, detection limits = 0.10 ppm.

2. Experimental

2.1. Chemicals

Thorium nitrate ($Th(NO_3)_4 \cdot 5H_2O$), ceric sulphate ($Ce(SO_4)_2 \cdot 4H_2O$) and sodium dihydrogen phosphate ($NaH_2PO_4 \cdot 2H_2O$) were procured from Loba Chemicals, Mumbai. Deionized water was used for all the studies.

2.2. Material Synthesis

CP and TP were synthesized by sol-gel method varying several parameters such as mole ratio of reactants, mode of mixing (metal salt solution to anion salt solution or vice versa), temperature, pH and rate of mixing. The main objective was to obtain a material with high CEC/protonating ability. Several sets of materials were prepared varying conditions in each case using CEC as the indicative tool. (SI - Tables 1 and 2 describe optimization of reaction parameters for synthesis of CP and TP respectively).

2.2.1. Synthesis of CP at optimized condition

A solution containing $Ce(SO_4)_2 \cdot 4H_2O$ [0.1 M, 50 mL in 10% (w/v) H_2SO_4] was prepared, to which $NaH_2PO_4 \cdot 2H_2O$ [0.3 M, 50 mL] was added dropwise (flow rate 1 mL/min) with continuous stirring for an hour at room temperature, when gelatinous precipitates were obtained (Step-I). The resulting gelatinous precipitate was allowed to stand for 3 h at room temperature, then filtered, washed with conductivity water to remove adhering ions and dried at room temperature (Step-II).

2.2.2. Synthesis of TP at optimized condition

An aqueous solution of $Th(NO_3)_4 \cdot 5H_2O$[0.1 M, 50 mL] was added drop wise (flow rate 1 mL/min) to an aqueous solution of $NaH_2PO_4 \cdot 2H_2O$ [0.2 M, 100 mL] with continuous stirring for an hour at room temperature, when gelatinous precipitates were obtained (Step-I).

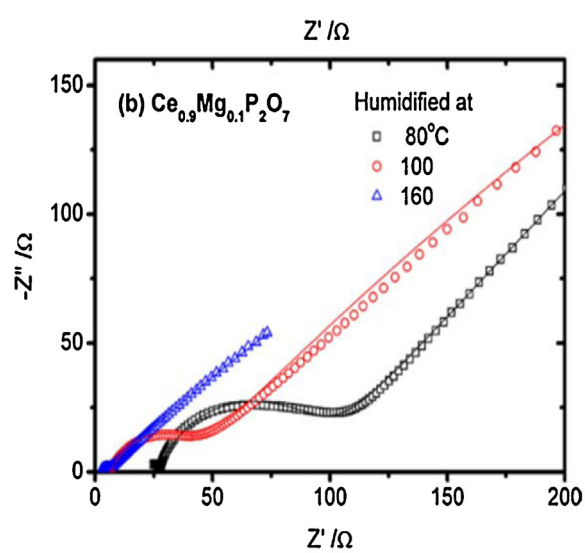

Fig. 1. Complex impedance plot [25].

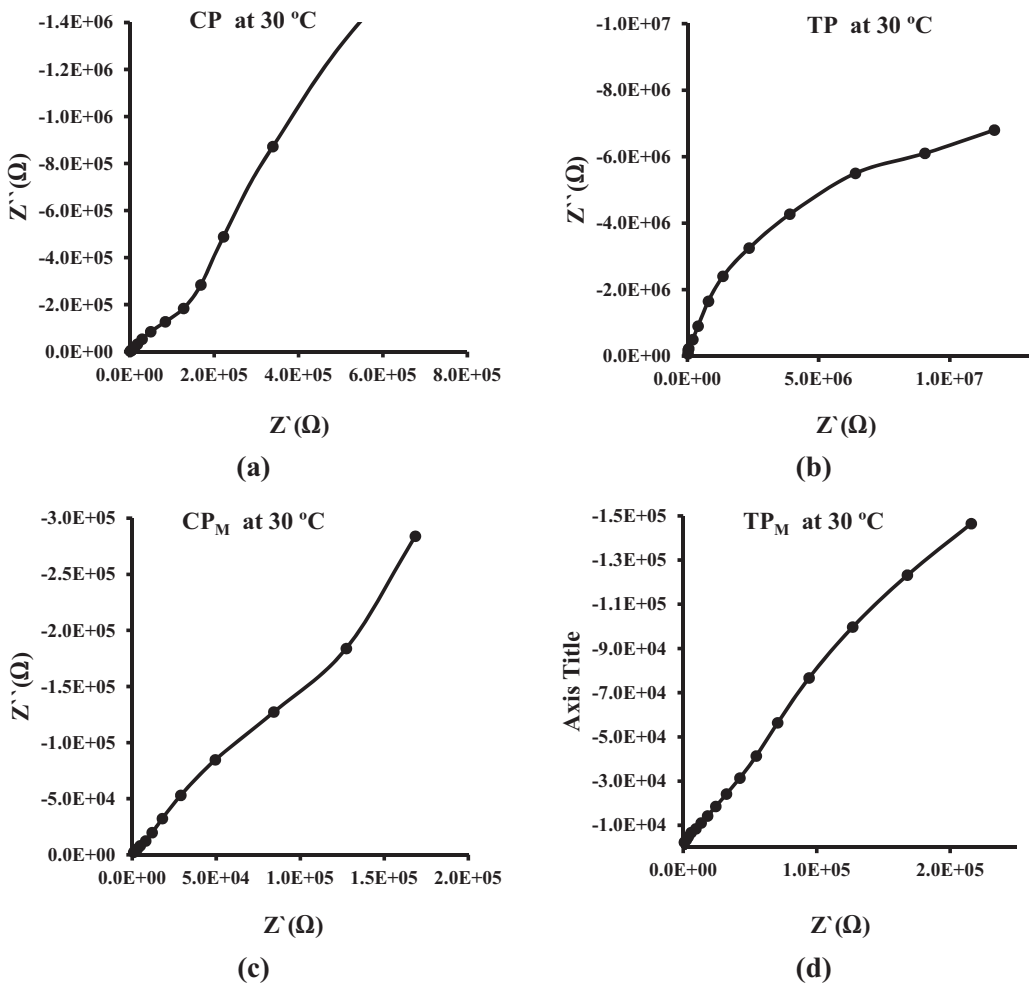

Fig. 2. Complex impedance (at 30 °C) for (a) CP (b) TP, (c) CP_M and (d) TP_M.

The resulting gelatinous precipitate was allowed to stand for 5 h at room temperature, then filtered, washed with double distilled water to remove adhering ions and dried at room temperature (Step-II).

2.2.3. Synthesis of CP and TP under microwave irradiation

Gelatinous precipitate obtained in step-I was subjected to microwave irradiation for optimum time and temperature (SI – Table 3), then filtered, washed with double distilled water to remove adhering ions and dried at room temperature (Step-II).

2.2.4. Acid treatment

The above dried materials obtained in step-II were broken down to the desired particle size [30–60 mesh (ASTM)] by grinding and sieving. 5 g of this material was treated with 50 mL of 1 M HNO_3 for 30 min with occasional shaking. The material was then separated from acid by decantation and treated with deionized water to remove adhering acid. This process (acid treatment) was repeated at least 5 times for both the materials. After final washing, the material was dried at room temperature.

2.3. Characterization

2.3.1. Chemical stability

The chemical stability of the materials in various acids (HCl, H_2SO_4, HNO_3), bases (NaOH and KOH) and organic solvent media (ethanol, propanol, butanol, benzyl alcohol, cyclohexane, toluene, xylene and acetic acid) was examined by taking 0.5 g of each of the synthesized material in 50 mL of the particular medium and allowed to stand for 24 h. The change in color, weight and nature was observed.

2.3.2. Cation exchange capacity (CEC)

The protonating ability of materials was determined as Na^+ CEC using column method by optimizing volume and concentration of sodium acetate solution [19,20].

2.3.3. Instrumentation

All synthesized materials were subjected to instrumental methods of analysis/characterization. FTIR spectra were recorded using KBr pellet on Shimadzu (Model 8400 S). Thermal analysis (TGA) was carried out on a Shimadzu (Model TGA 50) thermal analyzer at a heating rate of 10 °C/min and DSC was analyzed on Shimadzu (Model DSC-50). X-ray diffractogram ($2\theta = 10–80°$) was obtained on X-ray diffractometer (Bruker AXS D8) with Cu-Kα radiation with nickel filter. SEM and EDX of the sample were scanned on Jeol JSM-5610-SLV scanning electron microscope. Surface acidity was determined on Chemisorb 2720, by a temperature programmed desorption (TPD) of ammonia. All materials were preheated at 150, 200 and 700 °C temperatures and thereafter ammonia was chemisorbed at 120 °C and then desorption was carried out upto 700 °C at a heating rate of 10 °C/min in all cases.

2.3.4. Conductivity measurements

The conductivity of the materials was measured on pellets of 10 mm diameter and 1·5–2 mm thickness. The opposite sides of the

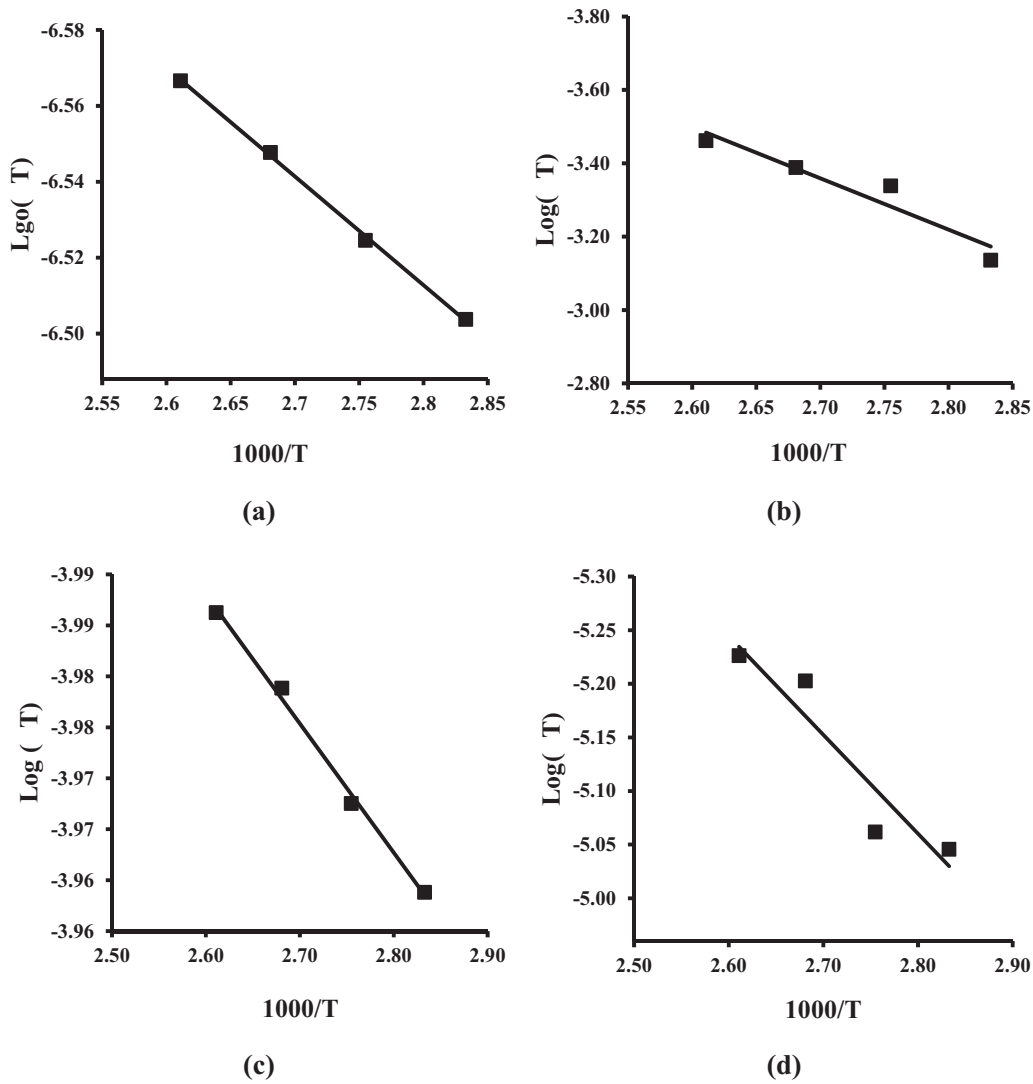

Fig. 3. Arrhenius plots (temperature range 90–120 °C) for (a) CP (b) TP, (c) CP_M and (d) TP_M.

pellets were coated with conducting silver paste to ensure good electrical contact. Complex impedance was measured in the temperature range 30–120 °C, at 10 °C intervals using Solartron Dataset Impedance Analyzer (SI 1260), over a frequency range 1 Hz-10 MHz at a signal level below 1 V, interfaced to a minicomputer for data collection. In all cases, since the impedance plots of the materials consist of single depressed semicircle, the conductivity was obtained by arc extrapolation to the real axis, taking into account the geometrical sizes of the pellets.

3. Results and Discussion

3.1. Material characterization

CP and TP were obtained as yellow and off white hard granules respectively. Elemental analysis performed by ICP-AES, for both CP and TP, show ratio of M:P to be 1:2, which is well supported by EDX analysis (SI - Figs. 1 and 2) (Table 1).

Thermal behavior of several TMA salts have been investigated and generally examined for loss of moisture ~80 °C, loss of external water molecules ~100–180 °C and for condensation of the structural hydroxyl groups ~180–500 °C and above [19]. TGA of CP and TP (SI - Fig. 3) reveals that CP exhibits the first weight loss ~13% and the second weight loss ~8% while TP exhibits the first weight loss ~11% and the second weight loss ~9%. The first weight loss (up to ~120 °C) is attributed to loss of moisture/hydrated water while the second weight loss in the range 120–500 °C is attributed to condensation of structural hydroxyl groups. DSC of CP and TP (SI - Fig. 4) shows an endothermic peak at ~128 °C and 133 °C for CP and TP respectively, attributed to loss of moisture/hydrated water.

Based on the elemental analysis (ICP-AES) and thermal analysis (TGA) data, CP and TP, are formulated as $Ce(HPO_4)_2 \cdot 5H_2O$ and $Th(HPO_4)_2 \cdot 6H_2O$. The number of water molecules in each case is calculated using Alberti and Torracca (1968) formula [21].

The FTIR spectra (SI - Fig. 5) of CP and TP exhibits a broad band in the region ~3400 cm^{-1} which is attributed to asymmetric and symmetric–OH stretching vibration due to residual water and presence of structural hydroxyl groups, H^+ of the –OH being Brønsted acid sites in nature. These bands indicate the presence of structural hydroxyl groups/catalytic sites in the materials. These sites are also referred to as defective P-OH groups [22]. A sharp medium band at ~1630 cm^{-1} is attributed to aquo H–O–H bending [23]. The band at ~1050 cm^{-1} is attributed to P = O stretching while the bands at ~620 cm^{-1} and ~500 cm^{-1} is attributed to Metal-O stretching [24].

The Na^+ CEC values/protonating ability were observed to be 2.48, 1.45, 2.90 and 2.41 for CP, TP, CP_M and TP_M respectively at room temperature (~30 °C).

Table 2
Specific conductance σ (S/cm) of CP, TP, CP_M and TP_M at various temperatures.

Temperature (°C)	σ CP	σ CP_M	σ TP	σ TP_M
30	4.57×10^{-7}	3.17×10^{-6}	3.33×10^{-8}	2.76×10^{-7}
40	4.44×10^{-7}	3.11×10^{-6}	3.17×10^{-8}	2.21×10^{-7}
50	4.18×10^{-7}	3.02×10^{-6}	3.04×10^{-8}	2.19×10^{-7}
60	3.30×10^{-7}	2.62×10^{-6}	2.86×10^{-8}	2.19×10^{-7}
70	3.28×10^{-7}	2.02×10^{-6}	2.71×10^{-8}	2.15×10^{-7}
80	3.11×10^{-7}	1.94×10^{-6}	2.55×10^{-8}	2.07×10^{-7}
90	2.97×10^{-7}	1.74×10^{-6}	2.39×10^{-8}	1.26×10^{-7}
100	2.81×10^{-7}	1.73×10^{-6}	1.68×10^{-8}	1.10×10^{-7}
110	2.70×10^{-7}	1.52×10^{-6}	1.55×10^{-8}	9.02×10^{-8}
120	2.28×10^{-7}	1.30×10^{-6}	1.16×10^{-8}	8.21×10^{-8}
E_a (kcal/mol)	2.10	1.15	7.30	4.86
CEC (meq/g)	2.45	2.90	1.48	1.90
Surface Acidity (mmol/g) (150 °C)	0.95	1.26	0.78	0.80

CEC values decrease on calcination, at higher temperatures due to loss of hydrated water and condensation of structural hydroxyl groups (SI -Table 4). This fact is also evident from the FTIR spectra of the calcined samples (SI - Fig. 6). It is seen that the intensities of the peaks at ~3400 cm^{-1} and ~1638 cm^{-1} corresponding to the –OH group diminish as temperature increases [20].

CP and TP are found to be stable in acid media, maximum tolerable limits being (1 N H_2SO_4, 2 N HNO_3, 5 N HCl) and also stable in organic solvent media. They are however not so stable in base medium, maximum tolerable limits being (0.5 N NaOH and KOH).

The absence of sharp peaks in the X-ray diffractograms of CP and TP (SI - Fig. 7), and CP_M and TP_M (SI - Fig. 8) indicates amorphous nature of all the materials. SEM images of CP, TP, CP_M and TP_M (SI - Figs. 9 to 12) shows irregular morphology.

Surface acidity for all the materials was determined by NH_3-TPD at 150 °C, 200 °C and 700 °C preheating temperatures (SI - Table 5 and Figs. 13 to 16).

3.2. Conductivity Measurements

An impedance spectrum is a plot of the in phase (imaginary Impedance) components of the vector impedance (z) as a function of the frequency of an ac electrical stimulus. Each point generated in complex plane corresponds to a measurement at a different frequency. This is also known as Nyquist plot or cole cole plot or Complex Impedance Plot [25].

The impedance diagrams measured on a sintered compact are shown in Fig. 1. They can be divided into three different contributions (Fig. 1) [25]. At low frequency a straight line is observed, characteristic of the sample-electrode interface. At high frequency, the bulk response of the sample gives rise to a semicircle. At intermediate frequencies a third contribution, that appears for the low temperatures and/or for the low relative humidity only, can be attributed to a grain boundary contribution, in agreement with similar works [25].

The results of specific conductance (σ) for CP, CP_M, TP and TP_M have been presented in Table 2. The complex impedance plots (at 30 °C) have been presented in Fig. 2. For all the materials, it is observed that specific conductivity decreases with increasing temperature (Table 2). Similar trend in TMA salts have been observed earlier by us [14–18]. This is attributed to the loss of water of hydration as well as condensation of structural hydroxyl groups with increasing temperature. This fact is also supported by study of the effect of heating on CEC, where CEC values decrease as calcination temperature increases. This suggests the mechanism of transportation to be of Grotthuss type [4], where the conductivity depends on the ability of the water located on the surface to rotate and participate. Further, the results are also in agreement with the suggestion that protons are not able to diffuse along an anhydrous surface, where the spaces between –OH groups are very large [26]. Besides, the fact that the loss of protons resulting from hydroxyl condensation causes considerable decrease in conductivity also indicates that the conduction is protonic. These factors reveal the importance of water in the conduction mechanism.

The order of specific conductance at 30 °C (Table 2) is found to be CP_M (3.17×10^{-6} S/cm) > CP (4.57×10^{-7} S/cm) > TP_M (2.76×10^{-7} S/cm) > TP (3.33×10^{-8} S/cm). This trend is also in keeping with the CEC values in parenthesis, CP_M (2.90) > CP (2.45) > TP_M (2.41) > TP (1.48). Higher CEC as well as surface acidity values indicate more exchangeable protons (H^+ of structural –OH group in present case) and hence more conducting protons (Table 2).

In the present study, since the phosphate anion is common for CP and TP, the proton conductivity of the phosphates should bear a correlation with the acidity of the cations. Acidity of a cation is related to ion size and charge. The ionic radius for Ce^{4+} is 1.05 Å (180 pm) and Th^{4+} is 1.08 Å (185 pm) [27]. Ce^{4+} with a smaller ionic radius and therefore a high charge density, exhibits higher proton conductivity. The specific conductivity of CP and TP is lower compared to amorphous zirconium(IV) phosphate (ZrP) {4.2×10^{-6} S/cm}[18], titanium(IV) phosphate (TiP) {1.3×10^{-6} S/cm}[18] and tin(IV) phosphate (SnP) {7.6×10^{-6} S/cm}[18]. However, the specific conductivity value of CP_M is comparable to ZrP.

E_a values depend on several factors such as high density of mobile ions, the availability of vacant sites, good connectivity among the sites, complexity in structure/steric effect and acidity of the metal ion [2,28]. Stenina et al. have attributed strong H-bonding to higher E_a values [29]. However, observed E_a is a result from the contribution of the above-mentioned factors. Depending on the predominant factor, the E_a values vary in each case. In Fig. 3 (Arrhenius plots, Log (σT) versus 1000/T) linearity is observed in the temperature range 90–120 °C for all the materials (Table 2). The energy of activation (E_a) (in parenthesis) has been found to be CP_M (1.15), CP (2.10), TP_M (4.86) and TP (7.30) kcal/mol. E_a values, follow the order TP > TP_M > CP > CP_M in the temperature range 90–120 °C, while, specific conductance values follow the order CP_M > CP > TP_M > TP. A lower value of E_a indicates ease of conduction and also suggests the mechanism to be Grotthuss type where E_a entirely

depends on reorientation of water molecules on the surface. In the present study trend in E_a and specific conductivity (σ) are supportive to each other.

4. Conclusions

TMA salts, CP and TP, exhibit good proton conductance. CP_M and TP_M synthesized under microwave irradiation in a much shorter reaction time exhibit higher conductance compared to CP and TP. The present study was a humble attempt to explore the proton conduction properties of amorphous CP and TP. Several studies based on synthesis of CP and TP will have to be performed, with an aim to carry out surface modifications that would offer higher CEC/surface acidity and hence proton conduction.

Acknowledgement

The authors thank DAE-BRNS (BARC-Mumbai) for providing financial support and research fellowship to one of them (Tarun Parangi).

Appendix A. Supplementary data

Supplementary data associated with this article can be found, in the online version, at http://dx.doi.org/10.1016/j.electacta.2014.10.032.

References

[1] J. Guitton, C. Poinsignon, J. Sanchez, Proton Conductors, in: P.H. Colomban (Ed.), Cambridge University Press, Cambridge, 1992.
[2] A. Clearfield, Structural concepts in inorganic proton conductors, Solid State Ionics 46 (1991) 35–43.
[3] W.H.J. Hogarth, J.C. Diniz da Costa, G.Q. Lu(Max), Solid acid membranes for high temperature (140(C) proton exchange membrane fuel cells, J Power Sources 142 (2005) 223–237.
[4] C.J.T. van Grotthuss, Sur la decomposition de leau et des corps quelletient en dissolution a laide de lelectricitegalvanique, Ann. Chim. 58 (1806) 54–73.
[5] H. Ikava, Proton Conductors, in: P.H. Colomban (Ed.), Cambridge University Press, Cambridge, 1992, pp. 551.
[6] M. Casciola, D.S. Costantino, Damico, ac Conductivity of cerium(IV) phosphate in hydrogen form, Solid State Ionics 28 (1988) 617–621.
[7] M.V. Le, D.S. Tsai, C.Y. Yang, W.H. Chung, H.Y. Lee, Proton conductors of cerium pyrophosphate for intermediate temperature fuel cell, Electrochim. Acta 56 (2011) 6654–6660.
[8] H. Onoda, Y. Inagaki, A. Kuwabra, N. Kitamura, K. Amezawa, A. Nakahira, Synthesis and electrical conductivity of bulk tetra-valent cerium pyrophosphate, J Cera. Proc. Res. 11 (3) (2010) 344–347.
[9] A. Nicole, B. Simon, L. Mun, N. Hannah Ray, B. Ross, C. Neaton, Lutgard, De Jonghel, Structure and electronic properties of cerium orthophosphate: Theory and experiment, Phys. Rev. B 83 (2011) 205104 205107.
[10] A. Gomez del Moral, D.P. Fagg, E. Chinaro, C.C. Abrantes Jao, J.M. Jurao, G.C. Mather, Impedance analysis of Sr-substituted $CePO_4$ with mixed protonic and p-type electronic conduction, Cera. Int. 35 (2009) 1481–1486.
[11] D. Failong, L. Zhongfang, S. Wang, Z. Wang, Synthesis and characteristics of proton-conducting membrane based on cerium sulphenyle phosphates and poly(2, 5-benzimidazole) by hot-pressing method, Int. J. Hydro. Energy 36 (2011) 11068–11074.
[12] A. A. Khan, Inamuddin, Cation-exchange kinetics and electrical conductivity studies of an 'organic-inorganic' composite cation-exchanger: Polypyrrole-Th (IV) phosphate, 105(5)(2007) 2806–2815.
[13] P. Barboux, R. Morineau, J. Livage, Solid State Ionics 27 (1988) 221–225.
[14] B. Beena, U. Chudasama, Transport properties in a mixed inorganic ion exchanger zirconium phosphomolybdate - in comparison to its single salt counterparts Chudasama, Bull. Mater Sci. 19 (1996) 405.
[15] B. Beena, B. Pandit, U. Chudasama, Transport properties of organic derivatives of zirconium molybdate Chudasama, Indian J Eng. Mater Sci. 5 (1998) 77.
[16] A. Parikh, U. Chudasama, A comparative study of the proton transport properties of metal (IV) tungstates, Proc. Ind Acad. Sci. 115 (2003) 1.
[17] H. Patel, A. Parikh, U. Chudasama, A comparative study of proton transport properties of metal (IV) tungstates and their organic derivatives, Bull. Mater Sci. 28 (2005) 137–144.
[18] H. Patel, U. Chudasama, A comparative study of the proton transport properties of metal (IV) phosphates, J. Chem. Sci. 119 (1) (2007) 35–40.
[19] R. Kunin, Ion Exchange Resin, Wiley, London, 1958.
[20] R. Thakkar, U. Chudasama, Synthesis and characterization of zirconium titanium phosphate and its application in separation of metal ions, J. Hazard Mater 172 (2009) 129–137.
[21] G. Alberti, E. Torracca, Crystalline insoluble acid salts of polyvalent metals and polybasic acids - VI: Preparation and ion-exchange properties of crystalline titanium arsenate, J. Inorg. Nucl. Chem. 30 (1968) 3075–3080.
[22] A. Bhaumik, S. Inagaki, Mesoporous Titanium Phosphate Molecular Sieves with Ion-Exchange Capacity, J Am. Chem. Soc. 230 (2001) 691–696.
[23] C.T. Seip, G.E. Granroth, M.W. Meisel, D.R. Talham, Langmuir-Blodgett films of known layered solids: Preparation and structural properties of octadecyl-phosphonate bilayers with divalent metals and characterization of a magnetic Langmuir-Blodgett film, J Am. Chem. Soc. 119 (1997) 7084–7094.
[24] A. Nilchi, M.M. Ghanadi, A. Khanchi, Characteristics of novel types substituted cerium phosphates, J Radioana. Nucl. Chem. 245 (2) (2000) 589–594.
[25] I. Hammas, K. Horchani-Kaifer, M. Ferid, Conduction properties of condensed lanthanum phosphates; $La(PO_3)_3$ and LaP_5O_{14}, J Rare Earths 28 (3) (2010) 321–328.
[26] G. Alberti, U. Costantino, R. Polambari, First International Conference on Inorganic Membranes, Montpellier, France, 1989, pp. 25.
[27] Pauling, Atomic radii and interatomic distances in metal, J Am. Chem. Soc. 69 (3) (1947) 542–553.
[28] T. Kudo, K. Flueki, Solid State Ionics, VCH, Publishers, New York, 1981, pp. Ch. 6.
[29] I.A. Stenina, A.D. Aliev, I.V. Glukhov, F.M. Spiridonov, A.B. Yaroslavtsev, Cation mobility and ion exchange in acid tin phosphate, Solid State Ionics 162 (2003) 192.

Desalination and Water Treatment
www.deswater.com
doi: 10.1080/19443994.2015.1008582

(2015) 1–9

Taylor & Francis
Taylor & Francis Group

Sorption and separation study of heavy metal ions using cerium phosphate: a cation exchanger

Tarun Parangi[a], Bina Wani[b], Uma Chudasama[a,*]

[a]*Faculty of Technology & Engineering, Applied Chemistry Department, The M.S. University of Baroda, Vadodara 390 001, Gujarat, India, Tel. +91 9426344434; emails: juvenile34@gmail.com (T. Parangi), uvcres@gmail.com (U. Chudasama)*
[b]*Chemistry Division, Bhabha Atomic Research Centre, Trombay, Mumbai 400 085, Maharashtra, India, email: bnwani@rediffmail.com*

Received 21 August 2014; Accepted 6 January 2015

ABSTRACT

Cerium (IV) phosphate (CP), material of the class of tetravalent metal acid salts has been used as cation exchanger. The sorption/ion exchange behavior of CP toward heavy metal ions (Co^{2+}, Ni^{2+}, Cu^{2+}, Zn^{2+}, Cd^{2+}, Hg^{2+}, and Pb^{2+}) has been studied using Langmuir and Freundlich adsorption isotherms. The distribution coefficient (K_d) (at optimum conditions) and breakthrough capacity for these metal ions have been determined. Elution behavior of these metal ions has been studied using acids and electrolytes. Based on the separation factor α a few binary and ternary metal ion separations have been performed.

Keywords: Cerium phosphate; Ion exchanger; Cation exchanger; Langmuir; Fruendlich; Separation

1. Introduction

Among various processes developed to remove metal ions from wastewater, it is observed that at low concentrations, the removal is more effective by ion exchange [1–4]. Inorganic ion exchangers have played a prominent role in water processing for the chemical and nuclear industries, and also used extensively for the removal and recovery of metal ions. Further, different types of metal pollutants from chemical process industries necessitate finding new ion exchangers, that have good ion exchange capacity, stability toward temperature, and oxidizing solutions and that are capable of removing toxic substances from aqueous effluents [2–4].

Several studies have shown that cerium (IV) phosphates (CPs) are interesting inorganic materials for cation exchange. Clearfield et al. have reported the ion exchange behavior of crystalline CP with alkali metal ions [5]. Varshney et al. have reported kinetics of ion exchange of alkali and transition metal ions using acrylamide and acrylonitrile-based fibrous CP [6–8]. Sorption studies of strontium and uranium ions on fibrous cerium (IV) hydrogen phosphate have been reported [9]. Nilchi et al. have reported analytical applications of disodium, dipotassium, and distrontium substituted cerium phosphate and molybdate as cation exchangers for alkaline earth metal ions [10]. Varshney has reported synthesis, characterization, and adsorption behavior of triton X-100 based CP as a new Hg(II) selective, surfactant-based fibrous ion exchanger [11], and analytical applications of Pb(II) selective, surfactant-based sodium dodecyl sulfate cerium

*Corresponding author.

phosphate [12]. Analytical applications of pyridine-based CP as fibrous ion exchangers have been reported by Varshney [13]. Suzuki et al. [14] have reported synthesis and characterization of Pb(II) selective membrane filter, fabricated from fibrous CP $\{CeO(H_2PO_4)_2{\cdot}H_2O\}$ by blending with cellulose fiber. Preetha and Janardanan [15] have reported synthesis, characterization, and application of cerium zirconium phosphate as cation exchanger for metal ion separations of some transition metal ions.

In earlier publication, the authors have reported synthesis, characterization, and application of CP as an ion exchanger [16]. Distribution coefficient (K_d) of heavy metal ions (Mn^{2+},Co^{2+}, Ni^{2+}, Cu^{2+}, Zn^{2+}, Cd^{2+}, Hg^{2+}, and Pb^{2+}) has been determined in aqueous as well as various electrolyte media/concentrations. The equilibrium exchange of these metal ions with H^+ ions contained in CP has been studied and thermodynamic parameters equilibrium constant (K), standard Gibbs free energy (ΔG°), enthalpy (ΔH°), and entropy (ΔS°) have been reported [16].

In the present endeavor, the sorption/ion exchange behavior of CP toward heavy metal ions (Co^{2+}, Ni^{2+}, Cu^{2+}, Zn^{2+}, Cd^{2+}, Hg^{2+}, and Pb^{2+}) has been studied using Langmuir and Freundlich adsorption isotherms. The distribution coefficient (K_d) (at optimum conditions) and breakthrough capacity (BTC) for these metal ions have been determined. Elution behavior of these metal ions has been studied using acids and electrolytes. Based on the separation factor α and elution behavior a few binary and ternary metal ion separations have been performed.

2. Experimental

All chemicals and reagents used are of analytical grade. Double distilled water (DDW) was used for all the studies.

2.1. Adsorption studies

2.1.1. Effect of pH, contact time, and temperature on adsorption/ion exchange

Adsorption/ion exchange of metal ions Co^{2+}, Ni^{2+}, Cu^{2+}, Zn^{2+}, Cd^{2+}, Hg^{2+}, and Pb^{2+} using CP [30-60 mesh (ASTM)] was carried out in the pH range 1–7. To 0.1 g of the exchanger, 10 mL of 0.002 M metal ion solution was added and pH adjusted in acidic range using dilute HNO_3 and in alkaline range using dilute NaOH and the mixture shaken for 30 min. The supernatant liquid was used to determine the metal ion concentration by EDTA titrations [4,17]. The percentage uptake has been calculated using formula, $[(C_0 - C_e)/C_0] \times 100$ where C_0 is the initial concentration of metal ion in mg/L and C_e is the final concentration of metal ion in mg/L. A maximum percentage uptake gives optimum pH for the sorption of respective metal ion. The metal ion solution (10 mL) of 0.002 M was equilibrated in stoppered conical flasks at the desired temperatures (303–333 K with 10 K interval) and at specific time intervals with increments of 10 min (10–200 min). In each case, the pH of the solution is adjusted to the value at which maximum sorption of respective metal ion takes place. The supernatant liquid was removed immediately after each prescribed time interval and the metal ion concentration evaluated by EDTA titrations [4,17].

2.2. Distribution study and BTC

Effect of metal ion concentration on distribution coefficient (K_d) values for Co^{2+}, Ni^{2+}, Cu^{2+}, Zn^{2+}, Cd^{2+}, Hg^{2+}, and Pb^{2+} (heavy metal ions) has been determined by batch method. To 0.1 g of CP in the H^+ form was equilibrated with 20 mL of varying metal ion concentration (0.002–0.01 M with interval of 0.002 M) for 6 h (maximum equilibrium time) at room temperature. The metal ion concentration before and after exchange was determined by EDTA titration.

The K_d was also evaluated at optimum condition (optimum metal ion concentration and pH of maximum adsorption for maximum equilibrium time) with 0.1 g of the exchanger in aqueous as well as various electrolyte media like NH_4NO_3, HNO_3, $HClO_4$, and CH_3COOH of 0.02 and 0.2 M concentration at room temperature. The K_d was evaluated using the expression, $K_d = [(I - F)/F] \times V/W$ (mL/g) where I = total amount of the metal ion in the solution initially; F = total amount of metal ions left in the solution after equilibrium; V = volume of the metal ion solution; and W = weight of the exchanger in gram [4,17].

For determination of BTC, 0.5 g of the ion exchanger, TP, was taken in a glass column [30 × 1 cm (internal diameter)] and washed thoroughly with DW, and flow rate adjusted to 0.5 mL/min. Five milliliter fractions of each individual metal ion [Co^{2+}, Ni^{2+}, Cu^{2+}, Zn^{2+}, Cd^{2+}, Hg^{2+}, and Pb^{2+}] of 0.001 M concentration were passed through the column and effluent collected, till the amount of metal ion concentration was same in feed and effluent. A breakthrough curve was obtained by plotting the ratio C_e/C_0 against the effluent volume, where C_0 and C_e are the concentrations of the initial solution and effluent, respectively. BTC is calculated using formula, $(C_0 V_{(10\%)})/W$ (mmol/g) where C_0 is concentration of metal ion in mol/L, $V_{(10\%)}$ is the volume of metal ion solution passed through column when exit concentration reaches 10%

of the initial concentration in mL, and W is the weight of the exchanger in gram [4,17].

2.3. Elution and separation studies

For elution studies (single metal), the column were prepared as discussed earlier. The metal ion solution (0.001 M, 10 mL) was loaded onto the column. The metal ion loaded was eluted with eluents like HNO_3, $HClO_4$, CH_3COOH, and NH_4NO_3 of 0.02 and 0.2 M concentration. The amount of metal ion recovered was calculated in terms of percentage elution expressed as, $\% \ E = (C_e/C_0) \times 100$ where C_e is the concentration of the metal ion in the eluted solution and C_0 is the concentration of metal ion loaded onto the column.

For binary and ternary separations, mixture of metal ion solutions (0.001 M, 10 mL of each metal ion) to be separated was loaded onto the column. The separation was achieved by passing suitable eluent through the column and percentage metal eluted was calculated using above equation in each case.

3. Results and discussion

3.1. Adsorption studies

The effect of experimental conditions such as pH, contact time, and temperature was studied to set the conditions for maximum adsorption/ion exchange of the metal ions by the ion exchanger.

At pH values less than ~3, very less sorption has been observed for all metal ions (Table 1). The lack of sorption at low pH could be attributed to high concentration of the hydrogen ions competing with the metal ions for sorption/exchange sites. Effect of contact time and reaction temperature toward percentage uptake of metal ion is presented in Table 2. It is observed that sorption increases gradually with increase in contact time and reaches a maximum value after which randomness is observed. Increase in percentage uptake could be attributed to two different sorption processes, namely, a fast ion exchange followed by chemisorption [18]. It is observed that percentage uptake of each metal ion increases with increase in temperature, which indicates the uptake to be an ion-exchange mechanism.

Table 1
Percentage uptake of metal ions varying pH using CP

	Uptake of metal ion (%)						
pH	Co^{2+}	Ni^{2+}	Cu^{2+}	Zn^{2+}	Cd^{2+}	Hg^{2+}	Pb^{2+}
1	18.51	1.00	2.10	15.12	18.10	1.20	27.64
2	12.28	4.76	22.75	28.25	16.00	1.73	36.54
3	*29.30*	15.61	*25.55*	*46.80*	21.00	2.50	55.45
4	18.08	*32.16*	11.76	11.20	37.00	*2.90*	*76.22*
5	11.15	16.25	17.97	–	*55.50*	–	–
6	4.42	–	–	–	28.00	–	–
7	2.24	–	–	–	31.00	–	–

Note: Maximum deviation in percentage uptake of metal ion = ±2%.
Italic values are indicating optimum pH value for respective metal ion.

Table 2
Effect of contact time and temperature on adsorption behavior of metal ions using CP

	Equilibrium time (min)			
Metal ion	303 K	313 K	323 K	333 K
Co^{2+}	60	60	50	40
Ni^{2+}	60	60	50	40
Cu^{2+}	60	50	50	40
Zn^{2+}	60	50	40	40
Hg^{2+}	90	90	70	60
Cd^{2+}	40	40	40	40
Pb^{2+}	170	170	120	100

Equilibrium behavior is described in terms of equilibrium isotherms, which depend on the system temperature, concentration of the solution, contact time, and pH [19,20]. Adsorption equilibrium is usually established when the concentration of an adsorbate (metal ions) in a bulk solution is in dynamic balance with that of the adsorbent (exchanger) interface. The variation in adsorption with concentration and temperature is generally expressed in terms of adsorption isotherms—Langmuir and Freundlich adsorption isotherms.

The linearized form of the Langmuir isotherm equation is given as: $C_e/(X/m) = 1/(bV_m) + C_e/V_m$ where X is the amount of adsorbate, m is the amount of adsorbent, and C_e is the equilibrium concentration of the adsorbate in the solution. The constant "b" represents adsorption bond energy, which is related to the affinity between the adsorbent and adsorbate, which is also a direct measure for the intensity of the sorption process. The V_m is a constant related to the area occupied by a monolayer of sorbate, reflecting the maximum adsorption capacity [20,21]. A dimensionless constant equilibrium parameter R_L can also be used to express an essential characteristic of the Langmuir isotherm. The R_L value indicates the shape of the isotherm and is expressed as $R_L = 1/(1 + bC_0)$. A value $0 < R_L < 1$ indicates favorable adsorption, $R_L = 0$ irreversible adsorption, and $R_L = 1$ means linear adsorption while a value, $R_L > 1$ indicates an unfavorable adsorption [21].

Freundlich isotherm is expressed as, $\log(X/m) = \log K + (1/n)\log C_e$ where X and m have the same

Table 3
Langmuir and Freundlich constants for heavy metal ions using CP

Metal ion	Temp. (K)	Langmuir constants				Freundlich constants		
		R^2	b (dm^3/mg)	V_m (mg/g)	R_L	R^2	K	$1/n$
Co^{2+}	303	0.917	0.0011	27.02	0.994	0.993	4.33	0.993
	313	0.941	0.0024	27.02	0.991	0.997	6.20	0.997
	323	0.989	0.0015	28.57	0.981	0.996	5.27	0.996
	333	0.988	0.0030	20.40	0.981	0.997	6.09	0.997
Ni^{2+}	303	0.917	0.0012	23.25	0.999	0.996	5.80	0.764
	313	0.934	0.0016	27.02	0.996	0.998	6.22	0.794
	323	0.957	0.0011	29.41	0.995	0.996	6.50	0.813
	333	0.925	0.0020	30.30	0.986	0.995	6.09	0.825
Cu^{2+}	303	0.942	0.0009	25.64	0.999	0.991	6.65	0.823
	313	0.915	0.0006	41.66	0.998	0.994	7.39	0.869
	323	0.981	0.0008	37.03	0.997	0.999	6.66	0.824
	333	0.983	0.0012	32.25	0.994	0.994	6.08	0.784
Zn^{2+}	303	0.969	0.0031	26.31	0.996	0.998	3.26	0.514
	313	0.971	0.0032	27.02	0.990	0.997	3.25	0.512
	323	0.971	0.0044	27.02	0.981	0.998	3.62	0.559
	333	0.973	0.0040	28.57	0.974	0.997	3.82	0.583
Cd^{2+}	303	0.945	0.0026	25.00	0.993	0.920	3.08	0.489
	313	0.958	0.0032	27.77	0.980	0.890	2.46	0.391
	323	0.938	0.0052	27.77	0.950	0.780	2.09	0.322
	333	0.950	0.0024	37.03	0.972	0.912	3.39	0.531
Hg^{2+}	303	0.919	0.0011	5.02	0.993	0.617	2.20	0.344
	313	0.600	0.0014	8.54	0.989	0.552	2.05	0.313
	323	0.813	0.0020	9.61	0.965	0.633	2.73	0.437
	333	0.838	0.0021	13.51	0.959	0.896	2.31	0.364
Pb^{2+}	303	0.991	0.0061	64.51	0.977	0.984	2.59	0.282
	313	0.999	0.0100	65.78	0.927	0.994	3.01	0.253
	323	0.995	0.0072	86.20	0.921	0.944	3.40	0.246
	333	0.990	0.0051	62.50	0.866	0.991	3.88	0.294

Table 4
Distribution coefficient (K_d) values varying metal ion concentration using CP

Metal ions	Distribution coefficient (K_d) values (mL/g)				
	0.002 M	0.004 M	0.006 M	0.008 M	0.010 M
Co^{2+}	115.60	*154.00*	155.00	158.00	158.00
Ni^{2+}	147.10	*189.00*	192.00	193.00	193.00
Cu^{2+}	177.00	*210.00*	210.00	212.00	212.00
Zn^{2+}	205.00	235.00	*260.00*	260.00	261.00
Cd^{2+}	290.00	325.00	*345.30*	347.00	348.00
Hg^{2+}	7.00	15.20	*29.50*	32.00	32.00
Pb^{2+}	2,410.00	2,500.00	*2,590.00*	2,600.00	2,600.00

Note: Italic values are indicating optimum metal ion concentration for respective metal ion.

meaning as described in Langmuir isotherm, K and $1/n$ are the Fruendlich constants, describing the adsorption capacity and intensity, respectively. A value, $0 < 1/n < 1$ indicates a normal isotherm, while $1/n > 1$ is indicative for cooperative sorption, for $n = 1$ the partition between the two phases is independent of the concentration [20,21].

The isotherm constants are important in understanding the adsorption mechanism and their subsequent application for prediction of some important design parameters. Plots of $C_e/(X/m)$ vs. C_e and $\log(X/m)$ vs. $\log C_e$ are drawn for Langmuir and Freundlich isotherms, respectively, which are straight lines from which the constants can be determined by the slopes and intercepts. In order to decide which type of isotherm fits better, the R^2 values (goodness of fit criterion) computed by linear regression for both type of isotherms and a value $0 < R^2 < 1$ indicates that the isotherm provides a good fit to the sorption experimental data where R^2 values should be close to unity.

Langmuir constants (b and V_m) and Freundlich constants (K and $1/n$) obtained from the slopes and

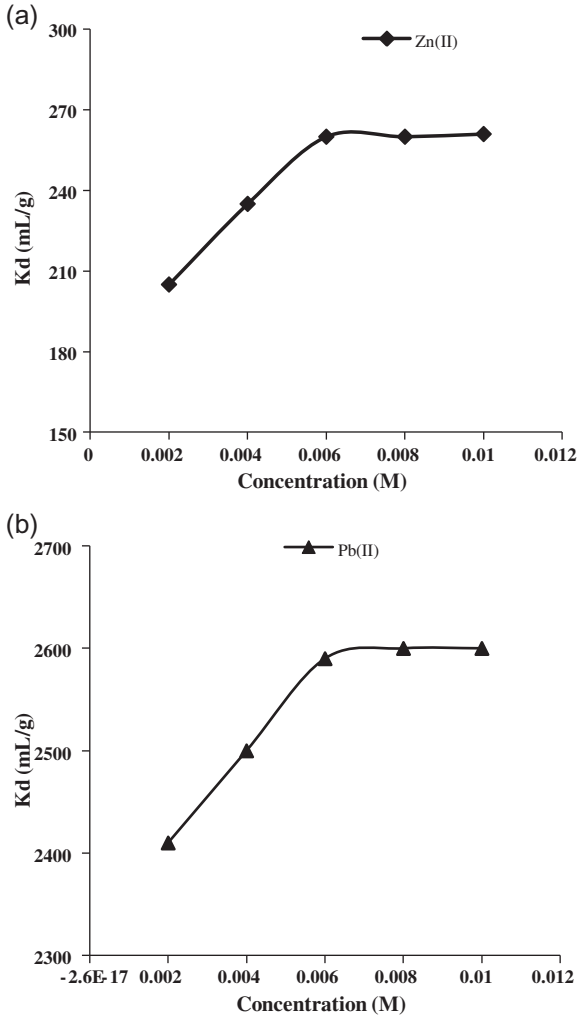

Fig. 1. (a) effect of metal ion (Zn^{2+}) concentration toward K_d and (b) effect of metal ion (Pb^{2+}) concentration toward K_d.

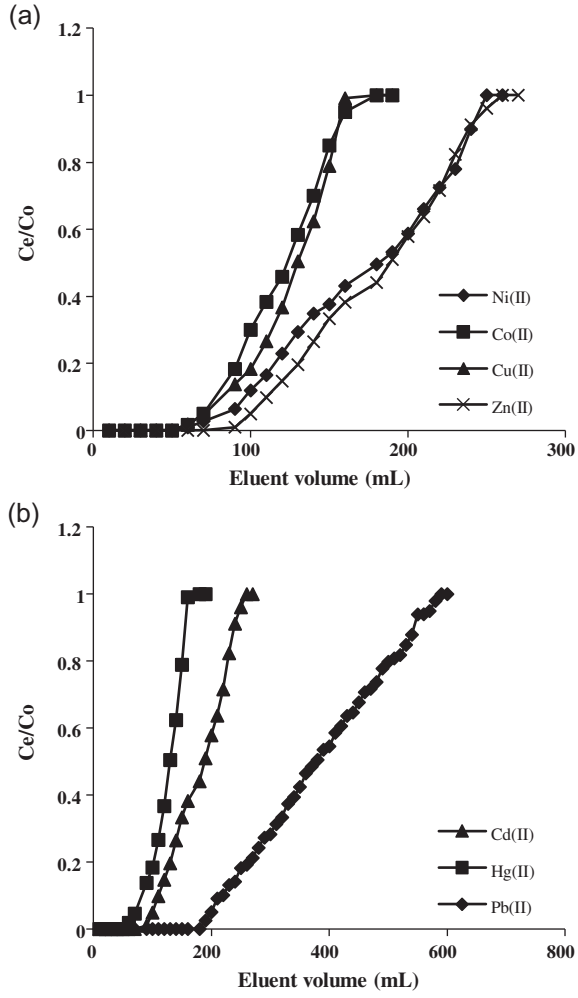

Fig. 2. BTC of heavy metal ions; (a) Ni(II), Co(II), Cu(II), Zn(II) and (b) Cd(II), Hg(II), Pb(II).

Table 5
BTC and distribution coefficient (K_d)* values for heavy metal ions using CP

Metal ion	Ionic radii (Å)	BTC (mmol/g)	K_d*values (mL/g) in aqueous and various electrolyte media/concentration								
				NH_4NO_3		HNO_3		$HClO_4$		CH_3COOH	
			DDW	0.02 M	0.2 M	0.02 M	0.2 M	0.02 M	0.2 M	0.02 M	0.2 M
Co^{2+}	0.72	0.37	201.20	117.00	42.00	27.40	5.00	30.00	16.00	236.50	200.50
Ni^{2+}	0.72	0.47	232.10	134.00	34.00	26.80	15.00	5.50	NS	235.00	155.00
Cu^{2+}	0.74	0.36	194.00	205.00	95.60	70.10	7.00	14.00	6.70	330.00	269.80
Zn^{2+}	0.74	0.50	298.00	196.00	84.70	81.00	28.10	46.80	32.00	304.10	214.00
Cd^{2+}	0.97	0.78	476.50	322.00	96.00	110.00	40.10	90.00	102.50	560.00	820.00
Hg^{2+}	1.44	0.04	31.00	79.50	48.50	78.30	55.80	30.00	4.50	94.00	68.00
Pb^{2+}	1.10	1.16	3,640.10	3,810.00	2,235.20	3,450.0	290.50	1,528.00	2,700.00	5,180.20	2,210.20

Notes: *K_d Values obtained at optimum condition (Optimum metal ion concentration, Optimum pH of solution, and maximum equilibrium time).
NS = No sorption; Maximum deviation in K_d values = ±3.

Table 6
Percentage elution (% E) of metal ions in different electrolyte media using CP

	NH_4NO_3		HNO_3		$HClO_4$		CH_3COOH	
Metal ions	0.02 M	0.2 M	0.02 M	0.2 M	0.02 M	0.2 M	0.02 M	0.2 M
Co^{2+}	81.30	83.35	92.15	97.00	92.64	94.10	85.80	88.70
Ni^{2+}	87.00	90.25	94.50	97.00	91.00	93.50	87.90	89.80
Cu^{2+}	87.00	90.30	94.40	97.22	92.10	93.50	86.20	89.40
Zn^{2+}	85.20	87.50	93.10	96.00	93.10	95.10	90.15	92.15
Cd^{2+}	85.10	89.35	94.70	95.20	91.50	93.60	89.20	95.40
Hg^{2+}	91.66	92.60	96.30	98.15	93.50	96.75	89.20	92.10
Pb^{2+}	84.20	86.50	88.45	91.35	86.55	89.40	78.80	80.35

Notes: Eluent volume = 70 and 60 mL for 0.02 and 0.2 M electrolytes, respectively.
Maximum deviation in % elution of metal ions = ±2.

Table 7
Binary separations of heavy metal ions using CP

		Metal ion (mg)		
Separation achieved	Eluent	Loaded (C_0)	Eluted (C_e)	Elution (%)
Co^{2+}-Zn^{2+}	(a) 0.2 M HNO_3 (Co^{2+})	0.5893	0.4980	84.50
	(b) 0.2 M $HClO_4$ (Zn^{2+})	0.6540	0.5295	80.95
Ni^{2+}-Zn^{2+}	(a) 0.02 M $HClO_4$ (Ni^{2+})	0.5869	0.5126	87.35
	(b) 0.2 M $HClO_4$ (Zn^{2+})	0.6540	0.5185	79.30
Cu^{2+}-Zn^{2+}	(a) 0.2 M $HClO_4$ (Cu^{2+})	0.6354	0.5480	86.25
	(b) 0.2 M HNO_3 (Zn^{2+})	0.6540	0.5244	80.20
Hg^{2+}-Pb^{2+}	(a) 0.2 M $HClO_4$ (Hg^{2+})	2.0059	1.8554	92.50
	(b) 0.2 M HNO_3 (Pb^{2+})	2.0720	1.7715	85.50
Cd^{2+}-Pb^{2+}	(a) 0.02 M HNO_3 (Cd^{2+})	1.1241	1.0229	91.00
	(b) 0.2 M HNO_3 (Pb^{2+})	2.0720	1.5430	74.50
Hg^{2+}-Cd^{2+}	(a) 0.2 M $HClO_4$ (Hg^{2+})	2.0059	1.8354	89.00
	(b) 0.2 M HNO_3 (Cd^{2+})	1.1241	0.8317	73.90

Note: Maximum deviation in % elution = ±2.

intercepts of the linear plots are listed in Table 3. It is observed that R^2 values are found to be close to unity for both isotherms and provide a good fit to the experimental data for sorption of all the metal ions taken (except Cd^{2+} for Fruendlich isotherm and Hg^{2+} for both isotherms). Variation in R^2 values is attributed to the fact that the surface adsorption is not a monolayer with single site. Two or more sites with different affinities may be involved in metal ion sorption [18]. In the present study, low values of b indicate favorable adsorption. Based on V_m values, that reflects maximum adsorption capacity of metal ions toward exchanger follows the order $Pb^{2+} > Cd^{2+} > Co^{2+} > Zn^{2+} > Cu^{2+} > Ni^{2+} > Hg^{2+}$ at 303 K. The values of $1/n$ and R_L are obtained between 0 and 1, which indicate normal isotherm and favorable adsorption, respectively, and agree with reported results [19,20].

3.2. Distribution studies and BTC

The effect of metal ion concentration on K_d values (Table 4) show that with increase in concentration K_d values increase. Above a particular concentration K_d values are constant which could be explained to be due to the fact that at lower concentrations, almost all the ions are exchanged due to availability of exchangeable sites, which are not available at higher concentrations. A plot of K_d values vs. metal ion concentration for Zn^{2+} and Pb^{2+} are presented in Fig. 1(a) and (b) showing optimum concentration for both metal ions, respectively.

The K_d values evaluated for the metal ions under study at optimum conditions (optimum metal ion concentration, optimum pH of solution, and maximum equilibrium time) toward CP have been presented in Table 5. In general, it is observed that the K_d values

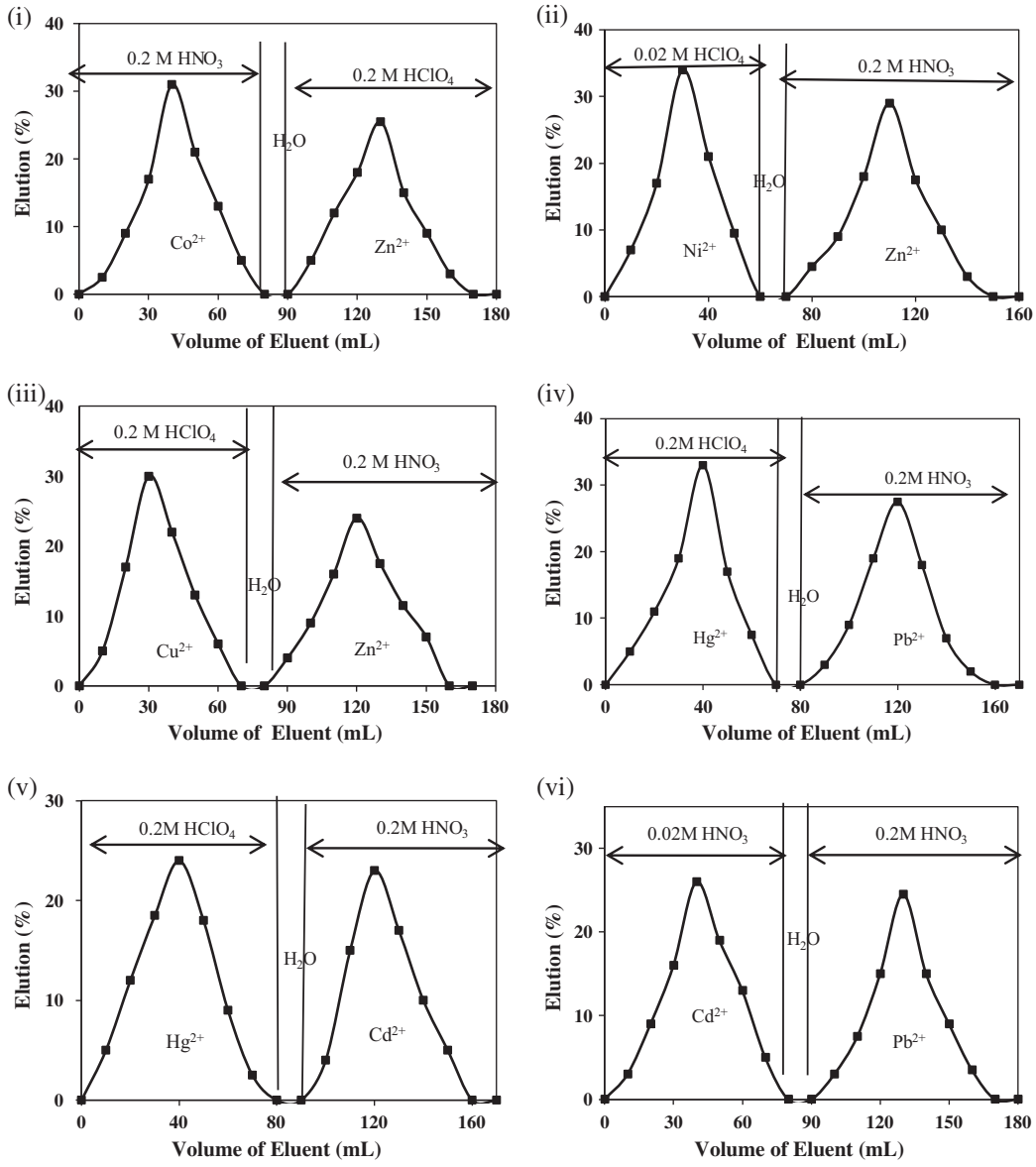

Fig. 3. Binary separation of (i) Co^{2+}-Zn^{2+}, (ii) Ni^{2+}-Zn^{2+}, (iii) Cu^{2+}-Zn^{2+}, (iv) Hg^{2+}-Pb^{2+}, (v) Hg^{2+}-Cd^{2+}, and (vi) Cd^{2+}-Pb^{2+}.

Table 8
Ternary separations of heavy metal ions using CP

Separations achieved	Eluent	Metal ion (mg)		Elution (%)
		Loaded (C_0)	Eluted (C_e)	
Ni^{2+}-Cu^{2+}-Zn^{2+}	(a) 0.02 M NH_4NO_3 (Ni^{2+})	0.5869	0.3257	55.50
	(b) 0.02 M $HClO_4$ (Cu^{2+})	0.6354	0.3113	49.00
	(c) 0.2 M HNO_3 (Zn^{2+})	0.6540	0.3099	47.40
Hg^{2+}-Cd^{2+}-Pb^{2+}	(a) 0.2 M NH_4NO_3 (Hg^{2+})	2.0059	1.2536	62.50
	(b) 0.02 M HNO_3 (Cd^{2+})	1.1241	0.5732	51.00
	(c) 0.2 M HNO_3 (Pb^{2+})	2.072	0.8598	41.50

Note: Maximum deviation in percentage elution = ±2.

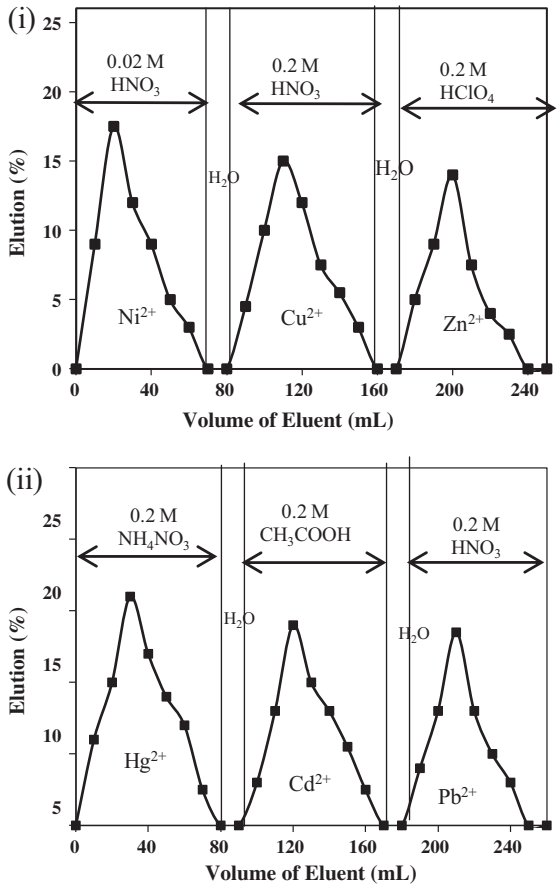

Fig. 4. Ternary separation of (i) Ni^{2+}-Cu^{2+}-Zn^{2+} and (ii) Hg^{2+}-Cd^{2+}-Pb^{2+}.

are lower in high concentration of electrolyte and vice-versa. In strong electrolyte media K_d values are lower as compared to weak electrolyte and aqueous media. This may be attributed to the high competition amongst ions for exchange in strong electrolyte media.

Breakthrough curves (a plot of C_e/C_0 vs. effluent volume) are presented in Fig. 2(a) and (b). BTC is the dynamic capacity or operating capacity of a known amount of ion-exchange material toward metal ion in column operation. In dynamic process, exchange of a particular metal ion depends mainly on the rate of exchange, contact time, flow rate of feed solution through the column, bed depth, selectivity coefficient, particle size, and temperature. The K_d values also give an idea of affinity of metal ion toward ion exchanger. However, K_d is determined by a batch process. It is expected that the metal ion affinity toward CP, based on K_d and BTC values should be the same, which is observed (Table 5) in the present study confirming the metal ion affinity toward CP.

3.3. Elution and separation studies

The elution behavior of single metal ions (under study) are carried out using different eluents such as HNO_3, $HClO_4$, CH_3COOH, and NH_4NO_3 of 0.2 and 0.02 M concentration, and results are presented in Table 6. The percentage metal eluted in all cases, is in the range 80–97%. Good elution is observed due to presence of single metal ion and non interference of elements. Higher concentration of eluent and acids in general are better eluents. To 0.2 M HNO_3 is the best eluent for most metal ions. Using 0.2 M HNO_3, order of percentage metal eluted is Hg^{2+} (98.14) > Cu^{2+} (97.22) > Co^{2+} (97. 05) > Ni^{2+} (97.00) > Zn^{2+} (96.03) > Cd^{2+} (95.05) > Pb^{2+} (91.34). This observation is in keeping with the fact that metal ions with high K_d values are less eluted and vice-versa [4,17,22]. All elution curves are symmetrical bell shaped indicating elution efficiency.

Separation factor α, at which two constituents separate on a column, given by, $\alpha = K_{d1}/\ K_{d2}$ where K_{d1} and K_{d2} are the distribution coefficients of the two constituents being separated, provides a guideline for metal separation. The greater the deviation of α from unity, better is the separation. The efficiency of an ion-exchange separation depends on the condition under which α has a useful value, or influencing in a direction favorable to separation. For a given metal ion pair, the electrolyte media in which the separation factor is the highest, is selected as the eluent. Thus, a study on distribution behavior of metal ions in various electrolyte media gives an idea about the eluents that can be used for separation [4,17,22].

Binary separations for following metal ion pairs, Co^{2+}-Zn^{2+}, Ni^{2+}-Zn^{2+}, Cu^{2+}-Zn^{2+}, Hg^{2+}-Pb^{2+}, Cd^{2+}-Pb^{2+}, and Hg^{2+}-Cd^{2+} have been performed using concept of high separation factor in a particular medium as discussed earlier in the text. In binary separations, separation efficiency is in the range 80–92% (Table 7). In all cases of binary separations, irrespective of metal ion pair, maximum percentage metal eluted is Hg^{2+} (92.50), Cd^{2+} (91.00), Ni^{2+} (87.35), Cu^{2+} (86.20), Pb^{2+} (85.50), Co^{2+} (84.51), and Zn^{2+} (80.97). This observation is in keeping with separation factor (α) and K_d values of metal ions. The % metal eluted decreases with decreasing separation factor and increases with increasing separation factor, and as explained earlier, metal ions with high K_d values are less eluted and vice-versa. Efficient separation in terms of % metal eluted is observed in case of Co^{2+}-Zn^{2+}, Ni^{2+}-Zn^{2+}, Cu^{2+}-Zn^{2+}, Hg^{2+}-Pb^{2+}, Cd^{2+}-Pb^{2+}, and Hg^{2+}-Cd^{2+} where α values are high, which is also supported by symmetrical bell-shaped curves (Fig. 3).

In ternary separations for Ni^{2+}-Cu^{2+}-Zn^{2+} and Hg^{2+}-Cd^{2+}-Pb^{2+}, the percentage metal eluted is in the range 47–55% and 41–62%, respectively (Table 8). In all cases, three distinct peaks are observed (Fig. 4), however, with tailing effects for every metal ion eluted. The percentage metal eluted is also lower as compared to single and binary metal ion separations. Probably the separation process becomes complex, attributed to the loss of metal ions during the change-over of the eluent, interference of metal ions, pH, simultaneous elution of two or more metal ions with the same eluent, and lastly, experimental errors involved in the determination of metal ions in the presence of other ions [4,17,22].

4. Conclusions

The most promising property of CP, is its high selectivity for Pb^{2+}. Lead is a toxic metal requiring stringent regulations to be applied to its content in wastes and water streams. An extremely high affinity of CP toward Pb^{2+} suggests the possibility of their application for lead separation from other pollutants.

Acknowledgment

The authors thank DAE-BRNS for providing financial support and research fellowship to one of them (Tarun Parangi).

References

[1] K.G. Varshney, M.A. Khan, in: M. Qureshi K.G. Varshney (Eds.), Inorganic Ion Exchangers in Chemical Analysis, CRC Press, Boca Raton FL 1991, pp. 28–29.
[2] K. Maheria, U. Chudasama, Synthesis and characterization of a new phase of titanium phosphate and its application in separation of metal ions, Indian J. Chem. Technol. 14 (2007) 423–426.
[3] A. Jayswal, U. Chudasama, Synthesis and characterization of a new phase of zirconium phosphate for the separation of metal ions, J. Iran. Chem. Soc. 4(4) (2007) 510–515.
[4] R. Thakkar, U. Chudasama, Synthesis and characterization of zirconium titanium phosphate and its application in separation of metal ions, J. Hazard. Mater. 172 (2009) 129–137.
[5] R.G. Hermant, A. Clearfield, Crystalline cerium(IV) phosphates-II. The ion exchange characteristics with alkali metal ions, J. Inorg. Nucl. Chem. 38 (1976) 853–858.
[6] K.G. Varshney, N. Tayal, U. Gupta, Acrylonitrile based cerium (IV) phosphate as a new mercury selective fibrous ion exchanger: Synthesis, characterization and analytical applications, Colloids Surf., A 145 (1998) 71–78.
[7] K.G. Varshney, N. Tayal, Ion exchange of alkaline earth and transition metal ions on fibrous acrylonitrile based cerium (IV) phosphate—A kinetic study, Colloids Surf., A 162 (2000) 49–53.
[8] K.G. Varshney, N. Tayal, U. Gupta, Kinetics of ion exchange of alkaline earth metal ions on acrylamide cerium(IV) phosphate: A fibrous ion exchanger, Colloids Surf., B 28 (2003) 11–16.
[9] Y. Onodera, T. Iwasaki, H. Hayashi, T. Ebina, A. Chatterjee, H. Mimura, Sorption of uranium on fibrous cerium(IV) hydrogenphosphate, WM'99 Conference, February 28–March 4 1999, Tucson, AZ.
[10] A. Nilchi, M.M. Ghanadi, A. Khanchi, Characteristics of novel types substituted cerium phosphates, J. Radioanal. Nucl. Chem. 245(2) (2000) 589–594.
[11] K.G. Varshney, M.Z.A. Rafiquee, A. Somya, Triton X-100 based cerium(IV) phosphate as a new Hg(II) selective, surfactant based fibrous ion exchanger: Synthesis, characterization and adsorption behavior, Colloids Surf., A 317 (2008) 400–405.
[12] A. Somya, K.G. Varshney, M.Z.A. Rafiquee, Synthesis, characterization and analytical applications of sodium dodecyl sulphate cerium (IV) phosphate: A new Pb(II) selective, surfactant-based intercalated fibrous ion exchanger, Colloids Surf., A 336 (2009) 142–146.
[13] K.G. Varshney, A. Agrawal, S.C. Mojumdar, Pyridine based cerium(IV) phosphate hybrid exchanger: Synthesis, characterization and thermal behavior, J. Therm. Anal. Calorim. 90(3) (2007) 731–734.
[14] T.M. Suzuki, M.A.L. Tanco, D.A.P. Tanaka, H. Hayashi, Y. Takahashi, Simple detection of trace Pb^{2+} by enrichment on cerium phosphate membrane filter coupled with color signaling, Analyst 130 (2005) 1537–1542.
[15] B. Preetha, C. Janardanan, Ion exchange method for the detection of trace amounts of Mn^{2+} using nano cerium zirconium phosphate cation exchanger, Ion Exch. Lett. 3 (2010) 12–18.
[16] T. Parangi, B. Wani, U. Chudasama, Synthesis and characterization and application of cerium phosphate as an ion exchanger, Desalin. Water Treat. 38 (2012) 126–134.
[17] P. Patel, U. Chudasama, Synthesis and characterization of a novel hybrid cation exchange material and its application in metal ion separations, Ion Exch. Lett. 4 (2011) 7–15.
[18] K. Maheria, U. Chudasama, Studies on kinetics, thermodynamics and sorption characteristics of an inorganic ion exchanger-titanium phosphate towards Pb(II), Bi(III), and Th(IV), J. Indian Inst. Sci. 86 (2006) 515–525.
[19] A.E. Kurtuoglu, G. Atun, Determination of kinetics and equilibrium of Pb/Na exchange on clinoptilolite, Sep. Purif. Technol. 50 (2006) 62–70.
[20] E. Voudrias, K. Fytianos, E Bozani, Sorption–desorption isotherms of dyes from aqueous solutions and waste waters with different sorbent materials, Global Nest: The Int. J. 4(1) (2002) 75–83.
[21] G.K. Akpomie, I.C. Ogbu, A.A. Osunkunle, M.A. Abuh, M.N. Abonyi, Equilibrium isotherm studies on the sorption of Pb(II) from solution by ehandiagu clay, J. Emerg. Trends Eng. Appl. Sci. 3(2) (2012) 354–358.
[22] P. Patel, U. Chudasama, Application of a novel hybrid cation exchange material in metal ion separations, Sep. Sci. Technol. 46 (2011) 1346–1357.